Wissenschaftszentrum Weihenstephan für Ernährung, Landnutzung und Umwelt

Lehrstuhl für Pflanzenernährung

# High-throughput phenotyping of winter wheat cultivars under field conditions

Sebastian Kipp

Vollständiger Abdruck der von der Fakultät Wissenschaftszentrum Weihenstephan für Ernährung, Landnutzung und Umwelt der Technischen Universität München zur Erlangung des akademischen Grades eines

## Doktors der Agrarwissenschaften (Dr. agr.)

genehmigten Dissertation.

Vorsitzender:           Univ.-Prof. Dr. Hans Rudolf Fries
Prüfer der Dissertation:    1. Univ.-Prof. Dr. Urs Schmidhalter
                         2. Univ.-Prof. Dr. Heinz Bernhardt

Die Dissertation wurde am 30.12.2013 bei der Technischen Universität München eingereicht

und durch die Fakultät Wissenschaftszentrum Weihenstephan für Ernährung, Landnutzung

und Umwelt am 18.06.2014 angenommen.

*Meinen Eltern*

# Publications arising from this thesis

**S. Kipp**, B. Mistele and U. Schmidhalter (2014): Identification of stay-green and early senescence phenotypes in high-yielding winter wheat, and their relationship to grain yield and grain protein concentration using high-throughput phenotyping techniques, *Functional Plant Biology*, 41, 227-235.

**S. Kipp**, B. Mistele and U. Schmidhalter (2014): The performance of active spectral reflectance sensors as influenced by measuring distance, device temperature and light intensity, *Computer and Electronics in Agriculture* 100, 24-33.

**S. Kipp**, B.Mistele, P. Baresel and U. Schmidhalter (2014): High-throughput phenotyping early plant vigour of winter wheat, *European Journal of Agronomy*, 52:271-278.

# Table of contents

# List of Tables

## List of Figures

**Summary**

Spectral remote sensing is widely used for land-use management, agriculture, and crop management. Spectral sensors are most frequently adopted for site-specific fertiliser applications and, increasingly for precision phenotyping. However the knowledge about their performance under varying ambient conditions and changing crop distances is still limited. Furthermore it is still unknown in which quantity different plant components (e.g. leafs, stem, ear) reflect the sensor signal and how deep the signal penetrates into the canopy. Such knowledge is indispensable, particularly for sensors being used for precision phenotyping measurements where only small differences in plant canopies or between cultivars need to be detected. The development of high-throughput phenotyping techniques as a non-invasive method to determine various plant characteristics in plot experimentation or for breeding purposes is the major target of this study. Nevertheless two basic experiments were conducted to improve the understanding about the performance of spectral sensors under varying ambient conditions and to obtain information about the spatial reflectance characteristics of plant canopies. The results could improve the applicability of spectral reflectance sensors for being used in the field.

For the second major part of the present study a two-year winter wheat experiment with 50 cultivars was conducted between 2010 and 2012 at the research station Dürnast of the Technische Universität München, Germany to provide high-throughput phenotyping experiments using spectral reflectance sensors mounted on the mobile phenotyping platform Phenotrac 4. In both years spectral measurements were conducted to detect genotypic differences in the plant vigour at early development stages, using digital imaging as suitable reference method. Cultivar specific differences for this specific trait could be observed and a spectral index was calculated to accurately detect the early plant vigour in large field trials using spectral reflectance as high-throughput phenotyping technique. In 2012 passive spectral sensing was established to identify stay-green and early-senescence phenotypes using the onset of senescence as distinctive feature. Significant relationships between the onset of senescence, yield and grain protein concentration indicated an important impact of the maintenance of green leaf area on carbon and nitrogen metabolism, which predominantly affect grain yield and protein concentration. The high-throughput character of our proposed phenotyping methods should help to improve the detection of important plant traits in large field trials as well as help us to reach a better understanding of underlying yield physiological processes.

**Zusammenfassung**

Spektrale Reflexionsmessungen finden eine breite Anwendung in der landwirtschaftlichen Pflanzenproduktion und im Nutzpflanzenmangement, wobei Sensorsysteme vorwiegend für das Bestandesmanagement eingesetzt werden und vermehrt auch zur Phänotypisierung von Pflanzenmerkmalen. Allerdings ist die Funktionalität spektraler Sensoren bei inkonstanten äußeren Messbedingungen und variablen Abständen zur Pflanzenoberfläche weitestgehend unklar. Desweiteren gibt es keine Informationen darüber welche Pflanzenteile in welchem Ausmaß das vom Sensor emittierte Licht reflektieren und wie tief das Lichtsignal in den Pflanzenbestand eindringt. Solches Wissen ist von großer Bedeutung für Sensoren, die zur Phänotypisierung von Pflanzen- oder Sortenmerkmalen eingesetzt werden, denn dort gilt es zu berücksichtigen, dass phänotypische Unterschiede oftmals sehr gering sind. Ziel dieser Arbeit ist die Entwicklung von Methoden zur Hochdurchsatz-Phänotypisierung, also zur nicht-invasiven Erfassung verschiedener Pflanzeneigenschaften in Feldversuchen. Dazu wurden zunächst Grundlagenversuche durchgeführt, um zu ermitteln, welche exogenen Faktoren einen Einfluss auf die Funktionalität spektraler Sensoren haben und inwiefern sich spektrale Reflexionseigenschaften von verschiedenen Pflanzenteilen unterscheiden. Die gewonnenen Ergebnisse lieferten wichtige Informationen für die korrekte Anwendung spektraler Sensoren im Feldversuchswesen zur Hochdurchsatz-Phänotypisierung von Weizen. In den Jahren 2010 bis 2012 wurde an der Forschungsstation Dürnast der Technischen Universität München ein zweijähriger Weizenversuch mit 50 Weizensorten durchgeführt. Die mobile Phänotypisierungsplattform Phenotrac 4, ausgestattet mit verschiedenen spektralen Reflexionssensoren, wurde dabei zur Hochdurchsatz-Phänotypisierung verschiedener Pflanzenmerkmale verwendet. In beiden Versuchsjahren konnten mittels Spektralmessungen deutliche Sortenunterschiede in Bezug auf die Wüchsigkeit junger Weizenpflanzen in frühen Entwicklungsstadien bestimmt werden. Als Referenzmethode erwies sich die Pixelanalyse von Digitalfotos am geeignetsten. Sortenabhängige Unterschiede konnten erfasst werden und ein spektraler Index wurde entwickelt um dieses Sortenmerkmal im Hochdurchsatz auf großen Feldversuchen zu phänotypisieren und um letztendlich visuelle Bonituren zu ersetzen. Im zweiten Versuchsjahr wurde eine Methode entwickelt um mit passiven Spektralmessungen sog. stay-green Sorten von frühabreifenden Sorten zu unterscheiden, wobei signifikante Beziehungen zwischen dem Beginn der Seneszenz und dem Ertrag, bzw. der Kornprotein-Konzentration ermittelt werden konnten. Die erzielten Ergebnisse lassen vermuten, dass die

Aufrechterhaltung der grünen Blattfläche von großer Bedeutung für den Kohlenstoff- und Stickstoffmetabolismus ist.

Die in dieser Arbeit entwickelten Methoden zur Hochdurchsatz-Phänotypisierung können einen wertvollen Beitrag liefern zur automatischen Erkennung verschiedener Pflanzenmerkmale, bzw. ertragsphysiologischer Prozesse, in groß angelegten Feldversuchen.

# 1    Introduction

## 1.1    Spectral reflectance on plant level

Spectral remote sensing is a widely used tool for agricultural production and crop management with respect to site-specific fertiliser applications (Dellinger et al., 2008; Barker and Sawyer, 2010). Its potential as a vehicle-based high-throughput phenotyping technology under field conditions has recently been demonstrated (Schmidhalter et al., 2001; Thoren and Schmidhalter, 2009; Winterhalter et al., 2011; Erdle et al., 2013). Various plant properties can be detected with spectral reflectance measurements, based on light reflectance in the visible (VIS; 400-750 nm) and near-infrared (NIR; 750-2500 nm) region of the light spectrum. NIR reflectance of plants is mainly affected by the scattering of light in mesophyll cells (Knipling, 1970) and water (Allen and Richardson, 1968). Reflectance and transmission of NIR light in plant canopies is much higher in comparison to VIS light. The sharp increase of reflectance between VIS and NIR, the so called red edge (Guyot et al., 1988) can be seen as indicator for the plants N-Status (Zillmann et al., 2006) or biomass, respectively. Visible light reflected by plant canopies is strongly affected by the amount of chlorophyll (Berger et al., 2010) and associated leaf pigments such as carotenoids and anthocyanins (Babar et al., 2006), which influence sensor readings in the visible spectrum. Because nitrogen is involved in chlorophyll formation, spectral indices can be indirectly used to quantify nitrogen supplies in crops and establish cost-saving site-specific application systems for fertilisers (Hatfield et al., 2008; Scharf et al., 2011). A number of optimised indices exist for quantifying parameters such as biomass (Erdle et al., 2011), N uptake (Mistele and Schmidhalter, 2008), N concentration (F. Li et al., 2010), water status (Elsayed et al., 2011; Winterhalter et al., 2011) or grain yield (Schmidhalter et al., 2003; Babar et al., 2006; Teal et al., 2006) of common crops.

## 1.2    Spectral reflectance sensors

Spectral sensors are increasingly being used in precision farming to convert spectral information directly into fertilisation recommendations (Dellinger et al., 2008; Barker and Sawyer, 2010), thereby enabling a cost-effective, site-specific application of fertilisers (Hatfield et al., 2008; Scharf et al., 2011). Spectral sensors for this purpose work either actively or passively (Erdle et al., 2011). Whereas active sensors are equipped with their own light sources, passive sensors are dependent on sunlight as the light source. Accordingly, active sensors are not influenced by ambient light conditions and can be used during the day and at night. The operating mode of both sensor systems is equivalent as they are equipped

with photodetectors that capture reflected light of specific wavebands in the visible (VIS) and near infrared (NIR) regions of the spectrum.

*1.2.1   Active Sensors*

Different active sensors have been developed for agronomic purposes. Whereas handheld systems are suitable for taking stationary "spot" samples (Govaerts et al., 2007; Verhulst et al., 2009), tractor-mounted sensors can be used for on-the-go precision farming (Reusch, 2004; Mayfield and Trengove, 2009; Tremblay et al., 2009). A related, emerging field is the application of proximal high-throughput phenotyping as a non-invasive method to determine various plant characteristics in plot experimentation or for breeding purposes (Schmidhalter, 2005; Thoren and Schmidhalter, 2009; Erdle et al., 2011).

Although active sensors are independent of solar radiation (Solari et al., 2004; Jasper et al., 2009), the choice of light source (e.g., LEDs or Xenon flash) and viewing angle (e.g., nadir or oblique) can still have important implications. For instance, the light source in combination with optical filters is crucial for the detected light and emitted wavebands. In addition, the measuring area (footprint size) is specific for each active sensor and varies with distance. The footprint size depends inter alia on the sensor's construction because the light signal is physically collimated, resulting in different viewing angles. Thus, at a given viewing angle, the footprint size changes according to the measuring distance and the area monitored by the sensor also changes simultaneously. The footprints of several commercially available sensors vary from oval (CropCircle ACS 470) to circular (N-Sensor ALS) to elongated (GreenSeeker RT100) types.

In addition, other potentially important factors that might affect the performance of active sensors include measuring distance and the resulting field of view depending on the sensors' positioning height (footprint size). Even with fixed sensor positions, differences in plant height in the field can change the measuring distances at fixed sensor positions. Handheld operating systems, where constant distances are not easy to maintain, will be more prone to such errors. Although the manufacturers of the active sensors provide recommendations for optimum measuring distances, it has not been demonstrated how the sensors' output values vary when the distance to the target changes during measurement, even within the recommended distances. Despite this, varying measuring distances have been adopted in different studies and some of the distances have been outside the manufacturers' recommended distances of 81 to 122 cm for GreenSeeker and 25 to 213 cm for CropCircle (Table 1). For example, the GreenSeeker and CropCircle were used at measuring distances

from 25 to 100 cm and 150 cm to 250 cm (Scharf et al., 2007; Roberts et al., 2009; Fitzgerald, 2010), although another study recommended distances of 60 to 110 cm for the CropCircle and 80 to 110 cm for the GreenSeeker (Solari, 2006). By contrast, the N-Sensor ALS can be used at distances of 140 cm (Portz et al., 2012) or more. However it is challenging to determine proper measuring distances between sensor and plant canopies considering that the penetration depth of the sensor signal is unknown.

Table 1: Optimum distances to the reference target as determined in this study compared to the manufacturer´s recommendations for three active canopy sensors and their field of view (FOV) at 1m measuring height.

| Sensor device | Optimum distance to target | Manufacturer´s recommendation | FOV (at 1m measuring height) |
|---|---|---|---|
| GreenSeeker NDVI | 70 – 140 cm | 81 – 122 cm | ~ 60 cm |
| GreenSeeker ($R_{770}/R_{650}$) | 70 – 110 cm | | |
| CropCircle ($R_{760}/R_{730}$) | 30 – 200 cm | 25 – 183 cm | ~ 54 x 25 cm |
| CropCircle NDVI | 30 – 200 cm | | |
| Active Flash Sensor | 50 – 200 cm (and more) | not specified | not specified |

When evaluating measuring distances, it must be considered that emitted light from a point source follows the inverse square law, which means the light intensity decreases four times when the measuring distance doubles. Thus, the spectral readings of a single waveband will change with varying distances to the target (Holland et al., 2012). Assuming that single wavelengths are sensitive to changing distances, a distance effect could be excluded by building spectral indices of two wavelengths. Thus, enabling spectral measurements, which are independent of varying distances, requires uniform changes in the reflectance magnitude of each wavelength. However, the stability of spectral indices with respect to measuring distance has not been tested by previous studies or suppliers' recommendations.

Other ambient factors that could affect the sensor performance are temperature and solar radiation/illumination. Both solar radiation and air temperature can affect the temperature of the sensor itself such that the device temperature may vary widely on measurement days with changing cloudy or sunny conditions. For the successful application of active sensors in the

6

field for precision-farming purposes, it is essential to determine whether and to what degree diurnal variations in temperature and light intensity might affect spectral readings. However, information regarding the effect of temperature or light intensity is rarely reported by sensor suppliers, and there are currently no associated relevant studies. Given the dependency of laser-induced chlorophyll fluorescence on ambient light and temperature conditions (Thoren et al., 2010), it remains to be tested whether such effects may also occur for other sensor systems.

Despite the obvious reliance of the performance of the active sensors, only little research has been done to assess the potential effect of external and internal factors on the active sensor performance. An exception is the study of Kim et al. (2010), who studied the effects of varying temperature and light intensity on the performance of the active sensor GreenSeeker. However, such general knowledge is indispensable, particularly when only small differences in plant canopies or between cultivars need to be detected and might be obscured by inherent measuring errors of the devices.

### 1.2.2 *Passive sensors*

Whereas active sensors are limited to single wavelengths, conventional passive spectrometers are able to detect a broad spectrum of wavelengths, including the VIS and NIR spectrum and various combinations of spectral indices can be computed. However sun light is needed for referencing the canopy reflectance. Thus the application of passive sensor devices is limited to daylight conditions considering that factors like changing solar zenith angle (Fitzgerald, 2010) can influence their performance. Long term measurements between morning and evening should be avoided because the solar angle changes during the daytime and across seasons. Because they use the sunlight as light source, which is not comparable to light emitting diodes (LED) used for active sensor systems, passive sensors work nearly independent from changing measuring distances. Thus, they are frequently used for ground-based sensing as well as for airborne and satellite observations.

### 1.3 High-throughput phenotyping of plant specific traits

Agronomists and plant breeders rely on the evaluation of various plant traits in the field to select favourable candidate plants or cultivars for further breeding steps. The amount of field trials and plots for breeding and research purposes is increasing (White et al., 2012), since modern breeding methods on genotype level (e.g. next-generation sequencing) accelerate the breeding process and more promising genotypes have to be tested in field trials. Thus, high-

throughput selection tools for phenotyping such traits are needed. Generally, spectral remote sensing has potential to be used as high-throughput phenotyping technique (Reynolds et al., 2009; Furbank and Tester, 2011; Walter et al., 2012; Fiorani and Schurr, 2013). To enable high-throughput measurements of large field trails researchers and plant breeders rely on vehicle based phenotyping platforms. Such platforms were already developed for field (Erdle et al., 2011, 2013; Montes et al., 2011; Comar et al., 2012; Winterhalter et al., 2012; Busemeyer et al., 2013) and greenhouse (Granier et al., 2006; Subramanian et al., 2013; Tisné et al., 2013) phenotyping. Many different plant traits are relevant for plant breeders and their scoring in the field could be substantially improved using spectral reflectance sensors for high-throughput phenotyping. In the present study spectral phenotyping methods for two important breeding traits, early plant vigour and the onset of senescence, are developed.

## 1.3.1   Early plant vigour

Yield formation of wheat starts in the early growth period when the seedlings´ vigour and several environmental factors influence the germination rate and early plant vigour. Seedling vigour is affected by various genetic traits (Richards and Lukacs, 2002; Ellis et al., 2004; Rebetzke et al., 2007) and reflects the plant vigour at early growth stages. Thus, early plant vigour has to be seen as an assessment criterion that substantially affects the final yield as a result of different tillering intensities (Valério et al., 2009).

Although many laboratory tests for assessing early plant vigour determining factors, such as seedling emergence or seedling vigour (Steiner et al., 1989; Boligon et al., 2011), exist, they are not suitable for selecting breeding lines under field conditions, where germination and early plant vigour are highly dependent on environmental factors (Steiner et al., 1989), such as temperature (Khah et al., 1989), soil moisture (Murungu, 2011), soil type, and other factors including seed storage conditions and seed age (Khah et al., 1989; Ghassemi-Golezani and Dalil, 2011), seed weight, or infection with pathogens (Rajala et al., 2011). Furthermore, the amount of mineral nitrogen, applied as fertilizer has an important influence on early plant vigour in terms of tillering intensity.

Scoring early plant vigour visually and with several persons in the field is laborious, biased and expensive. Even experienced persons determine early plant vigour subjectively. However, visual scoring of early plant vigour is still conventionally applied because of a lack of alternative methods. Counting the amount of tillers per plant in each plot would represent a possibly accurate method to detect early plant vigour but relating it to the extent of field trials in breeding programs it has to be seen critical in terms of laboriousness (Scotford and Miller,

2004), accuracy and representativeness (Taylor et al., 2000). A suitable method for detecting early plant vigour or crop coverage is the analysis for the proportion of green pixels in digital images.

Phenotypic differences in early plant vigour or crop coverage could be shown in experiments with increasing nitrogen levels or sowing densities (Lukina et al., 1999; Stevens et al., 2008; Wu et al., 2011) which increased the range of variation, but no study exists that tried to assess cultivar differences without experimental variation. Generally, spectral assessment of plants in early development stages was found to be difficult due to low soil coverage (F. Li et al., 2010).

### 1.3.2  *Onset of senescence*

Breeding simultaneously for both grain yield and grain protein concentration (GPC) confronts wheat breeders with the inverse genetic relationship that exists between these two traits (Feil, 1997; Pleijel et al., 1999; Blanco et al., 2012) and derives from interactions of the nitrogen and carbon metabolism affecting mainly the synthesis of amino acids or starch during grain filling, respectively, and therefore either GPC or grain yield (Novoa and Loomis, 1981). Considering the contribution of pre-anthesis stored assimilates to the final yield (e.g. ca. 57% in wheat (Gallagher et al., 1975) and 4-24.4% in barley (Przulj and Momcilovic, 2001a)), it is obvious that a large proportion of the final grain yield derives from post-anthesis accumulation and translocation of assimilates, in particular C and N (Przulj and Momcilovic, 2001a, 2001b). Thus, both grain yield and GPC are strongly affected by the length of the post-anthesis period and the maintenance of green leaf area as an indicator for photosynthetic activity. Thus, through the latter effect, post-anthesis leaf senescence should also influence grain yield and GPC.

Many studies have been conducted to identify stay-green and early-senescence phenotypes in wheat (Spano et al., 2003; Gong et al., 2005; Christopher et al., 2008; Bogard et al., 2011; Derkx et al., 2012; Lopes and Reynolds, 2012). Because the variability of the duration of greenness is also high in many plant species (Thomas and Smart, 1993), these results offer a valuable resource for attempts to improve grain yield and GPC of winter wheat cultivars (Foulkes et al., 2007). Thus, whereas mainly positive relationships between stay-green phenotypes and yield have been demonstrated (Verma et al., 2004; Christopher et al., 2008; Bogard et al., 2011; Lopes and Reynolds, 2012; Pask and Pietragalla, 2012), negative effects on yield have rarely been reported (Jiang et al., 2004; Kichey et al., 2007; Derkx et al., 2012). However there is a lack of studies dealing with large-scale phenotyping of stay-green and

early-senescence phenotypes under field conditions, which would enhance our understanding of the influence of senescence mechanisms on grain yield and GPC.

The onset of senescence, where the chlorophyll content of the plant decreases rapidly (Araus and Labrana, 1991) is a widely used measure to differentiate between stay-green and early-senescence phenotypes (Bogard et al., 2011; Lopes and Reynolds, 2012). However, use of this measure is complicated by the progress of senescence within the whole plant not being uniform, beginning initially in the older, lower leaf layers and progressing upwards through the plant such that the flag leaf remains green when all other leaves are already senescent (Fischer and Feller, 1994). Instead, there are good indications that senescence investigations should focus on the onset of this process in the flag leaf area because of its effects on both N-uptake (Hirel et al., 2007) and C remobilization (Tahir and Nakata, 2005) and thus potential impact on GPC and grain yield. For instance, as the youngest wheat leaf, the flag leaf contributes about 18% of the kernel N per spike (Wang et al., 2008) and about 30–50% of the assimilates for grain filling (Sylvester-Bradley et al., 1990). However, adverse environmental conditions such as drought or heat stress can distinctly affect plant physiological processes and consequently GPC and grain yield.

Different methods have been applied to assess flag leaf senescence, including visual scoring (Verma et al., 2004; Fois et al., 2009; Gaju et al., 2011), SPAD-meter measurements (Christopher et al., 2008; Derkx et al., 2012) and digital photo imaging (Adamsen et al., 1999). Although generally effective, these methods are not suitable for the high-throughput phenotyping that is needed to detect senescence properties of many cultivars in a reasonable timeframe. In this, spectral remote sensing could represent an ideal tool to bridge this gap (Reynolds et al., 2009; Furbank and Tester, 2011; Walter et al., 2012). Lopes and Reynolds (2012) applied a proximal sensing method to assess stay-green parameters, using the active spectral sensor GreenSeeker and SPAD readings. Such advanced methods are generally appropriate in terms of objectivity in comparison to visual scoring but still limited in meeting the demand of high-throughput phenotyping.

## 1.4    Objectives

Spectral reflectance sensors are widely used for agriculture, and crop management and more recently also for precision phenotyping approaches. However they are most frequently used for site-specific fertilizer application. Although the application of such sensors is very well established, there is a lack of studies dealing with potential factors, which could affect the sensor´s performance. With the use of active sensors in the field, it is inevitable that they will be used under varying ambient conditions and with varying crop distances, but it remains unclear how these factors affect the active sensors performance. Therefore the aims of *Section 1* were i) to investigate the impact of three external factors (measuring distance, device temperature, and amount of ambient light) on the performance of three different active sensor systems (NTech GreenSeeker RT100, Holland Scientific CropCircle ACS 470, YARA N-Sensor ALS) and ii) to exemplary quantify potential measuring errors on the basis of a winter wheat field trial with different nitrogen levels.

When using spectral sensors under field conditions it is still unclear, how deep the sensor signal penetrates into the canopy. Moreover the canopy reflectance is a mixture of different reflectance signals of all plant components and soil. Knowledge about the proportions of each plant component in the whole reflectance signal is necessary to achieve accurate measurements of plant canopies. *Section 2* of the present study therefore investigates i) how deep the emitted light by three different active sensors (NTech GreenSeeker RT100, Holland Scientific CropCircle ACS 470, YARA N-Sensor ALS) penetrates into the canopy, and ii) how accurate single wavelengths and spectral indices assess dry weight and N content of different plant components.

The major goal of the present study was the development of high-throughput phenotyping methods using spectral reflectance sensors. Such methods will help to improve and accelerate scoring of various plant traits for plant breeding purposes. Phenotyping methods of two different traits – early plant vigour and the onset of senescence – were developed for winter wheat cultivars grown under field conditions. Therefore field experiments in *Section 3* were conducted i) to rate the validity that pixel analysis of RGB images accurately reflects the early plant vigour for being used as reference method; ii) to demonstrate that early plant vigour is specific for each cultivar; and iii) to establish spectral reflectance measurements as a high-throughput phenotyping method to score early plant vigour in large field trials.

Phenotypic differences in the development of wheat plants between anthesis and maturity is usually been underestimated by agronomists and plant breeders, although it is well known that the timing of senescence clearly affects the carbon and nitrogen metabolism. Moreover

existing literature reports contrary effects of the maintenance of green leaf area on final grain yield or grain protein. Furthermore the visual identification of such stay-green genotypes under field conditions is difficult among large sets of cultivars. The aims of *Section 4* of this study were therefore i) to test whether high-throughput spectral reflectance measurements based on passive sensors can indeed be used to effectively and accurately identify stay-green and early-senescence phenotypes within a large range of certified winter-wheat genotypes and ii) to investigate the effects of these phenotypes on grain yield and grain protein concentration.

## 2    Materials and Methods

2.1    Active and passive spectral reflectance sensors

Four active (GreenSeeker RT100, CropCircle ACS470, Active Flash Sensor (AFS) and Hyperspectral Active Flash Sensor (HAFS)) and one passive spectral reflectance sensor devices were used for the following experiments.

The GreenSeeker RT100 possesses two separate LEDs emitting modulated light in either the near infrared (NIR, 770 nm) or the red region (650 nm) of the spectrum (Figure 1); the wavelengths are fixed and cannot be changed. The LEDs alternate their pulses, with each emitting 40 light pulses in 1 msec (= 40 kHz) before pausing for the other LED. A single silicon photodiode detector captures the reflected light of both LEDs. The most common index that can be generated by using the GreenSeeker´s wavelengths is the normalised difference vegetation index (NDVI = $(R_{770}-R_{650})/(R_{770}+R_{650})$), which can be used to estimate the photosynthetic area (biomass) or N-uptake of plant canopies.

A single LED is implemented in the CropCircle ACS 470, which with the use of PolySource light source technology (Holland Scientific, Lincoln, NE) is able to emit polychromatic light in wavelengths from 430 nm to 850 nm (Figure 1). To split the light signal into three different channels, optical interference filters are installed in front of the detector to regulate the incoming light reflectance and to enable the user to select the desired wavelengths. In this study, filters for 670, 730, and 760 nm were used. For the detection of the incoming reflectance, the CropCircle is equipped with a three-channel silicon photodiode array with a spectral range of 320 nm to 1100 nm (Holland-Scientific, 2008). The signal output rate for the CropCircle sensor is programmable within a range of 1 to 100 measurements per second. Compared with the GreenSeeker, the Crop Circle supports a broader range of plant indices because of the increased availability of wavelengths. Common indices that can be calculated are the soil-adjusted vegetation index (SAVI), the green difference vegetation index (GDVI), the ratio analysis of reflectance spectra (RARS) and NDVI, depending on user selectable filters which are used.

The AFS uses a xenon flash as its light source, which pulses monochromatic light at a frequency of at least 10 Hz (10 flashes per second) in a range between 650 nm and 1100 nm (Figure 1) in four different channels (Link and Reusch, 2006). Similar to the CropCircle, the AFS is equipped with interference filters to provide user-selectable wavelengths. Four filters (730, 760, 900, and 970 nm) were used in this study.
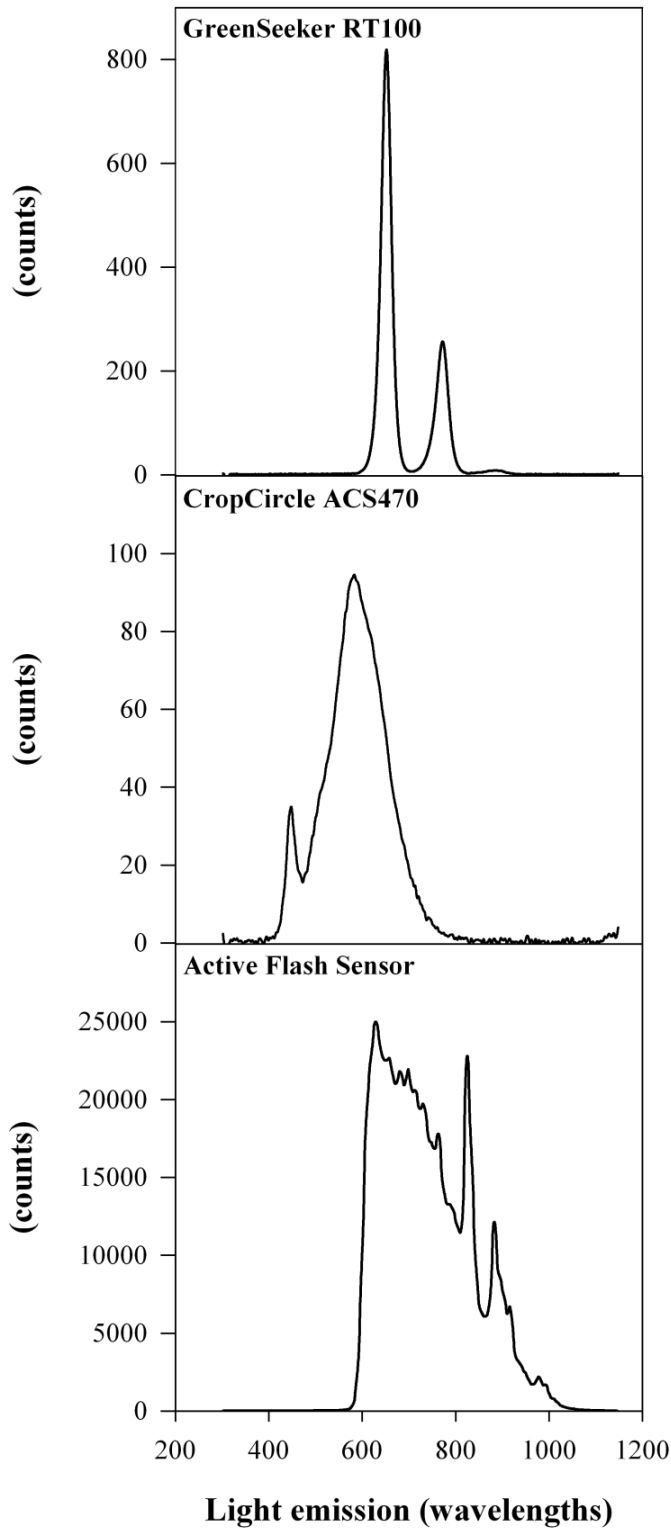
Figure 1: Emitted light quality of three active sensors measured with the diffuser of a passive spectrometer.

In comparison to the AFS the HAFS emits monochromatic light in a range between 370 nm and 1026 nm and light reflectance of single wavelengths could be measured every 7 nm. However the light source, a xenon flash, is similar to the AFSs one.

The passive spectrometer device (tec5, Oberursel, Germany) provides hyperspectral readings in a range of 400-1700 nm and a bandwidth of 3.3 nm (Mistele and Schmidhalter, 2010). The spectrometer comprises two Zeiss MMS1 silicon diode array spectrometers, which together measure canopy reflectance in a circular field of view (FOV) of approximately 0.28 m² in the centre of each plot. A second unit detects solar radiation as reference signal.

Depending on the experimental design (growth chamber, glass house or field) all sensors were either mounted on a moveable frame (Figure 2a) or on the mobile phenotyping platform PhenoTrac 4 (Figure 2b) developed by the Chair of Plant Nutrition, Technische Universität München (http://www.pe.wzw.tum.de). On the latter platform sensor readings were directly co-recorded along with GPS coordinates from the TRIMBLE RTK-GPS (real-time kinematic global positioning system; Trimble, Sunnyvale, CA, USA) to provide accurate sensor readings for single plots. All sensors were mounted in nadir position to enable vertical canopy measurements. The sensor-canopy distance in field measurements with the PhenoTrac 4 platform could be adjusted using a hydraulic measuring unit.
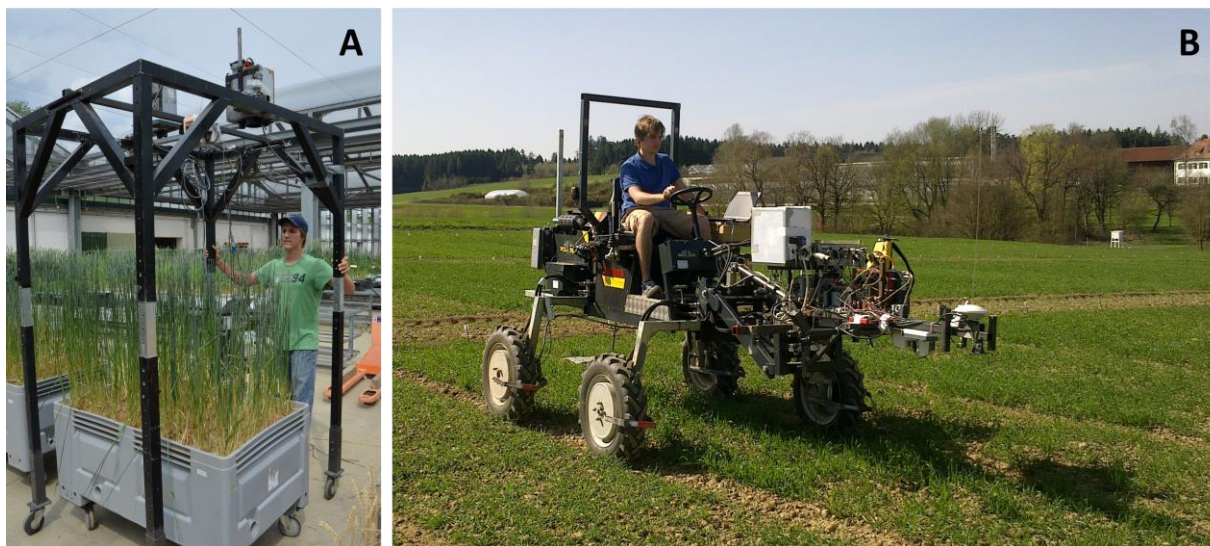


Figure 2: Experimental setup for canopy measurements in the growth chamber and glass house using a moveable frame (a). Field measurements were conducted using the mobile phenotyping platform Phenotrac 4 (b).

## 2.2 Growth chamber experiments for evaluating the performance of active sensors under varying conditions.

### 2.2.1 *Experimental design*

Measurements were performed in a temperature- and light-controlled walk-in growth chamber (York International, Mannheim, Germany) using metal halide lamps as a light source (MT 400DL, Osram, München, Germany). Airflow passed uniformly upward through the entire walk-in area to negate any effects from the heat of the lamp. A green, light-proof woven fabric (Vendela MW90G, IKEA, Munich, Germany) of 2 $m^2$ (2 m x 1 m) mounted on a wooden board was used as a reference surface for the reflectance measurements. To enable a uniform measuring area and to avoid creases, the fabric was tightly stretched over the board. Thus, identical spectral readings at each point of the fabric could be measured. The measuring reference surface was optimally suited for our investigation. The only possible alternative would be the use of a short-cut grass stand as used by Kim et al. (2010). Given the unknown penetration depths occurring in real plant stands, which also vary according to the type of sensor, it would be impossible to interpret results from such stands. Thus the only exact information can be obtained from a planar surface with reliably known vertical foot print distances. The reflectance characteristics of the green fabric were generally comparable to those of plant canopies or leaves. Figure 3 shows a spectral curve of the fabric measured with the handheld color spectrometer ColorEye XTH (X-Rite, Regensdorf, Switzerland). Plant specific reflectance attributes such as the absorption maximum of blue and red wavelengths and the red edge inflection are nearly identical to canopy reflectance. Additionally gloss properties of the green fabric were measured using again the color spectrometer. The gloss of the surface, defined as the ratio between specular and diffuse reflectance, was 2.8 %, which is nearly identical to the gloss effect of plant leaves. The sensors were installed on a mobile platform that enabled the measuring distances to be varied.
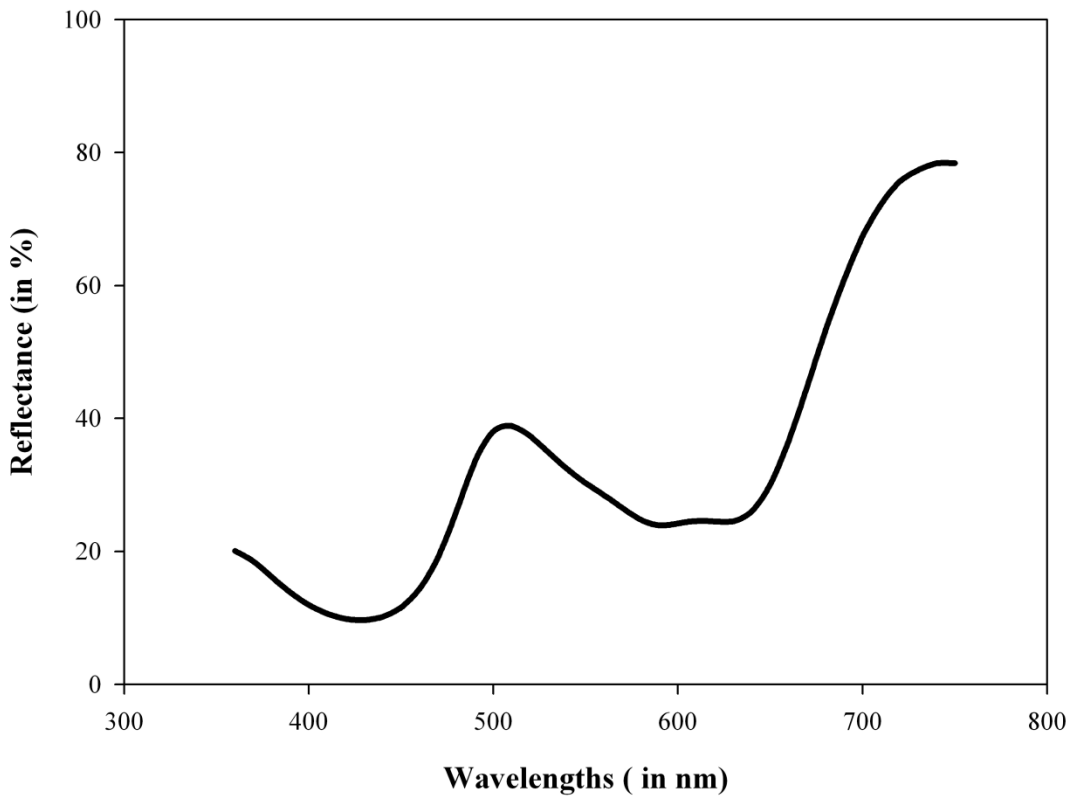
Figure 3: Spectral reflectance curve of the green fabric reference target, measured with a passive spectrometer device (tec5, Oberursel, Germany).

### 2.2.2 Spectral reflectance measurements

For evaluating effects of varying distances between sensor and target on the accuracy of active sensors, three active sensors (GreenSeeker, CropCircle, AFS) were mounted separately on the mobile measuring platform and fixed at different measuring distances. The sensor readings of the green measuring surface were recorded at incremental height intervals of 10 cm, starting at 10 cm and ending at 200 cm in the nadir position. The readings (5 readings/second) were averaged over 10 seconds and directly stored on a notebook via a USB connection. All measurements were repeated for distances between 10 and 160 cm to validate the repeatability of this experiment. Spectral measurements at distances above 200 cm were not possible due to the maximum height of the walk-in growth chamber where all measurements were conducted.

For detecting effects of varying device temperature on the sensor performance, the growth chamber was programmed to heat up from 5°C to 35°C over a 60-minute period and continuous sensor readings of the measuring surface were recorded. These measurements

were conducted twice for each sensor at two different measuring heights to verify if such measurements are repeatable. The temperature inside each sensor was measured with thermal detectors, which are standard components in the GreenSeeker and in the AFS. A thermal detector was also installed for the CropCircle for measuring the detector temperature. Again, the sensor reflectance values were recorded via USB to the notebook. Possible temperature corrections which could already being implemented by the manufacturer are not known.

To illustrate the effect of varying device temperatures under field conditions, we compared our measured values to spectral information obtained from a field experiment (Erdle et al., 2011) in which different amounts of nitrogen (10, 100, 160, and 220 kg N ha$^{-1}$) were applied in three dressings to the winter wheat (*Triticum aestivum L.*) variety "Tommi". The crops were scanned with all three active sensors (Erdle et al., 2011), and the respective index values were calculated and transformed to be expressed as kg N ha$^{-1}$. Potential error rates in index values for temperature shifts of ±1°C were calculated using measured data of the basic experiment in the growth chamber.

To investigate the effect of varying light conditions, all sensors were placed separately in the growth chamber at 5 °C considering enough heating time to achieve a stable temperature and to exclude temperature effects. Thereafter, five different light intensity levels (0, 100, 270, 410 and 580 μmol m$^2$*s$^{-1}$) were applied to the growth chamber while keeping the temperature constant within the ventilated room. The light intensity was reduced stepwise starting at 580 μmol m$^2$*s$^{-1}$ and after each step spectral reflectance measurements of the green fabric were performed. The overall measuring time was approximately 30 seconds for each sensor. Thus heating of the sensor body could be completely avoided. The light intensity levels were chosen to simulate photosynthetic active radiation, which reaches intensities of 500-600 W/m² under high net radiation conditions (Kyle et al., 1977; L. Li et al., 2010). The sensor readings at each illumination level were recorded to the notebook computer via the USB connection.

## 2.3 Pot experiments to detect reflectance characteristics of different leaf layers, stems and ears using active canopy sensors

### 2.3.1 *Experimental design*

A greenhouse winter wheat experiment was conducted at the research station Dürnast in 2012. Twelve containers with a surface area of 0.77 m² (0.7 x 1.1 m) were filled up with 480 kg homogenous soil (Cambisols of silty clay loam) with a N$_{min}$ content of 6.7 kg N ha$^{-1}$. The winter wheat cultivar "Scirocco" was manually drilled in a depth of 3 cm with a row spacing of 11.5 cm (320 kernels per m²). A total of 130 kg N ha$^{-1}$ was applied as ammonium nitrate

urea solution (AHL) at seeding (80 kg N) and stem elongation (50 kg N) and all other nutrients including P, K, S and the micronutrients, were adequately supplied to the crops.

The plants were daily watered by replacing the water loss of each container. The latter information was obtained from regular weighting of the containers.

### 2.3.2   Biomass sampling and spectral measurements

Biomass sampling and spectral measurements were conducted at two development stages (ZS 61 and ZS 75) for six containers at each date. Three active sensor devices (GreenSeeker, CropCircle, AFS) were mounted on the aluminum frame (Figure 2a), which could be moved above the containers, to provide a constant measuring distance of 1 m between the sensor and the plant canopy. All plant components, including stems and ears, were stepwise removed, starting with the lower leaf layers (up to 15 cm), the middle leaves (all leaves except flag leaves), flag leaves, ears and stems. Spectral measurements were conducted before the first leaves were removed and successively between each removal step, including the bare soil after cutting the stems. Sensor readings were averaged every 10 seconds and directly transmitted on a notebook via USB. Biomass samples from each removal step were separately weighed to determine the fresh weight. After drying in an oven at 100°C for 24 hours, all samples were again weighed to calculate the dry weight and the dry matter content. Dry samples were milled and analyzed for N concentration with mass spectrometry using an Isotope Radio Mass Spectrometer with an ANCA SL 20-20 preparation unit (Europe Scientific, Crewe, UK). The N-uptake was estimated by multiplying N concentration and dry weight.

The total fresh weight, dry matter content, dry weight, N concentration and N-uptake, respectively, were calculated by adding up the values of all samples which were removed from one container. Spectral data, including single wavelengths and spectral indices of each measurement step, were correlated with the remaining total biomass parameters excluding the components which were already removed. Results from six containers were averaged per measuring date.

### 2.4   Field experiment for high-throughput phenotyping of early plant vigor

### 2.4.1   Study site and experimental design

The 2-year field experiments were conducted in 2010/2011 and 2011/2012 at the Duernast research station of the Technische Universität München in southern Germany (11°41´60´´ E, 48°23´60´´ N). The field trial in 2012 was located 100 m away from the trial in 2011. Both

fields used were mostly homogeneous Cambisols of silty clay loam. The yearly average precipitation in this region is approximately 800 mm with an average temperature of 7.5 C°. The experimental design was identical in both years and was a randomised block design including four replicates. 50 winter wheat (*Triticum aestivum* L.) cultivars were mechanically drilled in a depth of 3cm using a small grain drill with a row spacing of 12.5 cm, whereas accurate soil tillage permitted an appropriate seed bed. The plot size was 12 m in length and 1.50 m in width. Comparable seed numbers per plot (320 kernels per m²) were sown by taking into account the thousand kernel weight. Agronomic management was conducted comparably in both years. The set of cultivars included all quality groups (A, B, C, E) being certified and listed by national authorities and regularly cultivated by German farmers. All cultivars are adapted to the climate conditions in Middle Europe and particularly in Germany. A total of 200 kg N ha$^{-1}$ was applied as ammonia nitrate urea solution (AHL) at tillering (80 kg N ha$^{-1}$), stem elongation (80 kg N ha$^{-1}$) and booting (40 kg N ha$^{-1}$), under consideration of soil N availability of 21 kg N ha$^{-1}$ in 2010 and 15 kg N ha$^{-1}$ in 2011. No fertilizer was applied before planting. All other nutrients, including P, K and S were adequately supplied to the crops. Reflectance measurements and photos were taken at tillering in Zadoks growth stage (ZS) 28 at April 15 in 2011 and ZS 23 at April 4 in 2012 (Zadoks et al., 1974). In 2011 the weather and soil conditions did not allow an earlier measurement. Figure 4 illustrates crop stands in 2011 and 2012 and indicates that the crop stands were not homogeneous. Integrated pest management kept the fields weed-free. Biomass sampling of a 2.7 m² area was performed in both years using a green forage chopper (Erdle et al., 2011), but no consistent data could be obtained in both years. In 2011 adhering soil particles compromised biomass samplings and in 2012 due to the early development stage it was not possible to cut the plants close enough to the soil surface. A manual sampling had to be excluded since previous experience indicated that it was highly subjective due to the individual cutting heights and the non-representativeness of such efforts. Clearly a point frame method using vertical needles to count the plants (Booth et al., 2006) in representative sites could not be adopted given the heterogeneity of the crop stand establishment (Figure 4) and also due to the high labour demand required by sampling 200 plots. Considering the lack of suitable methods, a pixel analysis of RGB images was chosen as reference method to accurately detect early plant vigour. Furthermore spectral reflectance measurements were applied to provide a high-throughput method for replacing the reference measurements, which is in fact very accurate but too laborious for being used as a high-throughput phenotyping tool.
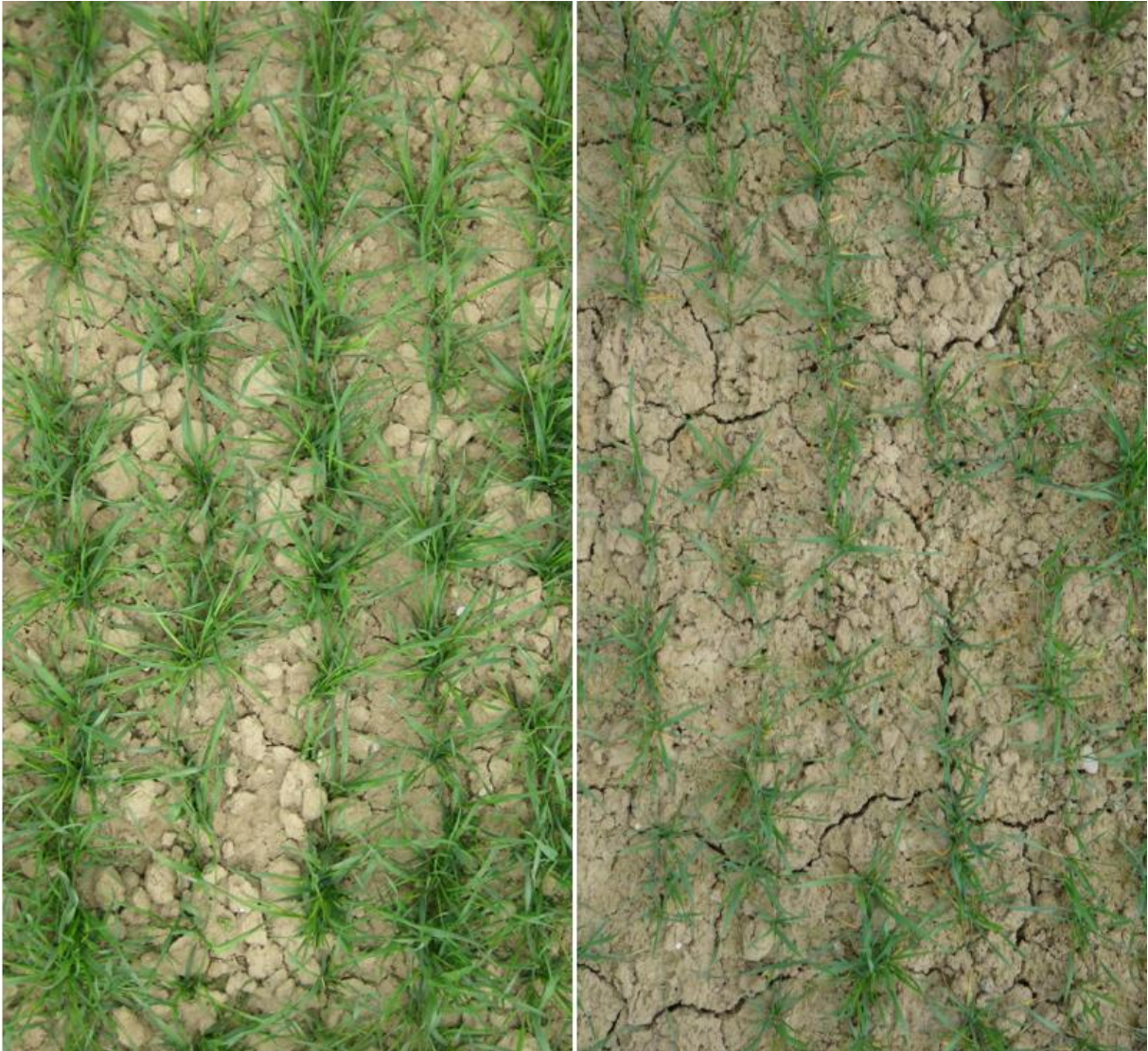
Figure 4: Comparison of digital photos in 2011 (a) and 2012 (b) for detecting early plant vigour.

### 2.4.2 *Pixel analysis of RGB images*

The photos were taken using a Nikon D5100 reflex camera under cloudy conditions to avoid shadows and to provide a constant operation mode. The camera was manually held and oriented vertically downwards over the canopy at a distance of 140 cm and approximately 6 rows of each plot were captured by the camera´s field of view (FOV). Two different methods of photo sampling were performed. In 2011, two photos were taken of each plot without any overlapping. In 2012, the multi shot mode was used while moving the camera from the beginning of each plot to the end. With this method 20-25 photos of each plot were taken, covering the entire plot and allowing the photos to be overlapped. Both methods produced photos with a pixel size of 1281 x 961 pixels, which were stored in JPEG (joint photographic

experts group) file format. Thereafter, the photos were converted into ppm (portable pixmap) file format and analysed for the relative amount of green pixels (RAGP) using R statistics 2.15 (R Foundation for Statistical Computing 2012). The R package "pixmap" was used for this procedure and green pixels could be quantitative separated from all other pixels according to RGB color. Therefore a segmentation index was calculated to extract the RAGP for each image:

$$\text{RGB - Index} = \frac{\text{Green-Red-Blue}}{\text{Green+Red+Blue}}$$

All photos were uploaded and the RAGP was automatically calculated with the software. The results of all photos for each plot were averaged to obtain the average early plant vigour of the whole set of wheat cultivars.

### 2.4.3   Spectral reflectance measurements

Spectral measurements were directly conducted at the beginning of the growing period using the hyperspectral active flash sensor (HAFS) mounted 1 m above ground on the mobile phenotyping platform PhenoTrac 4 in a nadir position to provide high-throughput measurements of all plots. Additionally spectral data of two other active sensor devices, GreenSeeker RT100 and Crop Circle ACS 470 were recorded, using the same phenotyping platform, to assess their ability to detect phenotypic differences at early growth stages.

Three methods were applied to identify optimal relationships between spectral information and the early plant vigour derived from pixel analysis by evaluating (i) combinations of all possible simple ratios and illustrated by contour plots (data not shown); (ii) testing of combined indices and (iii) applying multivariate modelling and prediction using the chemometric software package ParLeS (Viscarra Rossel, 2008). Overall the best performance was achieved with a newly developed combined spectral index, the early plant vigour index (EPVI), being better than all tested combined indices (e.g. NDVI and RVI) as well as the models suggested by the multivariate analysis. The EVPI was calculated, using three single wavelength values (670, 750 and 862 nm) as follows:

$$\text{Early plant vigour index (EPVI)} = \frac{R750 - R670}{R862}$$

The combination of NIR and VIS wavelengths was chosen since such spectral regions are well known for being used to predict biomass. The NDVI and RVI were calculated according to Raun et al. (2001) and Jordan (1969). Similar to the pixel analysis, replications were averaged to evaluate the early plant vigour of all wheat cultivars.

### 2.4.4 Statistical analysis

Early plant vigour as assessed by pixel analysis and the spectral index EPVI was separately correlated to each other for both years. An analysis of variance (ANOVA) and the Student-Newman-Keuls test were conducted to evaluate the heritability within the replications of each cultivar. To assess the ability of the spectral reflectance data to evaluate early plant vigour, plot averages of the EPVI and pixel analysis of RAGP were correlated. Coefficients of determination and regression equations were calculated to evaluate the relationship between both methods.

## 2.5 Field experiment for high-throughput phenotyping of stay-green and early senescence phenotypes

### 2.5.1 Study site and experimental design

All measurements were conducted in 2012 using the same field trial with 50 winter wheat cultivars as described in 2.4.1.

### 2.5.2 Phenology and crop measurements

Development stages between tillering and maturity were recorded for each cultivar every 1-2 days according to the Zadoks decimal code (Zadoks et al., 1974). Air temperature and rainfall conditions were recorded on-line in the field during the growth period using a mobile meteorological station (Figure 5). Following Przulj and Momcilovic, (2001$a$), average daily degree-days were calculated from the daily temperatures measured at 7:00, 14:00 and 21:00 h as $(T_7 + T_{14} + (2*T_{21}))/4$.
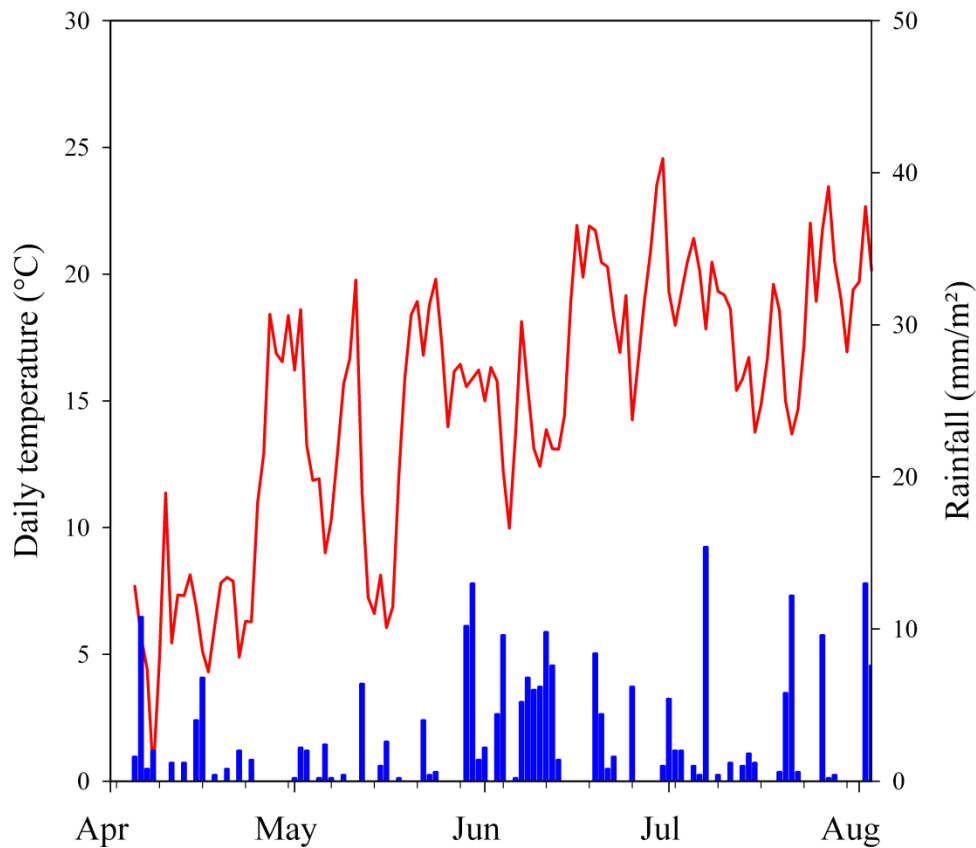
Figure 5: Temperature and rainfall conditions at the Dürnast study site during the main growing period from April to August 2012.

After maturity (1 August 2012), a 6.75 m² area of each plot was harvested using a combine harvester for a direct determination of grain yield. Representative grain samples of each plot were oven dried at 60°C for 48 hours and subsequently milled. The N concentration of each sample was detected with mass spectrometry using an Isotope Radio Mass Spectrometer with an ANCA SL 20-20 preparation unit (Europe Scientific, Crewe, UK) and GPC was taken to be 6.25 times the N concentration.

### 2.5.3   Color Measurements

Flag leaf color measurements of 20 of the 50 cultivars were conducted on 10 dates between anthesis and maturity. CIELab color coordinates (L, a, b) were measured using the handheld ColorEye XTH spectrometer (X-Rite, Regensdorf, Switzerland) within an 8°/d measuring geometry of an Ulbricht sphere, a D65 illuminant and 10° observer. A circular area with a diameter 5 mm of the leaf lamina was measured in the center of the fully developed flag leaf. Twenty measurements per plot were conducted in three replications, giving a total of 12000 samples for the 20 cultivars and 10 measuring dates. Although all perceptible colors can be

classified in the CIELab color space, only the collected b-values were used for the calculation of the onset of senescence because they measure the color-opponent dimensions blue-yellow and therefore best describe the typical color shifts into yellow that occur during the senescence process of wheat.

Flag leaf color measurements of three cultivars were stopped prematurely because objective measurements were not possible due to damage to the flag leaves through either the last fertilizer application at heading (cvs. W00984.2 and Arina) or heavy smutting with brown leaf rust (*Puccinia recondita* L.) (cv. Magnifik).

### 2.5.4   *Spectral reflectance measurements*

Spectral measurements were conducted within less than one day following the color measurements using the passive spectrometer device (tec5, Oberursel, Germany). The sensor device was mounted 1 m above the canopy on the mobile phenotyping platform PhenoTrac 4, (Figure 3b) in a nadir position.

### 2.5.5   *Multivariate data analysis*

To infer the onset of senescence for all cultivars (i.e., for the 30 for which color measurements were not taken directly), spectral reflectance data from the passive spectrometer were converted into predicted b-values by multivariate modeling and prediction using the chemometric software package ParLeS 3.1 (Viscarra Rossel, 2008). To accomplish this, a partial least square regression (PLSR) model was established to predict b-values. All data were pre-treated with mean centering to enhance subtle differences among spectra (Viscarra Rossel, 2008). B-values obtained from the ColorEye and the corresponding spectral information from the passive spectrometer (restricted to the spectrum from 400-800 nm) served as variables for the model. All data were split into calibration and validation datasets. Two thirds of all randomly ranked b-values and spectral data were used for the calibration dataset and the remaining one third for the validation dataset. To estimate the performance of the PLSR model, the coefficient of determination ($r^2$) and root mean square error (RMSE) were calculated for both datasets. Additionally, the normalized difference vegetation index (NDVI) was separately determined using the spectrometer data and compared with the associated b-values.

### 2.5.6 Calculating onset of senescence in flag leaves

The onset of senescence in the flag leaves was calculated from the anthesis date (ZS 61), daily growing degree-days, and b-values of each cultivar. The date of anthesis was estimated for each cultivar using the recorded phenological stages. Accumulated growing degree-days (GDD) starting at anthesis were calculated for each cultivar and related to the corresponding b-values. Thus, cultivar-specific progression curves of b-values according to GDDs or thermal time after anthesis (°Cd) were obtained (e.g., see Figure 6).
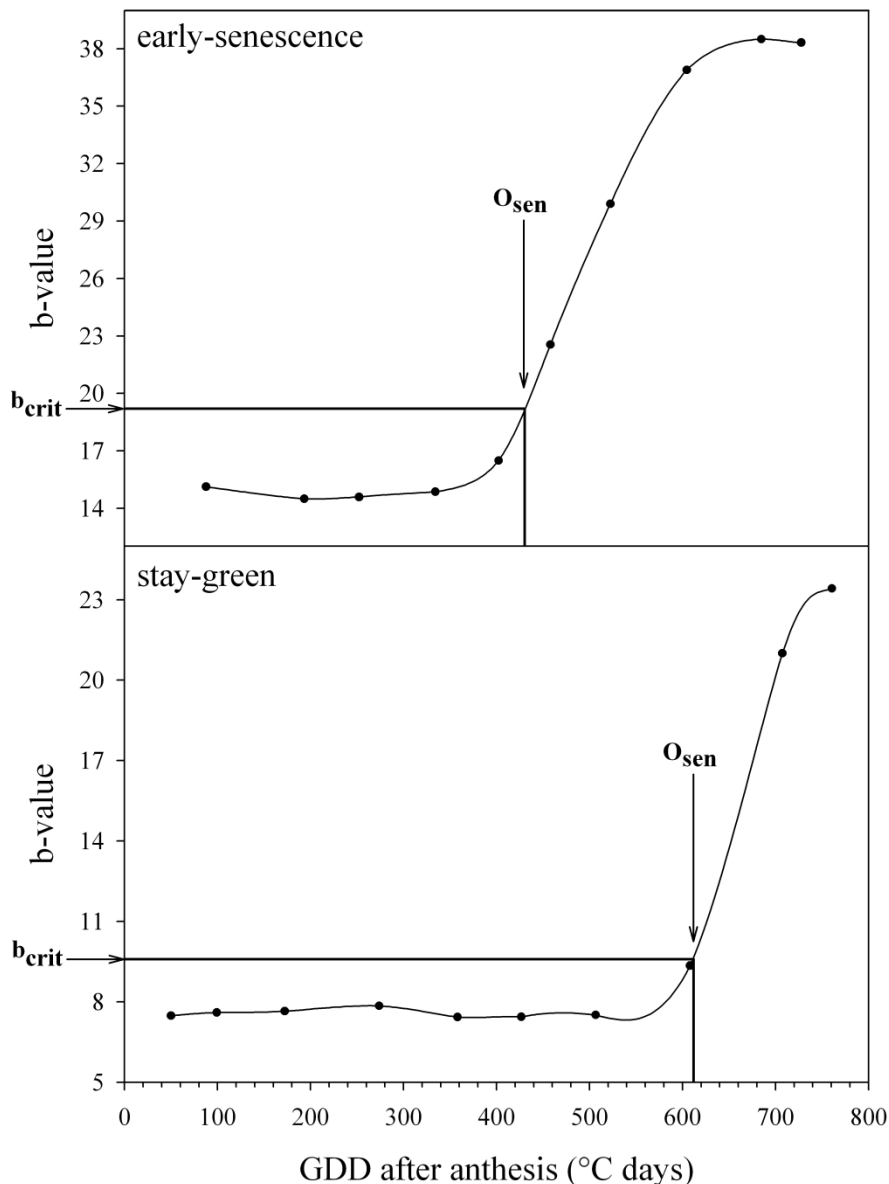


Figure 6: Exemplary calculation of the onset of senescence as the point of intersection between the critical b-value ($b_{crit}$; defined as 1.3 times the minimum b-value) and the corresponding accumulated thermal time or growing degree-days (GDD) after anthesis for an early-senescence and stay-green phenotype.

The onset of senescence ($O_{sen}$) was defined as the point where the b-value reached a level 1.3 times higher than the lowest b-value of the curve. We refer to this point as the critical b-value ($b_{crit}$) (Figure 6). Using this procedure, the cultivar specific onset of senescence could be estimated expressed in GDDs after anthesis.

# 3 Results

## 3.1 Section 1: The performance of active sensors as influenced by measuring distance, device temperature and light intensity

### 3.1.1 Measuring distance

Measurements at sensor-object distances from 10 cm to 200 cm resulted in highly variable spectral reflectance values, with the variability becoming increasingly manifest at the lower measuring distances (Figure 7). In particular, reflectance values obtained from distances lower than 50 to 70 cm – depending on the sensor – showed strong variation for each single wavelength as well as for the resulting indices. A specific range also existed for each sensor, where the respective indices remained nearly stable. As numeric criterion such ranges were ascertained by calculating a 5 % deviation from those heights where no marked changes in the spectral values occurred (GreenSeeker: 90 cm, CropCircle: 50 cm and AFS: 50cm). These ranges were markedly different for each sensor (Table 7), ranging from 70 to 140 cm for the NDVI index (70 to 110 cm for the $R_{770}/R_{650}$ index) calculated from the GreenSeeker reflectance data to 50 to 200 cm for the $R_{760}/R_{730}$ index for the AFS sensor and 30 to 200 cm for the same index for the CropCircle. In comparison to the GreenSeeker´s NDVI, the NDVI calculated with nearly comparable wavelengths for the CropCircle indicates an optimum range from 30 to 200 cm.
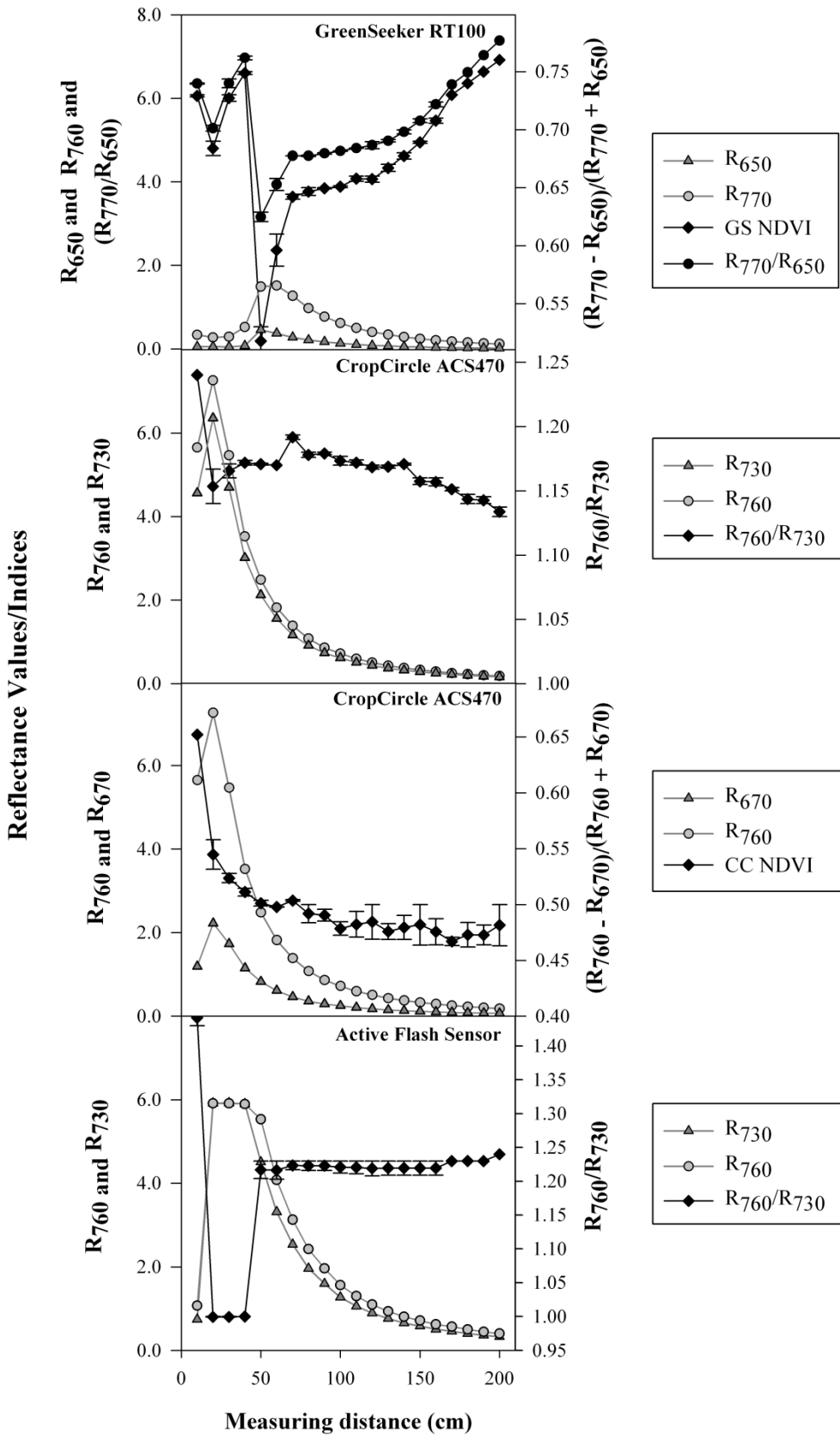
Figure 7: Sensor output values (indices and wavelengths) of three active sensors as a function of measuring distance (10-200 cm) to a green fabric reference target.

### 3.1.2   Device Temperature

An increase in the ambient temperature of the growth chamber led to an increase in the device temperature of each sensor. After approximately 50 minutes, all sensors reached a temperature equilibrium where device temperatures remained nearly stable. The device temperature profile of each sensor showed mainly a linear relationship between the device temperature and sensor output values as reflected in the different indices (Figure 8). Onset and maximum of device temperatures for each sensor can differ considering that also the activity of the sensor itself contribute to the warming of the sensor body. Whereas an increase in the device temperature caused a decrease in the NDVI and $R_{770}/R_{650}$ values for the GreenSeeker (Figure 8a+b), it resulted in an increase in the $R_{760}/R_{730}$ index for both the CropCircle (Figure. 8c) and AFS (Figure 8e). However, the CropCircle´s NDVI seems to be not affected by the device temperature (Figure 8d), because the values remain almost stable. All results were confirmed when repeating the measurements at different measuring heights for each sensor. However the curves for both indices of the CropCircle were parallelly shifted (Figure 8).
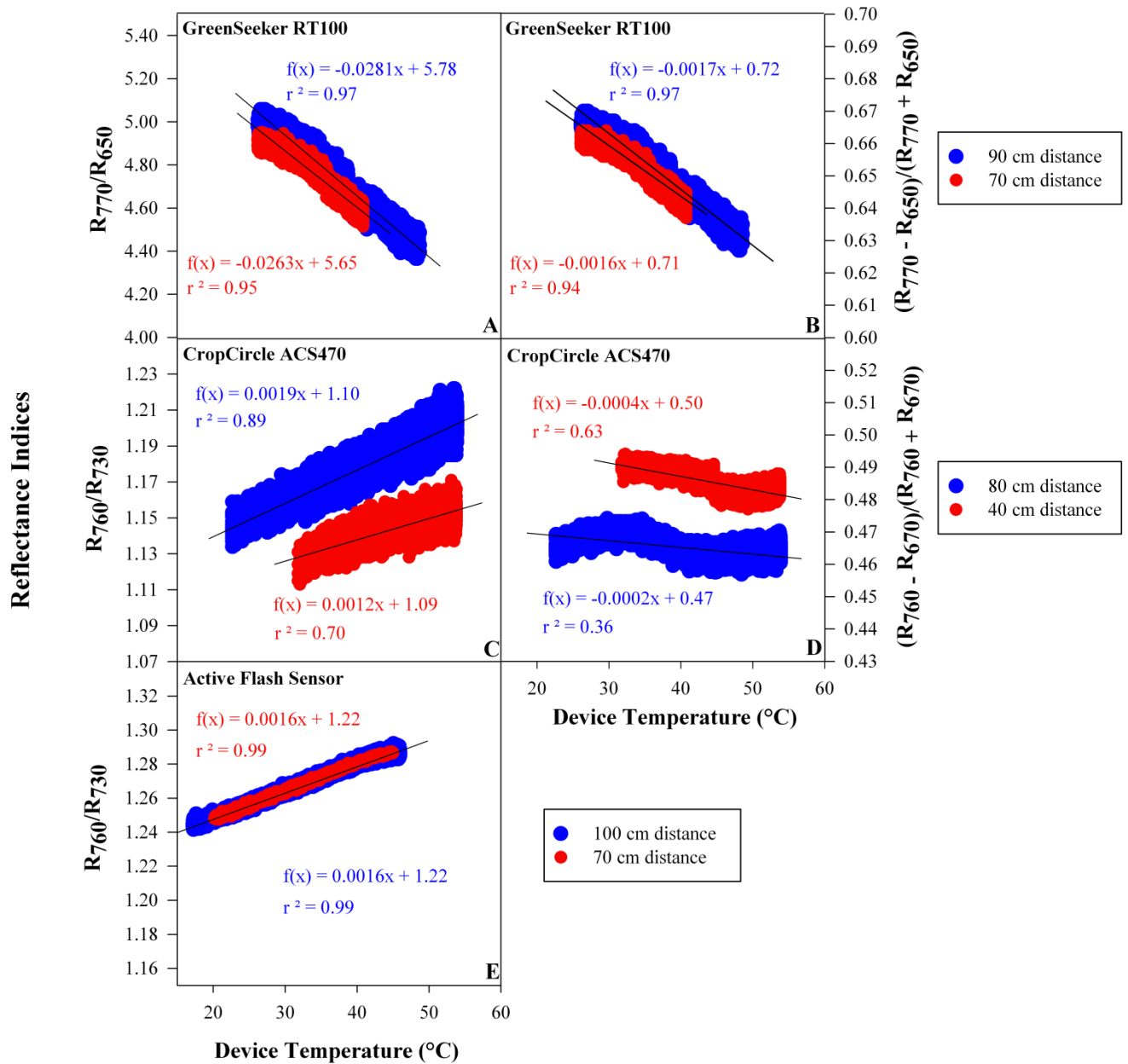
Figure 8: Variation of sensor indices of three active sensors at varying device temperatures.

The temperature effects measured in the growth chamber experiment, were transferred to a winter wheat field experiment with different N supplies to estimate potential error rates when the device temperature shifts by ±1°C.The linear relationship between the indices and the device temperature enables the index variation to be displayed with great accuracy when the device temperature shifted by ±1°C (Table 2).

Table 2: Analysis of a field experiment (Erdle et al. 2011) in which the winter wheat variety "Tommi" (*Triticum aestivum* L.) was fertilized at four different nitrogen application rates (0, 100, 160, and 220 kg N ha$^{-1}$). Each plot was measured with each of the three active sensors and index variations per kg N ha$^{-1}$ were calculated. In combination with index variations per °C device temperature shift, potential error rates in kg N ha$^{-1}$ could be estimated for device temperature variations of 1 °C.

| Sensor device | N application level | Δ Index/ kg N ha$^{-1}$ | Δ Index/°C | Error rate (kg N ha$^{-1}$/°C) |
|---|---|---|---|---|
| GreenSeeker (NDVI) | Δ1: N0 → N100 | 0.00161 | ± 0.0017 | ± 1.06 |
| | Δ2: N100 → N160 | 0.00123 | ± 0.0017 | ± 1.00 |
| | Δ3: N160 → N220 | 0.00005 | ± 0.0017 | ± 34 |
| GreenSeeker ( R$_{770}$/R$_{650}$) | Δ1: N0 → N100 | 0.01090 | ± 0.0281 | ± 2.58 |
| | Δ2: N100 → N160 | 0.01261 | ± 0.0281 | ± 2.23 |
| | Δ3: N160 → N220 | 0.00088 | ± 0.0281 | ± 31.93 |
| CropCircle (NDVI) | Δ1: N0 → N100 | 0.00236 | ± 0.0002 | ± 0.08 |
| | Δ2: N100 → N160 | 0.00206 | ± 0.0002 | ± 0.10 |
| | Δ3: N160 → N220 | 0.00007 | ± 0.0002 | ± 2.86 |
| CropCircle (R$_{760}$/R$_{730}$) | Δ1: N0 → N100 | 0.00431 | ± 0.0019 | ± 0.44 |
| | Δ2: N100 → N160 | 0.00475 | ± 0.0019 | ± 0.4 |
| | Δ3: N160 → N220 | 0.00018 | ± 0.0019 | ± 10.56 |
| AFS (R$_{760}$/R$_{730}$) | Δ1: N0 → N100 | 0.00195 | ± 0.0016 | ± 0.82 |
| | Δ2: N100 → N160 | 0.00248 | ± 0.0016 | ± 0.65 |
| | Δ3: N160 → N220 | 0.00015 | ± 0.0016 | ± 10.67 |

Results from the field experiment (Figure 9) show typical spectral reflectance values of plots that are indicative of low or high nitrogen application rates. Taking into account that the range of reflectance variation between each nitrogen application level is different (Figure 9), it is clear that each N level must be examined separately.
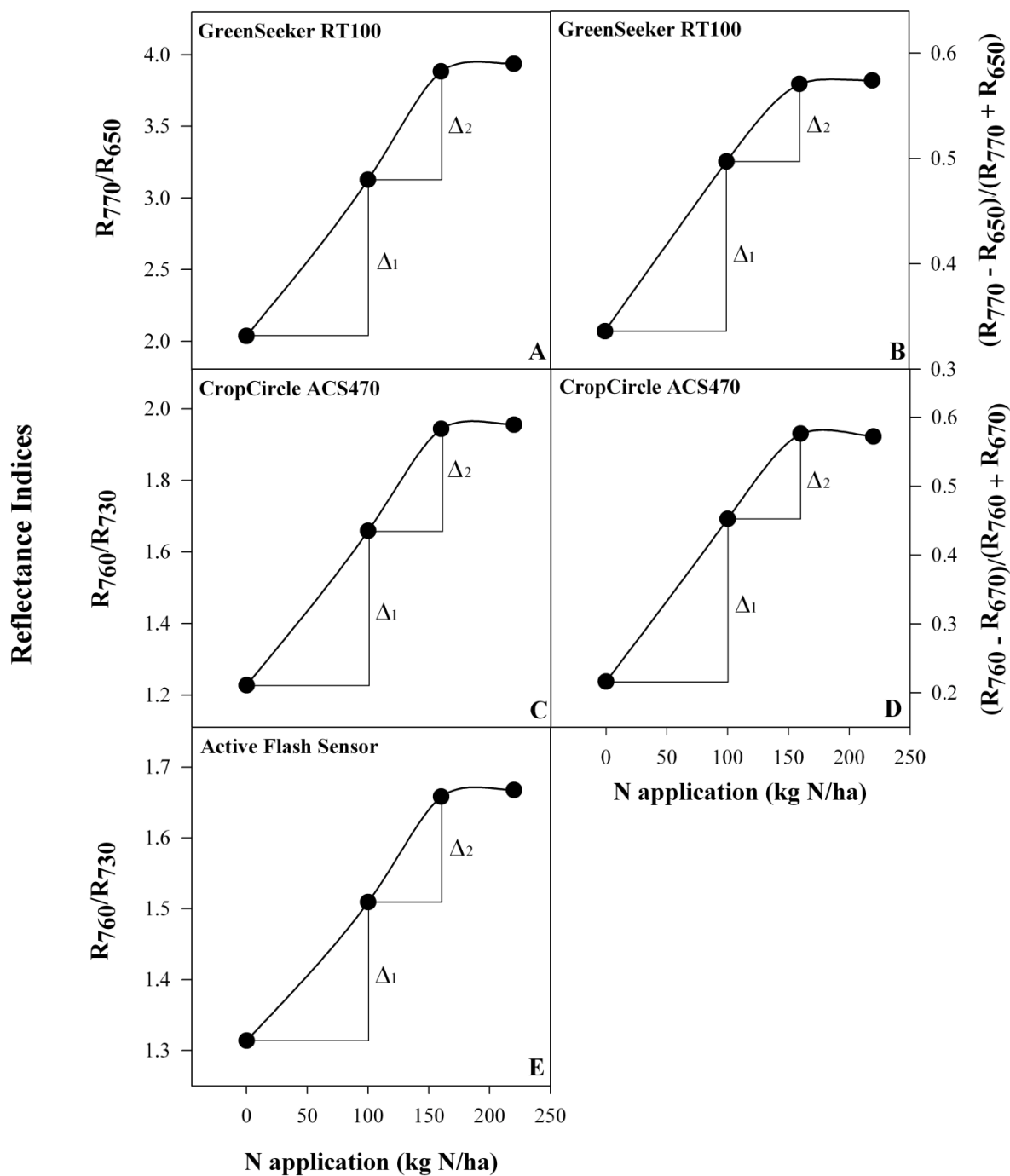
Figure 9: Spectral readings from field experiments with the winter wheat cultivar "Tommi" (*Triticum aestivum L.*) at nitrogen applications of 0, 100, 160, and 220 kg N ha^{-1}, split in three dressings. Differences between the first two pairs of nitrogen application rates are displayed as Δ1 and Δ2.

Although the differences in the spectral index values from the 0 N, 100 N, and 160 N treatments are strong, the index values are not significantly different due to the saturation effects in plots receiving high amounts of nitrogen (160-220 kg N ha$^{-1}$). By dividing the device temperature shift of $\pm 1°C$ (Table 2) by the mean index variation per kg N ha$^{-1}$ calculated in relation to the index differences between each N level ($\Delta_1$, $\Delta_2$) (Table 2), it can be shown that for each °C change in device temperature, the reflectance data would produce nitrogen errors rates (Table 2) of approximately 1.06 kg N and 1.00 kg N for the GreenSeeker NDVI, 2.58 kg N and 2.23 kg N for the GreenSeeker $R_{770}/R_{650}$, 0.08 kg N and 0.1 kg N for the CropCircle NDVI, 0.44 kg N and 0.4 kg N for the CropCircle $R_{760}/R_{730}$, and 0.82 kg N and 0.65 kg N for the AFS $R_{760}/R_{730}$ index, up to a nitrogen application level of 0-100 kg N ha$^{-1}$, respectively 100-160 kg N ha$^{-1}$. Calculating error rates for spectral data of nitrogen levels above 160 kg N is not of relevance because the index response cannot differ between such well fertilized canopies (Figure 9), and even a small change in temperature would lead to enormous misinterpretations in the applied doses of nitrogen. A device temperature effect on the sensor´s accuracy could not be shown for the CropCircle´s NDVI because this index reacts only slightly, if at all, to increasing temperatures.

### 3.1.3 Light Intensity

No external effect of different ambient light intensities was observed (Figure 10) and only marginal and very small variations were detectable and may occur due to scattering of the sensor values. However the $R_{760}/R_{730}$ index, derived by the AFS, changed slightly under low light intensity.
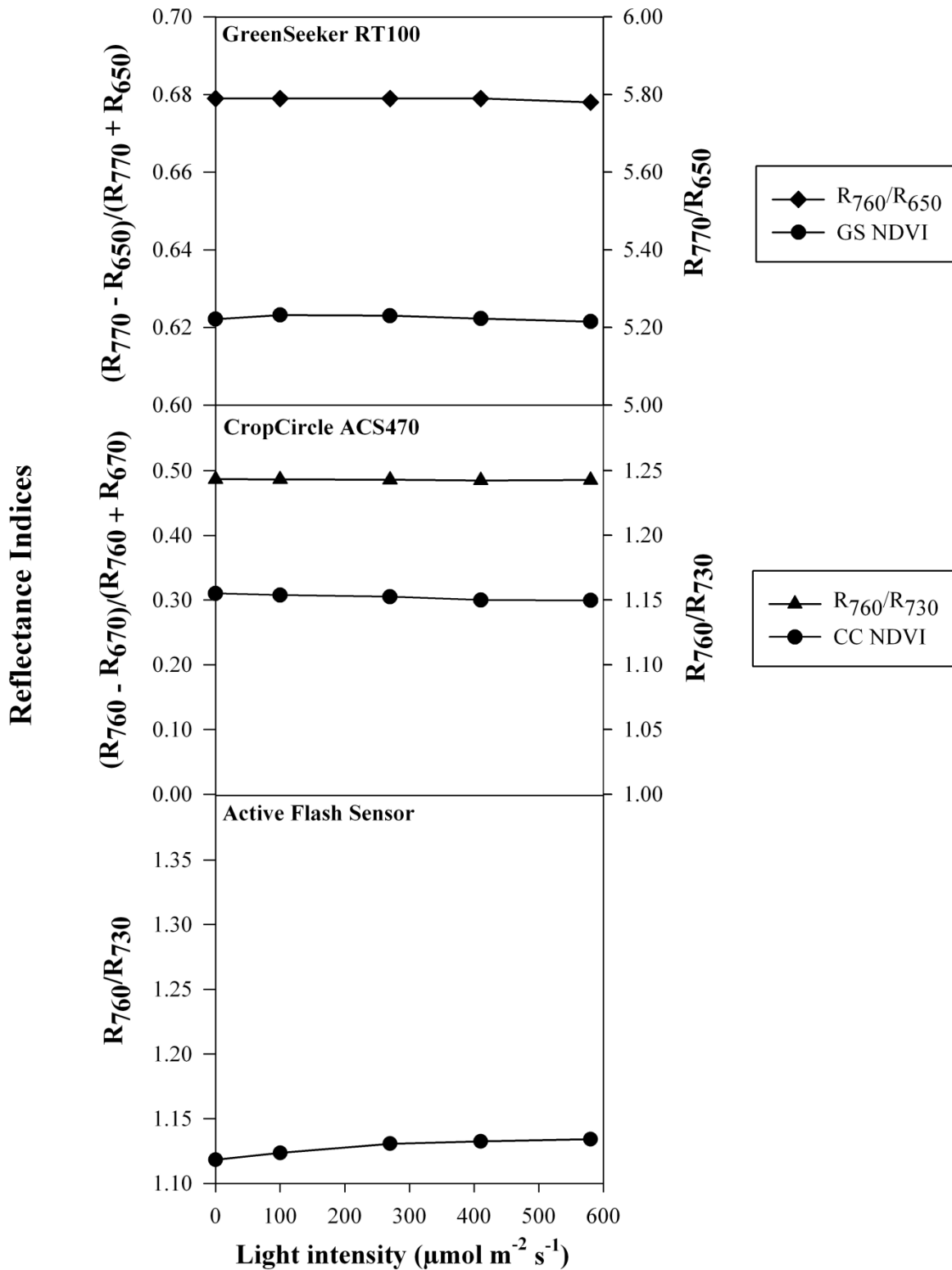
Figure 10: Spectral indices of three active sensors under varying light intensities.

3.2 *Section 2*: Reflectance characteristics of different plant components in a winter wheat experiment at two different development stages

*3.2.1 Distribution of dry matter and N content*

Samplings of all plant components were separately taken and analyzed for fresh weight (FW), dry matter content (DM), dry weight (DW), N concentration and N content (Table 3). Mean values and standard deviations indicated differences between each component and development stages. To assess the ability of active sensors to detect changes in biomass, after removing segmentally the different plant components, dry weight and N content were analyzed in detail.

Table 3: Fresh weight (FW), dry matter content (DM), dry weight (DW), N concentration (N) and N content of different plant components at ZS 61 and 75. Mean values and standard deviation are indicated.

| | | FW (g/container) | | DM (%) | | DW (g/container) | | N (%) | | N content (g/container) | |
|---|---|---|---|---|---|---|---|---|---|---|---|
| | Lower leaf layers | 420.83 | (± 61.0) | 20.07 | (± 0.02) | 84.54 | (± 13.4) | 3.40 | (± 0.16) | 2.88 | (± 0.5) |
| | Middle leaf layers | 908.23 | (± 98.6) | 19.65 | (± 0.01) | 178.19 | (± 15.2) | 4.79 | (± 0.19) | 8.56 | (± 1.0) |
| ZS 61 | Flag leaves | 265.92 | (± 19.7) | 26.52 | (± 0.00) | 70.51 | (± 4.3) | 4.82 | (± 0.09) | 3.39 | (± 0.2) |
| | Stems | 623.83 | (± 52.7) | 19.98 | (± 0.01) | 124.65 | (± 12.1) | 2.52 | (± 0.07) | 3.14 | (± 0.3) |
| | Ears | 2150.52 | (± 102.3) | 19.29 | (± 0.01) | 414.45 | (± 11.3) | 2.13 | (± 0.17) | 8.84 | (± 0.6) |
| | | | | | | | | | | | |
| | Lower leaf layers | 191.52 | (± 21.3) | 57.31 | (± 0.07) | 110.36 | (± 22.4) | 2.01 | (± 0.20) | 2.26 | (± 0.64) |
| | Middle leaf layers | 541.87 | (± 48.0) | 26.78 | (± 0.02) | 145.19 | (± 14.4) | 3.64 | (± 0.22) | 5.30 | (± 0.78) |
| ZS 75 | Flag leaves | 225.18 | (± 34.8) | 30.60 | (± 0.01) | 68.65 | (± 9.1) | 4.65 | (± 0.38) | 3.16 | (± 0.21) |
| | Stems | 1276.03 | (± 79.9) | 37.07 | (± 0.02) | 474.41 | (± 52.3) | 1.97 | (± 0.06) | 9.34 | (± 0.79) |
| | Ears | 1876.17 | (± 131.7) | 35.55 | (± 0.01) | 667.13 | (± 45.0) | 1.04 | (± 0.09) | 6.90 | (± 0.61) |

The distribution of dry weight between the different plant components was comparable within each development stage at anthesis (ZS61) and grain filling (ZS75) as shown in Figure 11 and Table 3. The middle leaf layers represent the largest dry weight in comparison to the contribution of lower leaves and flag leaves. The largest amount of dry weight was found in stems at both development stages and in the ears during grain filling. Comparing dry weight samplings at anthesis and grain filling only little changes in lower leaf layers were observed. However stem and ear dry weight clearly increased.
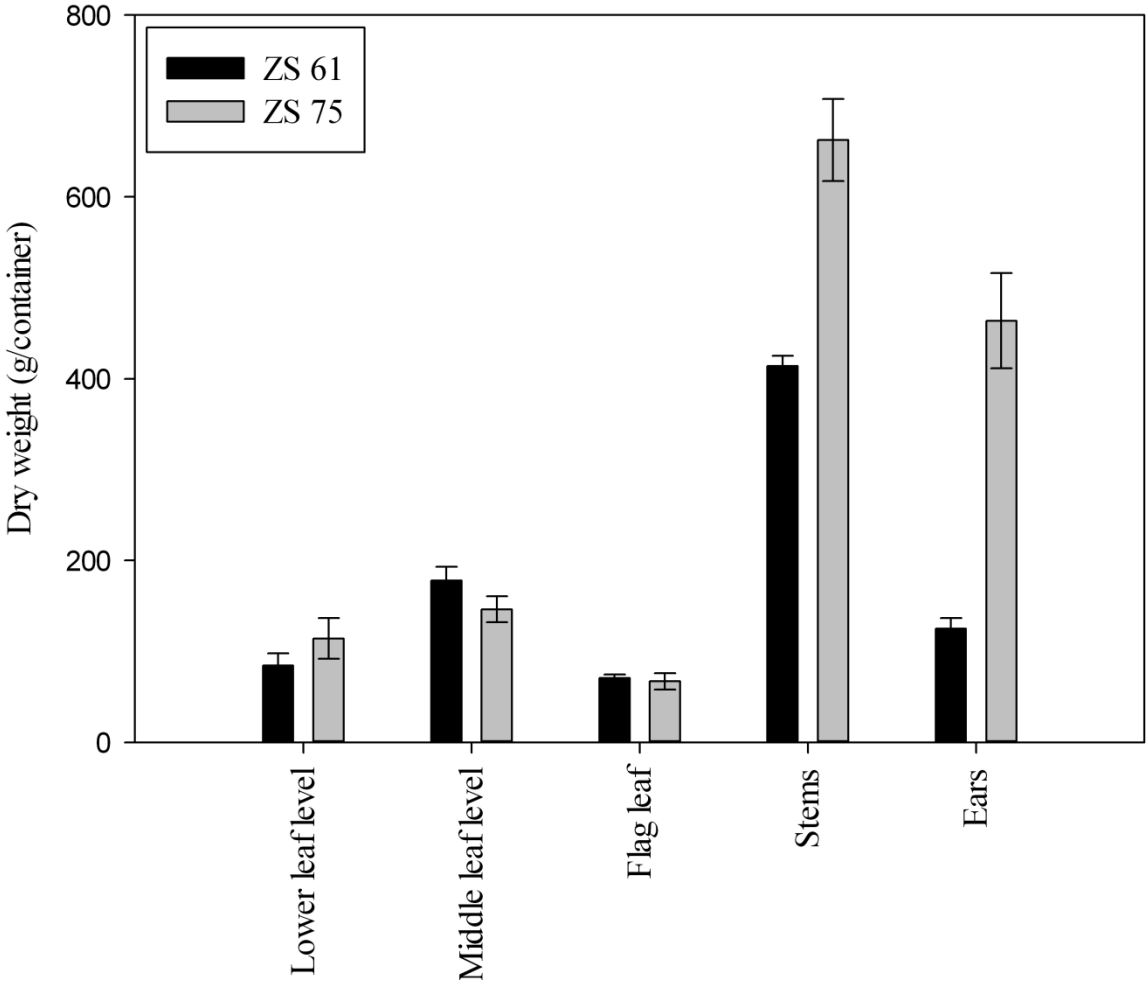


Figure 11: Dry weight of each plant component in g/container at ZS 61 and ZS 75. Standard deviations are indicated by error bars.

At anthesis N was stored mainly in middle leaf layers and stems (Figure 12) and the N content in lower leaf layers, the flag leaves and ears was significantly lower. At grain filling the N content in the middle leaf layers and stems decreased whereas N in the lower leaf layers and the flag leaves remained stable. Only the N content in ears increased considerably.
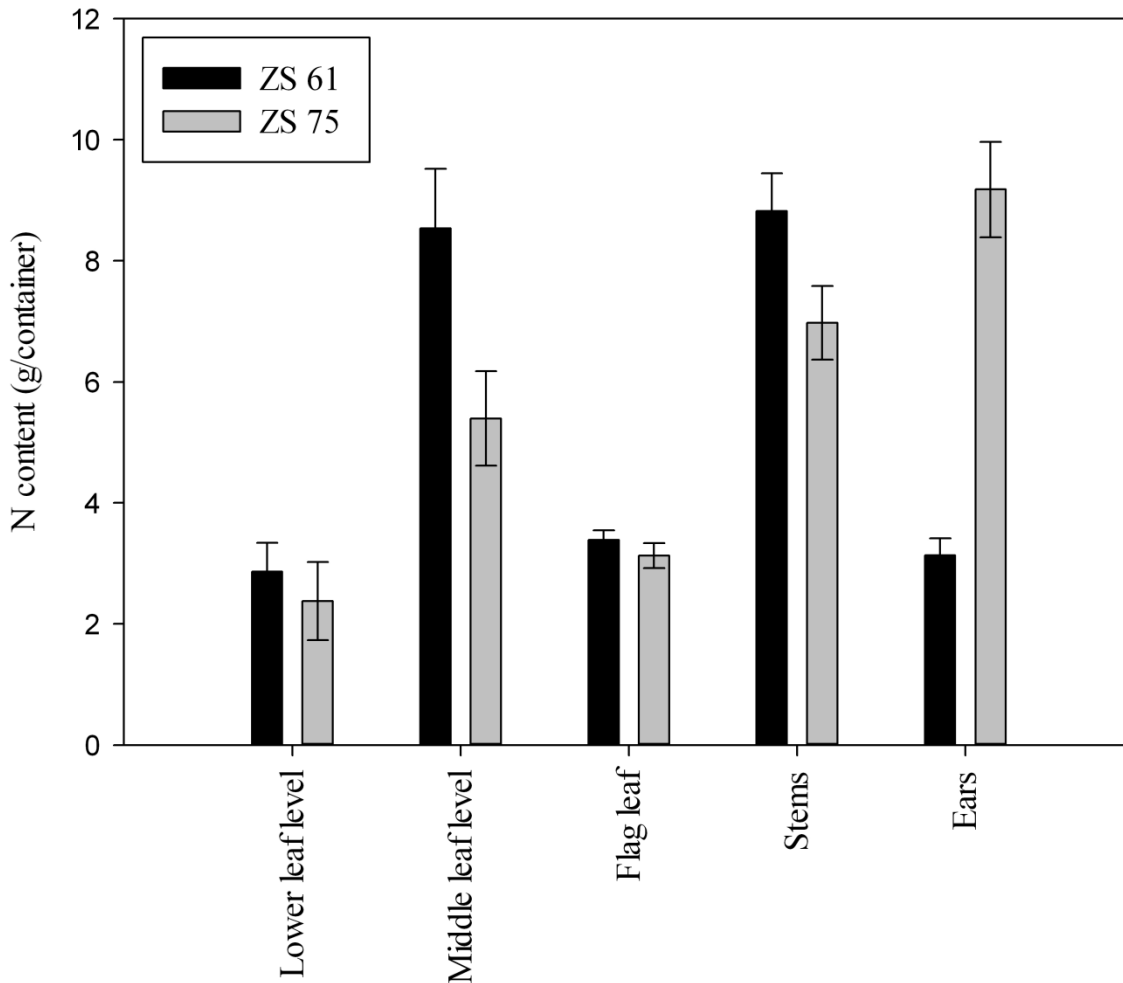
Figure 12: N content of each plant component in g/container at ZS 61 and ZS 75. Standard deviation is indicated by error bars.

### 3.2.2 *Spectral reflectance of different plant components*

The stepwise removal of plant components, indicated as R0 (whole plant), R1 removal of lower leaves, R2 (removal of middle leaves), R3 (removal of flag leaves), R4 (removal of ears) and R5 (removal of stems), differently influenced the reflectance intensities of single wavelengths and spectral indices (Figure 13).

The spectral reflectance by the GreenSeeker´s wavelengths 670 nm and 760 nm was differently affected by the removal of plant biomass. At 670 nm only marginal changes in reflectance intensities occurred at ZS 61 when stems were removed, and at ZS 75 after removal of flag leaves and stems. In comparison, at 760 nm the reflectance decreased rapidly at both development stages when middle leaf layers and flag leaves were removed and almost no effect on reflectance could be observed after removal of lower leaf layers, ears and stems.

The reflectance intensity of the CropCircle´s wavelengths 670, 730 and 760 nm was significantly higher at ZS 61 than at ZS 75. At 670 nm each removal step increased the reflectance similar. Only the removal of ears had no effect on the reflectance intensity. In comparison the reflectance at 730 and 760 nm was increased after removing the lower leaf layers before it decreased rapidly. Removal of middle leaf layers and flag leaves strongly affected the reflectance of these wavelengths.

In contrast to the CropCircle, the reflectance of the AFS wavelengths at 730 and 760 nm were higher at ZS 75 during each removal step and decreased rapidly after removal of lower and middle leaf layers. However the reflectance increased slightly after removing the stems.

Depending on the availability of the sensor specific wavelengths, different spectral indices ($R_{760}/R_{730}$, $R_{760}/R_{670}$ and NDVI) could be calculated which have frequently been applied in several scientific reports to indicate changes in biomass and N-uptake.

The index $R_{760}/R_{730}$ was calculated for the CropCircle and AFS, $R_{760}/R_{670}$ and NDVI for the CropCircle and GreenSeeker (Figure 13). Generally all indices were comparably affected by each removal step among all sensors. The index $R_{760}/R_{730}$ for CropCircle and AFS did not differ significantly between ZS 61 and ZS 75 and changed mainly after removal of the middle leaf layers and flag leaves. Removal of lower leaf layers, stems and ears showed nearly no effect on index values. The index values for $R_{760}/R_{670}$ of the CropCircle and GreenSeeker decreased also significantly after removing the middle leaf layers and flag leaves. However in the case of the GreenSeeker the index increased at ZS 61 and decreased at ZS 75 after removal of the lower leaf layers. In comparison to the whole value range of this index, almost no effect could be observed after removing stems and ears.

The NDVI of the CropCircle and GreenSeeker was the only index in this experiment, which reacted sensitively to the removal of ears and stems at both development stages. Lower leaf layers seemed to have no effect on the NDVI, but removal of middle leaf layers and particularly flag leafs affected the index values considerably.

Considering all changes in single wavelengths reflectance and index values, it is obvious that the middle leaf layers and flag leaves had the largest influence on active sensor readings.
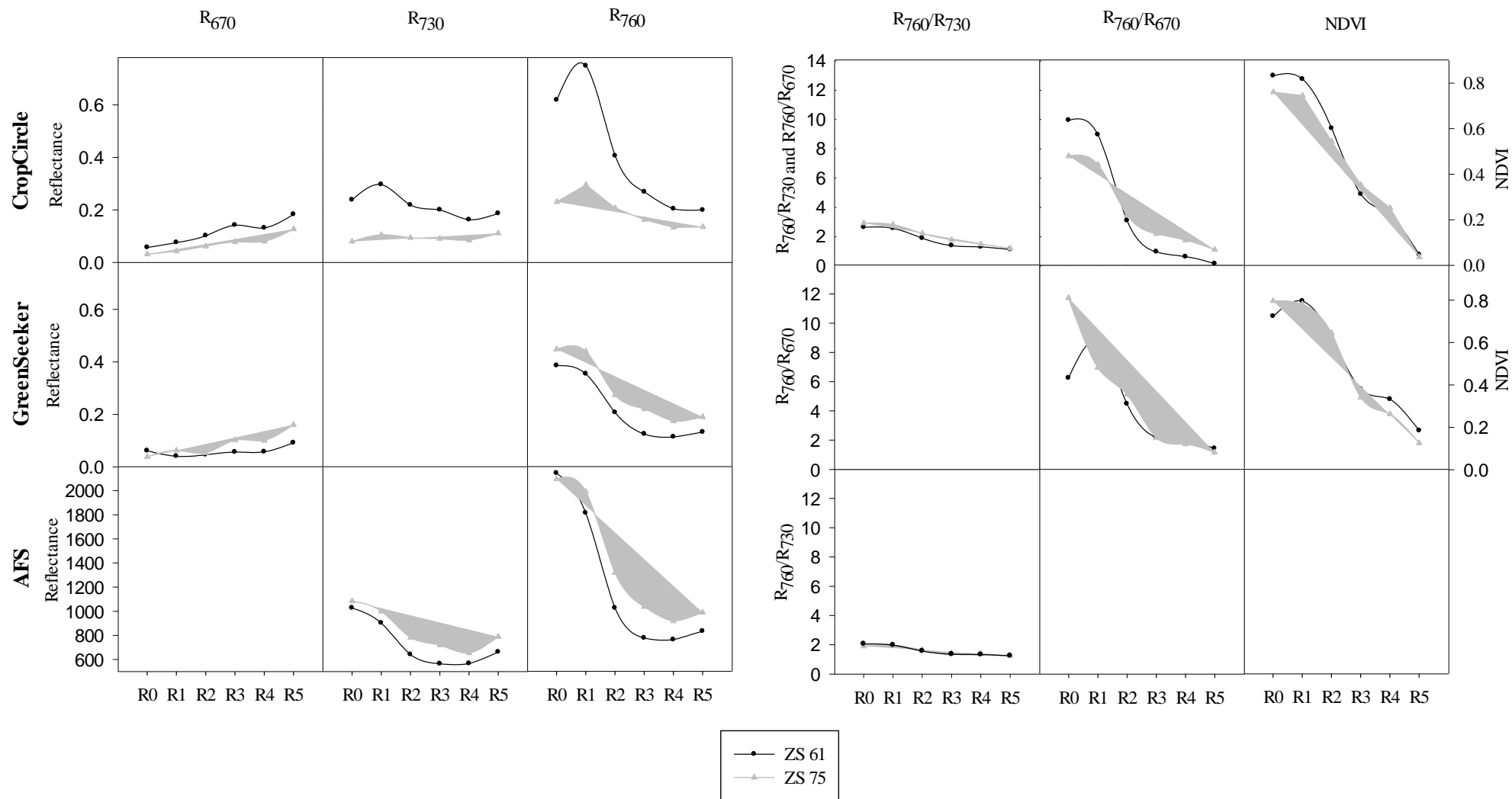
Figure 13: Changes in single wavelength reflectance and index values of the CropCircle, GreenSeeker and AFS after removing lower leaf layers (R1), middle leaf layers (R2), flag leaves (R3), ears (R4) and stems (R5). R0 represents the entire plant.

*3.2.3 Relationships between sensor readings and different plant components*

The relationships between sensor readings and the dry weight or N content were compared (Table 4 and 5) to observe whether the change in reflectance values according to the different removal step was predominantly affected by the amount of dry weight or N content. Relationships were calculated by correlating sensor readings at each removal step with the amount of remaining dry weight or the N content.

Reflectance at 670 nm responded significantly to the dry weight as well as the N content. Only in the case of the GreenSeeker no significant relationship existed between 670 nm and both parameters.

At 730 nm no significant relationship for the CropCircle and AFS could be found. The wavelength 760 nm, which was available for all sensors, showed significant relationships only for the N content. The index $R_{760}/R_{730}$ showed the most significant relationship with N content for all sensors. In contrast the correlations between $R_{760}/R_{730}$ and dry weight were less significant. The index $R_{760}/R_{670}$ poorly reflected the dry weight. Only in the case of the CropCircle a slightly significant relationship could be found at ZS 61. The relationships between this index and the N content were more significant, especially for the CropCircle at ZS 61. The NDVI seemed to be suitable to measure accurately the dry weight as well as the N content. Apart from the GreenSeeker´s NDVI at ZS 75 all sensors showed highly significant relationships between the NDVI and the dry weight or the N content. All relationships are summarized in Table 4 and 5.

Table 4: Coefficients of determination for the relationships between single wavelengths/indices and the dry weight of each plant component. Significance at $p \leq 0.05$ and $p \leq 0.01$ is indicated by * and **.

| | | $R_{670}$ | $R_{730}$ | $R_{760}$ | $R_{760}/R_{730}$ | $R_{760}/R_{670}$ | NDVI |
|---|---|---|---|---|---|---|---|
| | CropCircle | **0.91**\*\* | 0.47 | 0.67\* | 0.78\* | 0.68\* | **0.95**\*\* |
| ZS 61 | GreenSeeker | 0.63 | | 0.62 | | 0.65 | **0.85**\*\* |
| | AFS | | 0.41 | 0.57 | 0.74\* | | |
| | CropCircle | **0.91**\*\* | 0.28 | 0.56 | 0.79\* | 0.62 | **0.87**\*\* |
| ZS 75 | GreenSeeker | **0.87**\*\* | | 0.56 | | 0.56 | 0.79\* |
| | AFS | | 0.31 | 0.52 | 0.72\* | | |

Table 5: Coefficients of determination for the relationships between single wavelengths/indices and N content of each plant component. Significance at $p \leq 0.05$ and $p \leq 0.01$ is indicated by * and **.

| | | $R_{670}$ | $R_{730}$ | $R_{760}$ | $R_{760}/R_{670}$ | $R_{760}/R_{730}$ | NDVI |
|---|---|---|---|---|---|---|---|
| ZS 61 | CropCircle | **0.96**** | 0.61 | 0.82* | **0.92**** | **0.86**** | **0.87**** |
| | GreenSeeker | 0.48 | | 0.81* | | 0.78* | **0.91**** |
| | AFS | | 0.63 | 0.77* | **0.90**** | | |
| ZS 75 | CropCircle | **0.92**** | 0.16 | 0.73* | **0.93**** | 0.80* | **0.96**** |
| | GreenSeeker | **0.86**** | | 0.77* | | 0.74* | **0.91**** |
| | AFS | | 0.53 | 0.73* | **0.87**** | | |

## 3.3 *Section 3*: High-throughput phenotyping early plant vigour of winter wheat

### 3.3.1 *Pixel analysis and spectral reflectance measurements*

Because the photos were taken under cloudy conditions, shadows within the pictures could be completely avoided. The analysis of the RAGP in each photo (Figure 14) resulted in highly different means between 2011 and 2012 (Table 6). The RAGP of all 50 cultivars was 63.1 in 2011 and 27.0 in 2012. Thus, photos which were taken on April 15 in 2011 showed more than double RAGP than photos taken on April 4 in 2012. However, the mean values for "greenness" of all cultivars were in broad ranges from 29.4 (RCATF TF 174/1C) to 76.9 (Colonia) in 2011 and from 18.1 (Timber) to 39.2 (Kerubino) in 2012.

Table 6: Results of the relative amount of green pixels derived from digital images and EPVI values for 2011 and 2012, with each value representing the average of four replications. Cultivar rankings of RAGP and EPVI for 2011 and 2012 derived by the Student-Newman-Keuls test are indicated at $p \leq 0.05$.

| Cultivar | 2011 | | 2012 | |
|---|---|---|---|---|
| | Relative amount of green pixels | EPVI | Relative amount of green pixels | EPVI |
| W00984.2 | 64.2 [a,b,c,d,e,f,g,h] | 0.63 [a,b,c,d,e,f,g] | 26.6 [a] | 0.41 [a,b,c,d,e] |
| Alcazar | 60.9 [a,b,c,d,e,f,g,h] | 0.59 [a,b,c,d,e,f] | 18.3 [a] | 0.33 [a,b,c] |
| Magnifik | 65.1 [a,b,c,d,e,f,g,h] | 0.70 [c,d,e,f,g] | 24.7 [a] | 0.39 [a,b,c,d,e] |
| Figura | 62.3 [a,b,c,d,e,f,g,h] | 0.61 [a,b,c,d,e,f,g] | 26.2 [a] | 0.39 [a,b,c,d,e] |
| Oakley | 61.1 [a,b,c,d,e,f,g,h] | 0.65 [a,b,c,d,e,f,g] | 21.0 [a] | 0.35 [a,b,c,d,e] |
| Timber | 53.6 [a,b,c,d] | 0.57 [a,b,c] | 18.1 [a] | 0.33 [a] |
| Liman R | 53.4 [a,b,c] | 0.58 [a,b,c,d,e] | 19.6 [a] | 0.33 [a,b,c] |
| Arina | 63.3 [a,b,c,d,e,f,g,h] | 0.60 [a,b,c,d,e,f] | 21.7 [a] | 0.36 [a,b,c,d,e] |
| CH-111.13716 | 59.3 [a,b,c,d,e,f,g] | 0.63 [a,b,c,d,e,f,g] | 24.8 [a] | 0.39 [a,b,c,d,e] |
| CH-111.13930 | 58.4 [a,b,c,d,e,f] | 0.59 [a,b,c,d,e,f] | 18.8 [a] | 0.31 [a,b,c] |
| CH-111.13521 | 64.9 [a,b,c,d,e,f,g,h] | 0.63 [a,b,c,d,e,f,g] | 29.4 [a] | 0.40 [a,b,c,d,e] |
| Mirage | 57.5 [a,b,c,d,e,f] | 0.61 [a,b,c,d,e,f,g] | 22.8 [a] | 0.35 [a,b,c,d,e] |
| Piotta | 60.3 [a,b,c,d,e,f,g,h] | 0.65 [a,b,c,d,e,f,g] | 25.4 [a] | 0.36 [a,b,c,d,e] |
| Alchemy | 63.7 [a,b,c,d,e,f,g,h] | 0.67 [b,c,d,e,f,g] | 21.7 [a] | 0.37 [a,b,c,d,e] |
| CH-194.10518 | 63.2 [a,b,c,d,e,f,g,h] | 0.60 [a,b,c,d,e,f] | 23.0 [a] | 0.36 [a,b,c,d,e] |
| Cubus | 72.8 [f,g,h] | 0.72 [c,d,e,f,g] | 32.0 [a] | 0.46 [d,e] |
| Türkis | 71.0 [d,e,f,g,h] | 0.71 [c,d,e,f,g] | 30.0 [a] | 0.40 [a,b,c,d,e] |
| Akteur | 62.4 [a,b,c,d,e,f,g,h] | 0.61 [a,b,c,d,e,f,g] | 27.9 [a] | 0.43 [a,b,c,d,e] |
| Hermann | 68.9 [b,c,d,e,f,g,h] | 0.68 [b,c,d,e,f,g] | 27.7 [a] | 0.41 [a,b,c,d,e] |
| Impression | 58.2 [a,b,c,d,e,f] | 0.63 [a,b,c,d,e,f,g] | 28.9 [a] | 0.42 [a,b,c,d,e] |
| Schamane | 71.6 [e,f,g,h] | 0.68 [b,c,d,e,f,g] | 31.0 [a] | 0.41 [c,d,e] |
| Manager | 62.1 [a,b,c,d,e,f,g,h] | 0.69 [b,c,d,e,f,g] | 24.1 [a] | 0.37 [a,b,c,d,e] |
| Potenzial | 67.3 [a,b,c,d,e,f,g,h] | 0.68 [b,c,d,e,f,g] | 26.0 [a] | 0.40 [a,b,c,d,e] |
| Julius | 66.2 [a,b,c,d,e,f,g,h] | 0.64 [a,b,c,d,e,f,g] | 29.3 [a] | 0.39 [a,b,c,d,e] |
| Pamier | 51.8 [a,b] | 0.52 [a] | 22.4 [a] | 0.34 [a,b,c,d] |
| JB Asano | 72.9 [f,g,h] | 0.74 [e,f,g] | 29.0 [a] | 0.44 [b,c,d,e] |

| | | | | |
|---|---|---|---|---|
| Kredo | 56.1 [a,b,c,d,e,f] | 0.58 [a,b,c,d] | 20.9 [a] | 0.32 [a,b] |
| Famulus | 64.1 [a,b,c,d,e,f,g,h] | 0.67 [b,c,d,e,f,g] | 22.9 [a] | 0.36 [a,b,c,d,e] |
| Genius | 58.8 [a,b,c,d,e,f,g] | 0.59 [a,b,c,d,e,f] | 23.3 [a] | 0.35 [a,b,c,d,e] |
| Linus | 51.6 [a] | 0.55 [a,b] | 22.9 [a] | 0.33 [a,b,c] |
| Meister | 54.8 [a,b,c,d,e] | 0.58 [a,b,c,d] | 27.2 [a] | 0.40 [a,b,c,d,e] |
| Orcas | 54.8 [a,b,c,d,e] | 0.58 [a,b,c,d,e,f] | 23.2 [a] | 0.34 [a,b,c,d,e] |
| Muskat | 73.5 [f,g,h] | 0.71 [c,d,e,f,g] | 30.9 [a] | 0.39 [a,b,c,d,e] |
| Kerubino | 75.9 [g,h] | 0.74 [f,g] | 39.2 [a] | 0.48 [e] |
| KWS Erasmus | 63.8 [a,b,c,d,e,f,g,h] | 0.63 [a,b,c,d,e,f,g] | 29.4 [a] | 0.41 [a,b,c,d,e] |
| Matrix | 70.3 [c,d,e,f,g,h] | 0.73 [d,e,f,g] | 34.3 [a] | 0.42 [a,b,c,d,e] |
| Florian | 60.9 [a,b,c,d,e,f,g,h] | 0.64 [a,b,c,d,e,f,g] | 27.8 [a] | 0.38 [a,b,c,d,e] |
| Sailor | 60.8 [a,b,c,d,e,f,g,h] | 0.64 [a,b,c,d,e,f,g] | 30.9 [a] | 0.42 [a,b,c,d,e] |
| Norin | 58.3 [a,b,c,d,e,f] | 0.64 [a,b,c,d,e,f,g] | 27.1 [a] | 0.37 [a,b,c,d,e] |
| Komet | 72.9 [f,g,h] | 0.72 [c,d,e,f,g] | 34.0 [a] | 0.45 [a,b,c,d,e] |
| Colonia | 76.9 [h] | 0.75 [g] | 37.7 [a] | 0.45 [b,c,d,e] |
| Tabasco | 70.2 [c,d,e,f,g,h] | 0.71 [c,d,e,f,g] | 33.1 [a] | 0.45 [c,d,e] |
| Sophytra | 63.9 [a,b,c,d,e,f,g,h] | 0.66 [a,b,c,d,e,f,g] | 26.8 [a] | 0.38 [a,b,c,d,e] |
| Akratos | 64.8 [a,b,c,d,e,f,g,h] | 0.64 [a,b,c,d,e,f,g] | 28.8 [a] | 0.39 [a,b,c,d,e] |
| Sokrates | 60.6 [a,b,c,d,e,f,g,h] | 0.63 [a,b,c,d,e,f,g] | 28.5 [a] | 0.40 [a,b,c,d,e] |
| Winnetou | 66.2 [a,b,c,d,e,f,g,h] | 0.72 [c,d,e,f,g] | 32.5 [a] | 0.44 [c,d,e] |
| KWS Bogus | 62.2 [a,b,c,d,e,f,g,h] | 0.67 [b,c,d,e,f,g] | 32.9 [a] | 0.44 [b,c,d,e] |
| Wilson | 70.4 [c,d,e,f,g,h] | 0.73 [d,e,f,g] | 29.4 [a] | 0.42 [a,b,c,d,e] |
| Glaucus | 69.1 [c,d,e,f,g,h] | 0.71 [c,d,e,f,g] | 30.4 [a] | 0.44 [b,c,d,e] |
| SH 401 | 68.7 [a,b,c,d,e,f,g,h] | 0.68 [b,c,d,e,f,g] | 26.9 [a] | 0.39 [a,b,c,d,e] |
| | | | | |
| Mean | 63.7 | 0.65 | 27.0 | 0.39 |

The visualization of the green pixel analysis with R statistics showed that only plant parts were retrieved by the software as green pixels (Figure 14).
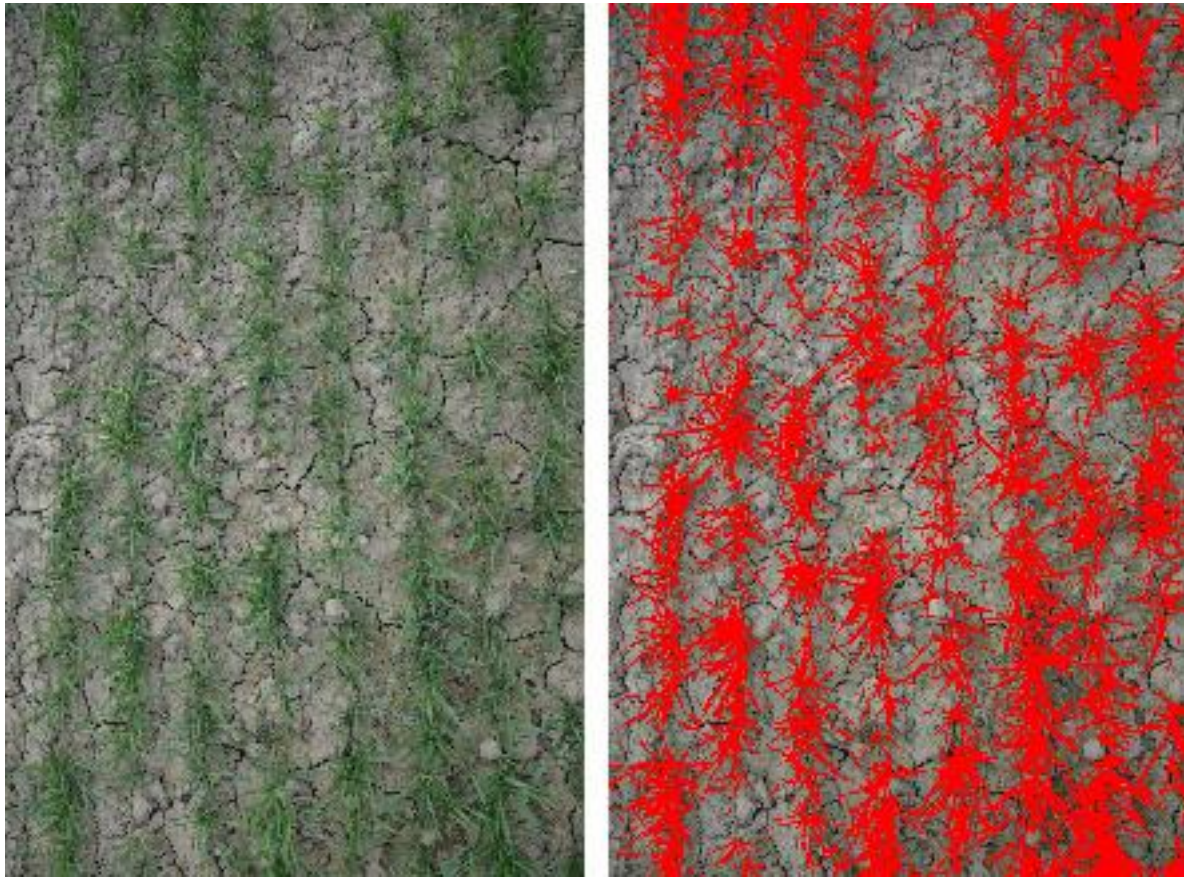


Figure 14: Analysis of the amount of green pixels (RAGP) in digital images of winter wheat plots. a) Original digital image of wheat plants at the tillering stage; b) Identical image after selecting green pixels by using R statistics.

The EPVI measured by the HAFS also indicated a high range of values. The values are non-dimensional and illustrate the relative differences between cultivars. Plots with higher or lower biomass or plant vigour respectively, showed a high differentiation in their spectral reflectance values. Figure 15 shows the reflectance curves of cultivar "Colonia" with high early plant vigour (i.e., RAGP), cultivar "Linus" with low early plant vigour (i.e., lower RAGP) and bare soil. The cultivar with the higher early plant vigour shows a higher light absorption than the cultivar with lower biomass and soil except in spectral regions higher than 725 nm. It is obvious that weak early plant vigour results in alignment of the spectral curve to that of bare soil.

Due to the automation of the sensor system, all 200 plots (50 cultivars x 4 replications) could be measured in 75 min at a driving speed of 2.8 km h$^{-1}$ (0.78 m s$^{-1}$).
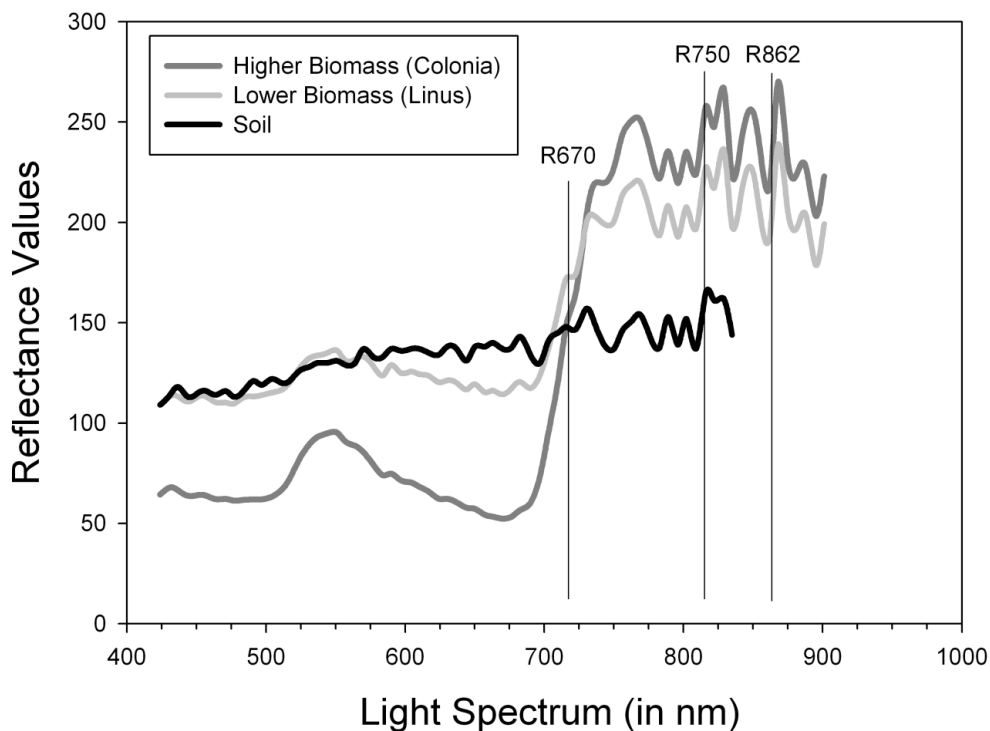
Figure 15: Spectral reflectance curves of winter wheat plots with weak ( = reduced biomass) and strong early plant vigour ( = higher biomass) and bare soil. The selected wavelengths are components of the EPVI (R750-R670)/R862.

### 3.3.2 Cultivar specific variation of the early plant vigour

Plot means of pixel analysis and the EPVI for 2011 and 2012 were correlated (Figure XX16) to observe if significant relationships in early plant vigour between both years existed, and to confirm that early plant vigour is a cultivar specific trait. A significant correlation between pixel analysis ($r^2$ of 0.55) and the EPVI ($r^2$ of 0.57) in 2011 and 2012 could be observed. Additionally an analysis of variance (Table 7) and the Student-Newman-Keuls test (Table 6) showed a significant cultivar effect on RAGP and EPVI for each single year.

Table 7: Oneway ANOVA results (*F*-values and its significance) for the cultivar effect. Significance at $p \leq 0.05$ is indicated by **

| Cultivar effect as | 2011 | | 2012 | |
|---|---|---|---|---|
| source of variation | dF | *F*-value | dF | *F*-value |
| RAGP | 49 | 4.147** | 49 | 1.825** |
| EPVI | 49 | 4.212** | 49 | 3.212** |
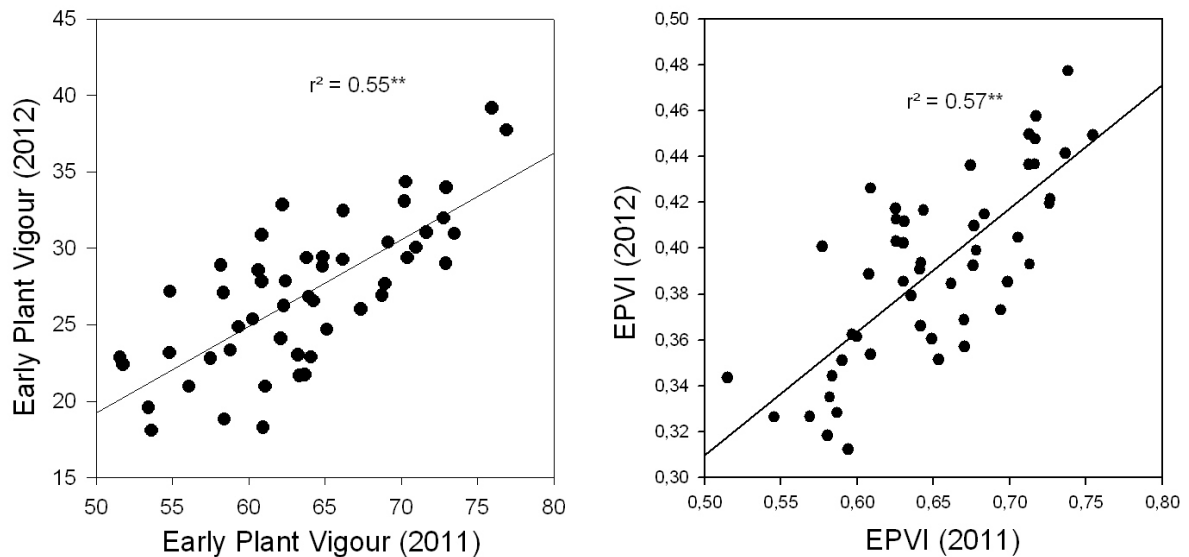
Figure 16: Correlations between 2011 and 2012 for the values of image analysis ($r^2 = 0.55$) and the EPVI ($r^2 = 0.57$) as indicator of early plant vigour as cultivar specific trait.

### 3.3.3   Relationship between pixel analysis and spectral reflectance measurements

The relationship between the plot means of the pixel analysis and the EPVI (Figure 17) was significant with an $r^2$ of 0.98 within both years. Furthermore, a very good relationship between the RAGP on photos and the spectral reflectance measurements existed. The EPVI index revealed to be slightly superior to the NDVI and RVI (Table 8), as other well known indices, and the analysis of all possible dual wavelengths combinations and the multivariate analysis did not result in enhanced relationships.

Table 8: Coefficients of determination for the relationships between early plant vigour obtained from analysis of green pixels and spectral indices EPVI, NDVI and RVI.

| Early plant vigour | EPVI | NDVI | RVI |
|---|---|---|---|
| 2011 | 0.81** | 0.78** | 0.77** |
| 2012 | 0.84** | 0.83** | 0.84** |
| 2011 + 2012 | 0.98** | 0.97** | 0.94** |

\* All results were significant at p < 0.001

Correlations between pixel analysis results and the NDVI derived from wavelengths provided by the GreenSeeker and the CropCircle showed also comparable results within both years. However, in 2012, a less close correlation between pixel analysis and the NDVI provided by the GreenSeeker ($r^2$ = 0.73) and the CropCircle ($r^2$ = 0.77) compared to the optimized index EPVI ($r^2$ = 0.85) derived from the HAFS was observed.
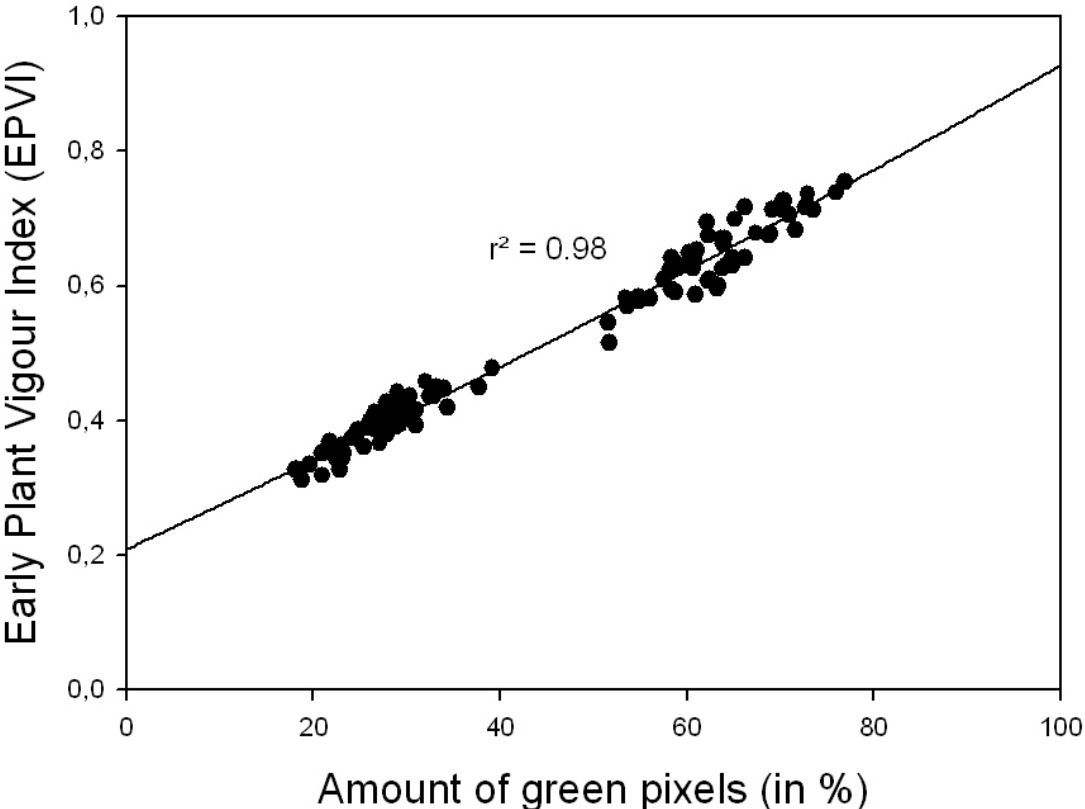


Figure 17: Correlations of the EPVI and the relative amount of green pixels (RAGP) derived from digital images of 50 winter wheat cultivars in 2011 and 2012.

3.4    *Section 4*: Identification of stay-green and early-senescence phenotypes and effects on grain yield and grain protein concentration using high-throughput phenotyping techniques

*3.4.1    Anthesis date and environmental conditions*

Large variation in the anthesis date existed among the 50 cultivars. Both early (e.g. W00984.2 and Liman R) and late flowering genotypes (e.g. cvs. Matrix and Magnifik) were identified, with the majority of anthesis dates occurring between 223 and 226 days after sowing (Table 9). Climate data as represented by daily temperature and rainfall conditions indicated stable growth conditions during the main growing season without the occurrence of any drought or heat stress periods. The maximum temperature exceeded 30°C only at one day in June and consequently a marked heat stress could be avoided.

Table 9: Average values and coefficients of variation of days to heading (DH), anthesis dates in days after sowing (AD), Onset of senescence ($O_{sen}$) in growing degree days (GDD) after anthesis, yield (in g m$^{-2}$) and grain protein concentration (GPC) of 50 winter wheat cultivars grown under comparable conditions in 2011/2012. The maturity group (MG) of cultivars which were certified and listed by German authorities are indicated.

| Cultivar | MG | DH | AD | $O_{sen}$ | | Yield | | GPC | |
|---|---|---|---|---|---|---|---|---|---|
| | | | | Average (GDD) | CV % | Average (g m$^{-2}$) | CV % | Average (in %) | CV % |
| W00984.2 | | 119 | 214 | | 1 | 677 | 2 | 17.8 | 1 |
| Alcazar | 5 | 127 | 224 | 554 | | 879 | 20 | 14.3 | 3 |
| Magnifik | | 132 | 233 | | 1 | 856 | 10 | 14.1 | 4 |
| Figura | | 126 | 222 | 549 | 5 | 952 | 6 | 13.9 | 3 |
| Oakley | | 128 | 227 | 512 | 4 | 1020 | 9 | 12.2 | 5 |
| Timber | | 125 | 224 | 561 | 0 | 944 | 6 | 14.0 | 3 |
| Liman R | | 119 | 214 | 617 | | 759 | 3 | 15.9 | 2 |
| Arina | 6 | 126 | 223 | | 3 | 890 | 3 | 16.4 | 1 |
| CH-111.13716 | | 127 | 219 | 611 | 0 | 747 | 6 | 15.8 | 4 |
| CH-111.13930 | | 125 | 217 | 617 | 3 | 751 | 8 | 16.2 | 2 |
| CH-111.13521 | | 125 | 221 | 583 | 5 | 860 | 3 | 14.4 | 3 |
| Mirage | 5 | 127 | 224 | 519 | 2 | 978 | 3 | 13.5 | 1 |
| Piotta | | 125 | 223 | 549 | 2 | 882 | 9 | 15.0 | 2 |
| Alchemy | | 132 | 229 | 488 | 0 | 1001 | 7 | 13.0 | 1 |
| CH-194.10518 | | 126 | 220 | 603 | 3 | 797 | 7 | 15.5 | 2 |
| Cubus | 4 | 128 | 224 | 555 | 2 | 974 | 2 | 14.0 | 1 |
| Türkis | 5 | 130 | 227 | 516 | 0 | 1004 | 3 | 14.0 | 1 |
| Akteur | 6 | 133 | 227 | 519 | 1 | 999 | 4 | 14.8 | 1 |
| Hermann | 6 | 132 | 227 | 505 | 1 | 1032 | 2 | 13.0 | 1 |
| Impression | 6 | 130 | 223 | 520 | 4 | 995 | 5 | 13.5 | 1 |
| Schamane | 5 | 126 | 223 | 509 | 4 | 1009 | 3 | 14.3 | 2 |
| Manager | 6 | 126 | 224 | 550 | 0 | 994 | 4 | 13.4 | 1 |
| Potenzial | 6 | 131 | 227 | 513 | 3 | 1027 | 5 | 13.3 | 1 |
| Julius | 6 | 128 | 228 | 523 | 1 | 988 | 4 | 13.5 | 0 |
| Pamier | 5 | 128 | 226 | 507 | 1 | 1001 | 4 | 14.8 | 4 |

| | | | | | | | | | |
|---|---|---|---|---|---|---|---|---|---|
| JB Asano | 4 | 126 | 223 | 527 | 3 | 1004 | 1 | 14.5 | 3 |
| Kredo | 6 | 126 | 224 | 523 | 1 | 1019 | 2 | 13.9 | 4 |
| Famulus | 5 | 127 | 223 | 553 | 2 | 919 | 4 | 15.8 | 4 |
| Genius | 5 | 126 | 223 | 534 | 3 | 954 | 4 | 15.0 | 6 |
| Linus | 6 | 125 | 229 | 471 | 2 | 1059 | 5 | 14.1 | 4 |
| Meister | 6 | 132 | 229 | 454 | 3 | 1045 | 6 | | 1 |
| Orcas | 5 | 127 | 223 | 533 | 1 | 957 | 3 | 13.6 | 1 |
| Muskat | 5 | 125 | 223 | 528 | 1 | 975 | 1 | 13.4 | 1 |
| Kerubino | 5 | 126 | 223 | 534 | 2 | 939 | 2 | 14.3 | 3 |
| KWS Erasmus | 6 | 130 | 225 | 500 | 0 | 999 | 2 | 12.3 | 3 |
| Matrix | 6 | 130 | 231 | 481 | 2 | 1053 | 3 | 12.6 | 2 |
| Florian | 6 | 130 | 225 | 519 | 1 | 930 | 6 | 14.3 | 5 |
| Sailor | 5 | 130 | 224 | 540 | 1 | 965 | 6 | 14.5 | 9 |
| Norin | 4 | 126 | 224 | 513 | 1 | 953 | 5 | 13.8 | 5 |
| Komet | | 128 | 227 | 482 | 1 | 1060 | 3 | 14.1 | 4 |
| Colonia | 5 | 128 | 225 | 518 | 2 | 969 | 2 | 14.1 | 2 |
| Tabasco | 7 | 132 | 229 | 467 | 1 | 1068 | 6 | 13.0 | 3 |
| Sophytra | 5 | 128 | 227 | 468 | 1 | 1025 | 4 | 13.6 | 2 |
| Akratos | 5 | 128 | 226 | 517 | 1 | 971 | 3 | 13.2 | 2 |
| Sokrates | 5 | 128 | 225 | 506 | 1 | 982 | 2 | 14.0 | 3 |
| Winnetou | 5 | 128 | 227 | 486 | 1 | 1082 | 6 | 13.0 | 3 |
| KWS Bogus | | 132 | 226 | 486 | 2 | 965 | 4 | 14.3 | 1 |
| Wilson | | 128 | 227 | 485 | 0 | 1004 | 2 | 14.3 | 3 |
| Glaucus | 7 | 132 | 226 | 534 | 2 | 996 | 1 | 14.1 | 2 |
| RCATF TF 174/1C | | 126 | 218 | 572 | 1 | 813 | 4 | 15.4 | 2 |

### 3.4.2 Flag leaf senescence

Compared to the senescence process of the lower leaf layers, that of the flag leaves was much delayed. Among all cultivars, the b-values of the flag leaves measured with the handheld ColorEye XTH remained approximately stable until June 29. Thereafter, each cultivar showed a rapid increase of its specific b-value until July 9 at the latest (e.g., see Figure 6).

### 3.4.3 Identification of stay-green and early-senescence phenotypes

The onset of senescence showed a broad variation among all cultivars (Table 9), with the time between anthesis and the onset of senescence being highly cultivar specific. Both cultivars that long maintained the greenness of the flag leaf (stay-green phenotypes: cvs. CH-111.13930, CH-111.13716 and Liman R) and those with an earlier onset of senescence (early-senescence phenotypes: cvs. Meister, Tabasco and Sophytra) were clearly identifiable. The flag leaf senescence of the stay-green phenotypes did not start before 600 °Cd, whereas that of the early-senescence phenotypes already occurred after less than 500 °Cd (Table 9).

### 3.4.4 Partial Least Square Regression Model (PLSR)

Considering the RMSE and Akaike Information criterion (AIC) and avoiding over- or underfitting, the optimum amount of principal components (PC) for the calibration model was five (Table 10). The statistical information of the PLSR model (Table 10) indicates a good ability for predicting b-values in the validation dataset with an $r^2$ of 0.73.

Table 10: Calibration and validation statistics, including principal components (PC) and random mean squared error (RMSE) for the PLSR model using b-values as color reference and multispectral data (500 – 700 nm) for the determination of senescence progress in 50 winter wheat cultivars.

| | Calibration dataset | | | | | Validation dataset | | | |
|---|---|---|---|---|---|---|---|---|---|
| | n | Range (b-value) | PC | $r^2$ | RMSE (b-value) | n | Range (b-value) | $r^2$ | RMSE (b-value) |
| Winter wheat cultivars | 309 | 7-39 | 5 | 0.67 | 2.8 | 154 | 8-33 | 0.73 | 1.9 |

*3.4.5   Relationship between stay-green duration, yield and grain protein concentration*

The onset of senescence (expressed as GDD after anthesis) was compared to yield and GPC to evaluate possible relationships between these traits (Figure 18). Both, yield and onset of senescence were specific for each cultivar, as shown by the analysis of variance (Table 11).

Table 11: One-way ANOVA results (*F*-values and its significance) for the cultivar effect. Significance at $p \leq 0.001$ is indicated by ***.

| Cultivar effect as source of variation | dF | *F*-value |
|---|---|---|
| Yield | 49 | 8.314*** |
| $O_{sen}$ | 49 | 7.885*** |
| GPC | 49 | 1.097 |

A strong negative relationship was observed between the onset of senescence and yield ($r^2 = 0.81$), indicating that stay-green phenotypes achieved lower yields than early-senescence ones. By contrast, the onset of senescence and GPC showed a weaker, but positive relationship ($r^2 = 0.48$). However, a significant relationship exists also for days after sowing (AD) and yield or GPC, respectively (Table 12).

Table 12: Correlation matrix with coefficients of determination for anthesis dates in days after sowing (AD), days to heading (DH), onset of senescence ($O_{sen}$), yield and grain protein concentration (GPC). Significance at $p \leq 0.01$ is indicated by **.

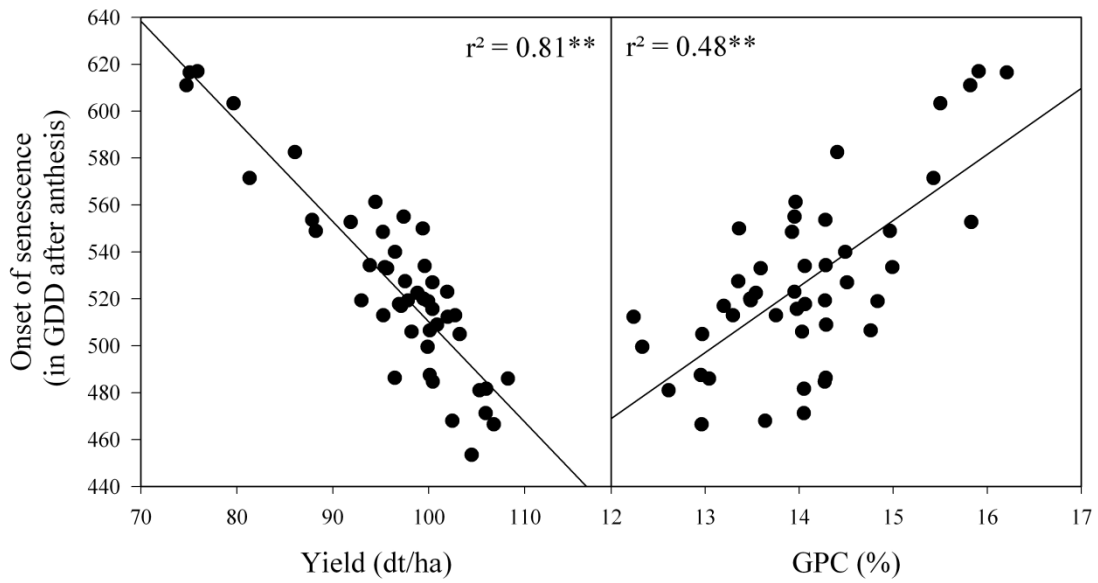| | AD | DH | $O_{sen}$ | Yield | GPC |
|---|---|---|---|---|---|
| AD | - | 0.50** | 0.78** | 0.61** | 0.51** |
| DH | 0.50** | - | 0.35** | 0.30** | 0.22* |
| $O_{sen}$ | 0.78** | 0.35** | - | 0.81** | 0.48** |
| Yield | 0.61** | 0.30** | 0.81** | - | 0.59** |
| GPC | 0.51** | 0.22* | 0.48** | 0.59** | - |

Figure 18: Linear regression and coefficients of determination for relationships between the onset of senescence (in growing degree-days after anthesis) and either grain yield or grain protein concentration. Significance at $p \leq 0.01$ is indicated by **.

# 4 Discussion

## 4.1 *Section 1*: The performance of active sensors as influenced by measuring distance, device temperature and light intensity

### 4.1.1 *Measuring distance*

Each wavelength shows significant changes in the reflected light at different measuring distances (Figure 7) because both the light emitted by the sensor and that reflected by the green fabric follow the inverse square law (Holland et al., 2012). Thus, given that the reflected light decreases when the measuring distance increases, it is necessary to use indices of single wavelengths to obtain reliable data at varying heights. Moreover, it is obvious that active sensors react sensitively with respect to the measuring distance, because the distance-reflectance curve for each wavelength shows the same progression within a small range of distances to the target.

The greater variability in the reflectance data, and thus also in the spectral indices derived from them, at low or small measuring distances (Figure 7) can be explained by the technical properties of the active sensors. Because the detectors and light sources are spatially separated, the footprint of the light emitted by the light source will fall outside the region where the detector captures the reflectance if the sensor is positioned too close to the measured target. By contrast, the output values stabilize when the detector is able to capture the entire footprint. The minimum distances at which this occurs is 70 cm for GreenSeeker, 30 cm for CropCircle, and 50 cm for AFS; at shorter distances, the sensor can hardly detect any reflectance. The curve progression of single wavelengths (Figure 7) also indicates that signal attenuation occurs at measuring distances of more than 2 m because the detector captures only marginal portions of the light emitted by the light source from that point onwards.

As discussed previously, a specific range of "optimum" measuring distances exists for each active sensor, where spectral indices remain stable as a consequence of the identical curve progression of the single wavelengths contributing to them. Within this tolerance range (Table 1), which is unique for each sensor, the effects of changing measuring distances on spectral indices are negligible. Table 1 shows that the manufacturers' recommendations concerning the optimum distance to the target largely agree with our experimental results. In case of the GreenSeeker´s NDVI the optimum measuring distance even exceeds the manufacturer´s recommendation subject to the chosen reference conditions. However the GreenSeeker´s $R_{770}/R_{650}$ index seems to be slightly more sensitive to distances above 110 cm, whereas the

manufacturer recommends measurements until 122 cm. Generally distances to target have to be considered critical as long as no reliable information exists on how to define the distance. In contrast to passive spectrometers (Winterhalter et al., 2012) it is unclear how deep the active sensor signal penetrates into the canopy. Thus it can be denoted as impossible to adjust particular measuring distances. The variation of sensor indices within the optimum ranges shown in this study as well as within the measuring distances recommended by the manufacturers may be marginal but as long as the distance to the plant canopy cannot be determined certainly, it has to be considered that reflectance values can be falsified if measuring distances are chosen which are close to the lower or upper limits of the tolerance ranges. The uncertainty of plant canopies as measuring surface with fixed distances was the determining factor to use a reference surface for all experiments to provide a reliable analysis of the technical ability of each sensor at particular measuring distances. Altogether, knowledge of the optimum measuring distances is crucial for the appropriate in-field application of the active sensors, making it possible to adapt the sensor-to-target distance to specific plant heights. Given that heterogeneous plant populations naturally exist in the field, this information can provide enhanced quality when assaying crop parameters non-destructively. Although handheld sensor systems may be particularly prone to varying distances and might require increased attention to maintain measurements within optimised distances, mobile sensor platforms might also require adjustment to varying plant heights despite their use of fixed distances.

An additional complicating factor is that the optimal distances to the target will depend on how dense the canopy is because the penetration depth of the sensor's light signal will differ between sparse or dense canopies. Thus, tracking optimum distances will be more difficult in row crops if they are not measured directly above the row and also because the exclusion of the inter-row needs to be factored in comparison with the more uniformly dense stands of non-row crops. For row crops such as maize, it is also difficult to determine the leaf levels from which the reflectance signals are being captured by the sensors. Differences are also expected between cultivars that have either planophile or erectophile leaves, and information can also vary at different growth stages. The contribution of different leaf levels to the output signal can therefore depend on both the plant architecture and the growth stage, thereby influencing the interpretation of the data and potentially confounding differences recorded among cultivars. The influence of varying distances is probably augmented in taller row crops compared with denser and shorter cereal stands. It may even be difficult to identify optimum measuring distances for active sensors using real plant populations (Solari, 2006). Together,

these factors stress that further intensive investigations are necessary to evaluate the role that leaf architecture plays and how deep the signals from active sensors penetrate into the canopy.

### 4.1.2 Device Temperature

A close relationship between the device temperature and sensor readings clearly exists (Figure 8), with the challenge being to answer whether the temperature affects the light source directly or the performance of the detector. Because the output values of each wavelength change differently, this suggests that it is the light source that is affected by the changing temperature conditions. Further evidence comes from the GreenSeeker, which captures the light of every wavelength with a single detector. Here it is apparent that the device temperature does not affect the detector's performance because the reflectance at each wavelength would otherwise show the same shift. Thus, the temperature apparently affects the light quality of the different light emitting diodes (one diode for one wavelength) differentially. Consequently, it must remembered during the application of active canopy sensors that they are temperature sensitive, which, in turn, depends on solar radiation and can vary diurnally (e.g., sunny versus cloudy periods). Thus, long-term measurements over a period of a couple of hours are susceptible to such influences because of potential differences in the device temperature over this period.

The reproducibility of spectral reflectance measurements affected by varying device temperatures could be shown by repeating this experiment for each sensor at different measuring heights (Figure 8). Nearly identical index values could be obtained from each sensor when the device temperature increased. The parallel shift of the CropCircle´s NDVI and $R_{760}/R_{730}$ index results from the sensor-target distance of 40 and 80 cm. At a measuring height of 40 cm the $R_{760}/R_{730}$ index values are slightly lower than at 80 cm and NDVI values are higher. Regarding CropCircle´s $R_{760}/R_{730}$, this index still reacts sensitive to increasing device temperature even if the measurement starts at a temperature equilibrium of 30°C.

To illustrate the effect of this error under field conditions and its potential impact on recommended nitrogen fertilisation rates, our measured values were compared to spectral information obtained from a field experiment (Erdle et al., 2011). Potential error rates for each sensor and index could be calculated when the device temperature shifted by ±1°C (Table 2).

These findings indicate that misinterpretations of spectral measurements in the case of the CropCircle can be easily avoided when choosing the NDVI for describing N-Uptake or biomass instead of the $R_{760}/R_{730}$ index. In contrast the GreenSeeker´s NDVI seems to be more affected to varying device temperatures. Although Kim et al. (2010) reported that there is no

impact of device temperature on the performance of the GreenSeeker, our study shows that such impacts may indeed occur, even if they seem to be insignificant. Thus, if small differences between plant canopies are to be expected, it is especially crucial to exclude device temperature effects. However the application of active sensors in precision farming is also affected by this influence considering that the diurnal temperature could change substantially between morning, midday and evening time and a stable temperature equilibrium does not exist in the practical application of active sensors Additionally the device temperature effect can be nearly eliminated by warming up the sensor body until it reaches a stable temperature. However it should be considered that comparisons of several measurements, performed under variable temperature conditions, could lead to false estimation of reflectance values.

### 4.1.3   *Light intensity*

The lack of any appreciable effect of varying light conditions on the performance of the active sensors can be explained by the devices being designed to emit their own light source at one or more wavelengths and record the specific reflectance. Thereby, the electrical circuits in the detector are able to filter and differentiate between the emitted "artificial" light and ambient light originating from the sun. Thus, our results show clearly that the assumption that active sensors are susceptible to varying light conditions as observed for other sensor systems, such as laser-induced chlorophyll fluorescence (Thoren et al., 2010), is false. Instead, the results agree with other experiments in terms of the lack of any apparent influence of ambient light on sensor performance (Solari et al., 2004; Jasper et al., 2009; Kim et al., 2010) and support that active sensors can work independently of bright daytime and dark night-time conditions. That being said, it is worth noting that external light could have an indirect temperature-based effect on the active sensors because increased light often generates higher temperatures, which again affects the device temperature and therefore performance. In case of the AFS, the slight decrease of the $R_{760}/R_{730}$ index could be explained with such a little variation in device temperature

4.2   *Section 2*: Reflectance characteristics of different plant components in a winter wheat experiment at two different development stages

The distribution of dry weight in lower leaf layers, middle leaf layers, flag leaves, stems and ears differs between ZS61 and ZS75 (Figure 11), which can be mainly explained by the post-anthesis translocation of assimilates. The contribution of post-anthesis assimilates to grain

filling is substantial for the final grain yield, because pre-anthesis assimilates contribute only 11-29 % in wheat (Gebbing et al., 1999) and 4-24.2 % in barley (Przulj and Momcilovic, 2001a). However the total leaf dry weight (Figure 11) does not increase by the post-anthesis assimilation, because assimilates are directly transferred into stems and ears. Therefore the stem and ear dry weight increased rapidly between ZS61 and ZS75. However the stem dry weight is expected to decrease until maturity because they store assimilates only temporary (Borrell et al., 1989). In comparison the N content in leaves and stems decreased rapidly between anthesis and grain filling (Figure 12), because the available N, stored in leaves and stems, has already been transferred into the grains.

Three different active sensors (CropCircle, GreenSeeker and AFS) were assessed in terms of their penetration depth into the canopy. Different plant components, including lower leaf layers, middle leaf layers, flag leaves, stems and ears were stepwise removed (starting at lower leaves) and changes in reflectance of sensor specific wavelengths and indices were observed. Dry weight and N content of each removal step were calculated and set in relation with sensor readings to assess the sensors ability to detect such parameters accurately within the whole plant.

The reflectance of single wavelengths during the removal of each plant component differs, depending on the spectral region. Reflectance at 670 nm increases when biomass in terms of leaves, stems and ears was stepwise removed, whereas reflectance in the NIR region at 730 and 760 nm decreases. Considering that plant canopies have their absorption maximum at 670 nm and NIR light is mainly reflected, this phenomenon can be explained with the increase of the soil reflectance with each removal step. Soil reflects more light than plants at 670 nm and less light in the NIR region. Thus the reflectance at 670, 730 and 760 nm aligns to the soil reflectance curve, which means that the reflectance increases at 670 nm and decreases at 730 and 760 nm.

The main variation in reflectance could be assessed after removing middle leaf layers, following lower leaf layers and flag leaves. This order is consistent with the relative portion of each leaf layer of the total leaf dry weight. In fact the plant dry weight is mainly localized in stems and ears, but their vertical orientation to the sensor position reduces the area which can be measured by the sensor. Thus sensor readings are predominantly affected by the leaf biomass and leaf area. Small changes in reflectance after removing ears and stems can be attributed to the measuring angle of each sensor because emitted light penetrates into the canopy also in an oblique direction, which still enables reflectance of these components.

The summary of reflectance intensities of single wavelengths and indices in Figure 13 could lead to misinterpretations without knowing the proportional distribution of dry weight of each plant component. The extent of variation in reflectance after each removal step has to be related to the proportional dry weight of the plant component which has been removed. A small variation at 760 nm of the GreenSeeker after removing the lower leaf layers in comparison to high variation after removing the middle leaf layers does not mean that the GreenSeeker is not able to penetrate deep into the canopy. In fact the lower leaf dry weight is much lower than in the middle leaves and the influence on the reflectance intensity is much lower. To avoid such misinterpretations, sensor readings of each removal step were correlated with the corresponding amount of dry weight and N content. Thus reliable information about the penetration depth of each sensor could be given.

The relationships between sensor readings and corresponding dry weight and N content values (Table 4 and 5) indicate differences between single wavelengths, sensor type and growth stage regarding the potential to detect changes in dry matter and N content when different plant components were removed. Among single wavelengths the best relationship could be found at 670 nm. Only in case of the GreenSeeker at ZS 61 no significant relationship exists. The absorption maximum of chlorophyll *a* and *b* in plant canopies at 670 nm, (Chappelle et al., 1992) mainly explains the good relationship to N content, since much of the plants nitrogen is integrated in chlorophyll (Mistele and Schmidhalter, 2008). No significant relationship between 730 nm and dry weight and N content at both development stages could be found. The spectral region at 730 nm is also called red edge position (REP), where the light reflectance of plant canopies increases rapidly due to the transition from the visible (VIS) to the near infrared light spectrum. Several former studies reported that the REP shows significant relationships to chlorophyll concentration (Hatfield et al., 2008) and it should be expected that at least a significant relationship to N content exists. In our experiment the non-significant relationship to both parameters can be explained with the last measurement taken on bare soil after removing the stems. The reflectance at this stage increases slightly, although biomass was removed. If the last measurement is omitted in the calculation the coefficient of determination increases to a highly significant level.

The NIR wavelength at 760 nm was better correlated to N content than to the dry weight, which is due to the reflectance response after removing stems. Almost the half of the total dry weight is accumulated in the stems at both development stages but reflectance values at 760 nm change only slightly in comparison to the other removal steps. This weak response in reflectance leads to insignificant relationships between 760 nm and dry weight.

Both simple ratios, $R_{760}/R_{730}$ and $R_{760}/R_{670}$ were better correlated to N content, but the NDVI seems to be suitable to detect both, dry weight and N content. However $R_{760}/R_{730}$ shows a more significant relationship to N content than $R_{760}/R_{670}$. Although both indices $R_{760}/R_{670}$ and NDVI contain similar wavelengths, the normalized index is better adapted to small changes in biomass.

Getting back to the question, if active sensors were able to penetrate deep enough into the canopy it can be concluded that each wavelength reacts sensitive when removing the lower leaf layers. Thus each tested sensor penetrates deep enough into the canopy to detect reflectance of the lowest leaves. For the NIR wavelengths such as 760 nm this is well known, because NIR irradiation can hardly be absorbed by plant canopies but highly transmitted (Heege et al., 2008), which leads to a deep penetration into the canopy. In comparison red wavelengths such as 670 nm causes mainly surface reflectance (Heege et al., 2008) due to low transmittance rates. Therefore it is surprisingly that reflectance at 670 nm shows sensitivity to the removal of lower leaf levels.

4.3    *Section 3*: High-throughput phenotyping early plant vigour of winter wheat

Early plant vigour is an early selection criterion in breeding programs for wheat and other cereals since it indicates the ability of plants to achieve sufficient biomass for yield productivity. Therefore, the present study represents an approach to establish a high-throughput phenotyping tool for plant breeding and field experimentation using spectral reflectance measurements. For referencing spectral data with early plant vigour values, pixel analysis of RGB images was chosen to be the most suitable reference method for such a large number of plots (200 plots). Visual field scoring cannot be used as an accurate reference method because it is impossible to detect small differences in early plant vigour between numerous plots as was the case in this study. Attempts to cut a 2.7 m² area of each plot with a green forage chopper were not successful, resulting from difficulties to cut at a pre-defined plant height at early plant stages above the soil terrain that naturally is not smooth. The same difficulties were observed in manually cutting plants at pre-defined heights at this early stage which resulted in large differences among individual persons and the biomass sampling was further influenced by a variable degree of adhering soil particles. In agreement with Scotford and Miller (2004) counting single plants or tillers in selected areas of each plot as it was conducted in previous studies (Phillips et al., 2004; Scotford and Miller, 2005) was found to be infeasible. The early plant vigour differed also markedly within the plots, thus counting a small area within a plot would not be representative enough for the entire plot. Counting

plants or leaves directly within point frames based on the intercept method (Booth et al., 2006) is amenable only to a reduced number of plots, but with respect to the large number of assessments required in our experiment, it was found to be not applicable. It is also supposed that the soil coverage is better estimated by the integral analysis of the image or the spectroscopic assessment than by the line intersection method.

Thus, no better reference method than pixel analysis could be identified meeting the need for assessing a large number of field plots with high accuracy and the latter was thus established as reference method for scoring early plant vigour by analyzing the RAGP on digital photos taken at ZS 28 in 2011 and ZS 23 in 2012. The non-invasive character, its applicability in very early development stages and the coverage of the entire plot are key factors for this method for being used in large breeding programs. The amount of green pixels represented the early plant vigour for each cultivar (Table 6). The difference in the RAGP in photos taken in 2011 and 2012 (Figure 6) was due to the differing development stages, ZS 23 and 28 in 2012 and 2011, respectively. Due to the later sampling date in 2011, the tillering process was nearly terminated. Thus, a higher fraction of green biomass covered the ground and the RAGP in the photos was higher. Differences in early plant vigour were expected due to the broad spectrum of wheat cultivars, which included all quality groups (A, B, C, E) being certified and listed by national authorities and regularly cultivated by German farmers. Integrated pest management and adequate nutrient supply allowed for healthy vegetation free of weeds. Neither the spectral sensor nor the color-based information from the digital camera would differentiate between wheat plants and weeds. The absence of weeds and the presence of healthy crops being adequately supplied with nutrients and adapted pest management are necessary to correctly identify early plant vigour. However, the degree of greenness could be identified as well. The visualization of the green pixels of each photo (Figure 14) shows that the software was able to differentiate exactly between green plant parts and soil. Thus, the early plant vigour could be determined with high accuracy. Pixel analysis of RGB images could also be suitable for scoring the early plant vigour, but it still requires a rather laborious post-processing procedure that decreases the practical use of this technique.

The EPVI is considered as an approach to replace the pixel analysis of plots. The wavelengths on which the EPVI is built were selected from regions in the visible (VIS) and near-infrared (NIR) spectrum of light where differences between plots with high and low biomass content become apparent (Shibayama and Akiyama, 1989; Smith et al., 1993). The VIS region of the spectrum, especially wavelengths at 670 nm, as a component of the EPVI is characterized by high light absorption due to the presence of chlorophyll in the palisade layers of leaves

(Campbell, 2002), whereas in the NIR region, 750 nm and 862 nm in the EPVI, biomass (e.g., cellulose, cell walls, etc.) reflects a large portion of the incoming light (Figure 15). Additionally, plants reflect more light in the green part of the VIS spectrum (500 nm – 550 nm) in comparison to other VIS wavelengths. Due to the disparity of reflectance in the VIS and NIR spectrum, which is highly related to the amount of biomass, ratios and indices of VIS and NIR wavelengths are very useful to describe differences in biomass (Raun et al., 2001; Erdle et al., 2011). Thus, the simple ratio of 670 nm and 750 nm is an indicator of the amount of green biomass related to other NIR/Red indices of former studies (Shibayama and Akiyama, 1989). Thus, the differentiation between plant biomass and soil should be provided by using such indices because soil does not show a rapid increase in reflectance between VIS and NIR (Figure 15). Previous studies have shown that soil could affect the spectral determination of biomass at early growth stages using a vertical measuring direction (Schmid, 2008). In contrast to this observation, the results from this study demonstrate that the selected combination of the EPVI wavebands was not affected by soil reflectance information, as shown by the good relationship between EPVI and RAGP for both years (Figure 17). However, previous studies have shown that various indices are suitable for characterization of plant parameters in growth stages starting at ZS 28 (Mistele and Schmidhalter, 2010). Considering that measurements in 2011 were conducted at ZS 28, other indices might also provide comparable results. Based on the sensitivity of the EPVI wavelengths to green biomass, the EPVI should be able to distinguish between green plant parts and soil for evaluating the plant vigour at early growth stages. However, pixel analysis as a reference method must be further established to confirm this hypothesis. Some previous studies have already shown good correlations between pixel analysis and spectral indices such the NDVI (Lukina et al., 1999) or RVI (Wu et al., 2011) and several reports describing the detection of the leaf area index (LAI) or tiller density (Scotford and Miller, 2004; Taylor et al., 2000) in field trials with different N-treatments or sowing densities can be found in literature but there is a lack of studies dealing with phenotypic differences of crop cultivars grown under comparable conditions.

To confirm the hypothesis that the rate of early plant vigour is specific for each cultivar consequently affected by the genotype it is crucial to prove whether early plant vigour as specific trait of each cultivar shows a similar behaviour in both experimental years.

Figure 16 shows significant correlations between 2011 and 2012 for the values of image analysis ($r^2 = 0.55$) and EPVI ($r^2 = 0.57$), although values of different development stages were compared. These results indicate that early plant vigour revealed to be cultivar specific

being confirmed in the two experimental years. Additionally the Student-Newman-Keuls test showed comparable cultivar rankings for RAGP and EPVI in both years (Table 6).

The analysis of green pixels to distinguish between plant material and soil revealed to be an accurate method to evaluate early plant vigour, but showed limitations in terms of time and effort. For breeding purposes or other large-scale field trials, it is impractical to take two or more photos of each plot in large field trials and to analyse those photos with a software as used in this study. Although such a method would be very accurate and useful, the laborious procedure will prohibit its application in the near future.

In contrast, spectral reflectance measurements have been suggested for high-throughput phenotyping purposes (Schmidhalter, 2005; Furbank and Tester, 2011; Walter et al., 2012). The application of spectral reflectance sensors in field trials enables researchers to establish high-throughput phenotyping platforms for measuring large field trials rapidly (White et al., 2012). However, a reference method is always required to relate spectral data to plant traits such as early plant vigour.

The present study demonstrates that the pixel analysis is the most accurate reference method for scoring early plant vigour. Relationships between the RAGP and EPVI of 50 wheat cultivars showed close relationships of $r^2 = 0.98$ for both years, $r^2 = 0.81$ for 2011 and $r^2 = 0.84$ for 2012. Two other indices (NDVI and RVI), which are frequently used in literature for detecting tiller density, soil coverage or leaf area index were additionally compared with pixel analysis to assess the accuracy of EPVI (Table 8). Both indices showed also significant correlation for both years but the EPVI proved to be more accurate within single years. The results indicate that the EPVI is an accurate indicator for the amount of green plant material in plots measured with the HAFS. However comparable relationships between pixel analysis and the NDVI provided by two other active sensors may indicate that these commercially available active sensors, the GreenSeeker and the CropCircle are also suitable to detect the early plant vigour. The wavelengths chosen to construct the EPVI were highly sensitive in distinguishing soil or green biomass, and this feature most likely contributes to the high accuracy of this novel index. Soil correction factors as they are implemented in other spectral indices, e.g., SAVI (Huete, 1988) and OSAVI (Rondeaux et al., 1996) are not necessary because the EPVI shows a close relationship to green biomass as a result of the sensitivity of the wavelengths chosen for the EPVI index. Significant relations for both years indicate that the EPVI can be used for scoring early plant vigour under different environmental conditions. Additionally, small differences in growth stages as found in the present study between 2011 and 2012 did not affect the accuracy of the index. The method could also provide

measurements at earlier growth stages for directly scoring field emergence. The differences obtained between the two years do not represent an obstacle being in line with the observation that genotypes are frequently evaluated on a relative basis.

The EPVI will not be able to give information about the number of seedlings or tillers, but it will be useful for the relative comparison of early plant vigour. It can further replace manual field scoring of early plant vigour, as commonly applied in plant breeding, due to its rapidity in scoring large field trials. In this study, 200 plots could be measured within 75 min at a driving speed of 2.8 km/h. Considering that the plot size was rather large (12 m in length x 1.5 m in width), measuring time could be substantially reduced for smaller sized-plots. Further, multiple measurements from alongside the plots result in a more representative assessment compared to visual scoring, which frequently is conducted only at the front (head) side of the plots.

Altogether the high-throughput character, the higher representativeness and the more objective assessments of the suggested method represent an advanced alternative compared to visual field scoring. The EPVI can accelerate the breeding process through its time- and cost-saving nature.

4.4 *Section 4*: Identification of stay-green and early-senescence phenotypes and effects on grain yield and grain protein concentration using high-throughput phenotyping techniques

In this study, stay-green and early-senescence phenotypes could be identified within a field experiment by measuring the onset of flag leaf senescence (expressed as GDD after anthesis) for 50 winter wheat cultivars. The selected set of cultivars included all quality groups (A, B, C, E) being certified and listed by national authorities and regularly cultivated by German farmers. All cultivars are adapted to the climate conditions in Middle Europe and particularly in Germany. The significant negative relationship between the onset of senescence after anthesis and yield together with the positive relationship with GPC indicate that stay-green phenotypes are negatively correlated with grain yield, but positively with GPC. A significant negative relationship exists also between AD and the onset of senescence, indicating that an early anthesis results in a longer maintenance of the green leaf area. However, if cultivars with similar AD (within 3-4 days) were considered, the relationship between onset of senescence and yield still remains significant negative. Thus the AD of cultivars could have an effect on stay-green duration among others. The effect of AD on stay-green probably varies depending on the region of cultivation. In areas with moderate temperature regimes and

66

adequate rainfall, the anthesis date is of lesser importance, whereas in regions in western Asia with early heat periods cultivars with early AD are favored.

The presented result are in contrast to other studies that report a positive relationship between yield and the onset of senescence (Borrell et al., 2000; Verma et al., 2004; Bogard et al., 2011). By contrast, Derkx et al. (2012) found a lack of increased yield in a stay-green phenotype in comparison to fast-senescing phenotypes in agreement with Kichey et al. (2007), who concluded that prolonged leaf metabolic activity influenced grain productivity. These conflicting findings can be explained in part by the fact that few data exist investigating a large number of cultivars that were grown under comparable conditions, but without being affected by drought stress or different N-levels. Bogard et al. (2011) found a positive relationship between the onset of senescence and grain yield in an experiment with standard and low N-treatment, but limiting these analyses to the standard N-treatment (as investigated in our study) the positive relationship turns into a negative one. Thus, any positive (or negative) effects on yield of stay-green phenotypes have to be interpreted with some degree of caution given that different N-levels or drought stress often appear to affect the results.

However it should be emphasized that the present results are limited to a 1-year experiment at one location. Unfavorable climate conditions such as drought stress periods which could affect the senescence process did not occur in this study. Thus it should be considered that the negative relationship between stay-green and yield could be a result of regional growing conditions in south-east Germany. Null or opposite effects of stay-green on yield and GPC as they may occur in comparable studies cannot be excluded until the results are verified in multi-year and multilocational field trials. However, transferring the present results to different environments with drought conditions, high rainfall, or shorter vegetation periods as being the case in many agricultural regions worldwide, should be done with caution.

In the present study, stay-green phenotypes were characterized by the longer maintenance of flag leaf greenness, lower yield and higher GPC. The negative relationship between grain yield and GPC frequently results from a dilution effect caused by increased starch accumulation (Campbell et al., 1997; Feil, 1997). Whereas, yield is affected mainly by starch synthesis and its carbon (C) requirements, amino-acid synthesis, which mainly uses N as a source, affects GPC such that the balance between starch and amino acids in the individual grains determines the extent of yield versus GPC (Novoa and Loomis, 1981). Although glucose from photosynthesis is required for both starch and protein synthesis, almost twice as much is needed for the latter (1 g glucose yields 0.45 g protein versus 0.86 g starch; (De Vries et al., 1974) because the degradation of glucose provides the necessary C for the C-skeleton

of the amino acids. Given that a prolonged green flag leaf area results in increased N-uptake during grain filling (Hirel et al., 2007), stay-green phenotypes will be comparatively better supplied with nitrogen and more glucose will be consumed to assimilate the additional N into grain protein. As a result of this wasting of glucose for protein synthesis (De Vries et al., 1974), the synthesis of starch is reduced at this time in these phenotypes, potentially lowering yield.

The discrepancy between the results of former studies (Verma et al., 2004; Bogard et al., 2011; Lopes and Reynolds, 2012; Gregersen et al., 2013) and those of the present study can be explained with an altered investment in starch versus protein synthesis under such adverse environmental conditions compared to more favorable growth conditions used in this study. Starch synthesis is more negatively affected by adverse growing conditions than the protein synthesis (Campbell et al., 1981; Bhullar and Jenner, 1985; Jenner et al., 1991). This fact, in turn, results in potential differential effects on grain yield and GPC between adverse and favorable growing conditions.

The genetic and physiological pathways resulting in a stay-green phenotype are diverse (Thomas and Howarth, 2000) and also highly dependent on environmental conditions (Bogard et al., 2011).

Spectral reflectance measurements from a passive spectrometer were successfully applied in this study to identify both stay-green and early-senescence phenotypes. Furthermore, CIELab color data of 20 wheat cultivars derived from a handheld Color Eye XTH spectrometer could be extrapolated to all 50 cultivars using PLSR models. Although the spectral information from the passive spectrometer includes information from the whole canopy, whereas the Color Eye measurements were restricted only to the flag leaf, the PLSR analysis was uniquely able to extract only those wavelengths from the spectra that could accurately predict the b-values of the Color Eye measurements. The $R^2$ of 0.73 in the validation dataset indicates a high accuracy of the developed PLSR model. For comparison, we tested all possible simple ratios for potential correlations to the b-values using contour map analysis as well as additional combined indices, but no stable relationships were found.

Thus, PLSR models appear to provide a most promising, labour-effective method to extract flag leaf specific traits for senescence mechanisms from the spectral information provided by the passive spectrometer using a handheld color spectrometer device as an initial calibration unit. Noteworthy here is the intensive nature of the latter, with 20 handheld measurements of the 20 cultivars requiring approximately 4 hours. By contrast, using the mobile phenotyping platform PhenoTrac 4 enabled us to record spectral measurements of the whole canopy of all

50 cultivars within 75 minutes, a time savings of 8 times compared to handheld measurements as conducted by Lopes and Reynolds (2012). As such, this high-throughput phenotyping method linked to PLSR analysis of the recorded spectra would appear to represent a novel, effective method to identify stay-green and early senescence phenotypes in large field trials.

The present results indicate a clear, negative relationship between stay-green phenotypes and grain yield in contrast to the majority of former studies as well as the resulting, widespread assumptions about the nature of this relationship. However, it should be stressed that our data are based on only a single year of experimental data and further field trials are necessary to confirm the present hypothesis. Importantly, comparable measurements should be conducted for a different set of wheat cultivars to test if these novel findings are transferable to other genotypes. In addition, partitioning processes of N and C should be investigated further and in more detail by taking samples of leaf, stem and ears at different growth stages of wheat to elucidate the physiological background behind the whole senescence process. Nevertheless, the present study should still shed new light on the potential effects of stay-green and early-senescence traits on yield and GPC.

# 5    General Discussion

The development of high-throughput phenotyping methods for the assessment of various plant traits requires detailed knowledge about the functioning and capabilities of sensor devices for this purpose. Therefore to basic experiments were conducted to evaluate the performance of active spectral reflectance sensors and to identify potential factors which could affect spectral measurements.

The first experiment (Section 1) was performed under standardized conditions in a growth chamber to evaluate whether ambient factors affect the accuracy of three different active canopy sensors (GreenSeeker, CropCircle, and AFS). Two major effects were found. As first effect, varying device temperature had variable results depending on sensor and spectral index and mostly a linear index response to increasing temperature was found. If changing temperatures are not considered and corrected, they can easily lead to misinterpretations when analysing the reflectance values from the sensors obtained under field conditions.

As second effect, the distance between active sensors and target surface was revealed to be the major factor to be considered, depending on the sensor type. A range of measuring distances exists where the sensors generate stable reflectance data. The ranges found in this study are overall similar to the manufacturer´s recommendations. Thus, to enable accurate field measurements with active sensors, the optimum distance to the plant canopy must be investigated and adjusted for each sensor, taking into account factors such as the plant architecture and growth stage. By considering the influence of external effects as shown in this study, all active sensors show a good performance in detecting the biomass and nitrogen status. Because of the complexity of the interactions in this instance, a second controlled environment experiment was conducted using wheat canopies to determine from where the signals are derived, how deeply and effectively the sensor light penetrates into wheat canopies.

As second experiment the penetration depth of active sensors into the canopy was investigated using winter wheat plants grown in large containers. After removing each plant component stepwise, starting with the lower leaf layers, it could be concluded that each of the tested sensor reacted sensitively when removing already lower leaves. Thus we can expect that active sensors detect changes in biomass also in the lowest leaves even if several other leaf layers cover such leaves.

For the second part of this study a 2-year field experiment with 50 winter wheat cultivars was conducted to develop high-throughput phenotyping techniques for scoring phenotypic differences of early plant vigour and the onset of senescence.

For detecting early plant vigour, different reference methods were compared and the pixel analysis of RGB images was found to be the best method for evaluating early plant vigour by analyzing the relative amount of green pixels (RAGP). Simultaneously, spectral reflectance measurements were conducted by using the HAFS, and a novel index, the EPVI, was developed to accurately reflect the rate of early plant vigour. Relationships between the EPVI and the RAGP on photos taken from each plot were significant within both years ($r^2 = 0.81$ in 2011 and $r^2 = 0.84$ in 2012). The results show that the EPVI can be used for high-throughput scoring of early plant vigour, even though soil coverage is low at such early development stages. The two other investigated active sensors, the GreenSeeker and the CropCircle, showed quite comparable results regarding the relationships between pixel analysis and the spectral index NDVI, thus demonstrating also the potential for detecting phenotypic differences in early plant vigour.

As second phenotyping method stay-green and early-senescence phenotypes could be identified among the 50 winter wheat cultivars using passive spectral sensing as a high-throughput phenotyping tool to estimate the onset of senescence of flag leaves in each cultivar. Carbon and nitrogen metabolism were hypothesized to be responsible for the opposing effects on the onset of senescence after anthesis on yield and GPC, with a significant negative relationship between the onset of senescence and grain yield ($r^2 = 0.81$) and a positive relationship with GPC ($r^2 = 0.48$) being observed. Thus, stay-green phenotypes were characterized by higher N-uptake during grain filling and a longer maintenance of greenness. In addition, their use of photosynthetic glucose for synthesis of amino acids rather than for starch affects yield and GPC.

Finally, spectral remote sensing was found to represent a suitable method for the high-throughput phenotyping of flag leaf senescence. Using a hand held color spectrometer as calibration unit, PLSR models were successfully applied to convert spectra of the whole canopy into color values measured at the flag leaf level. The high-throughput nature of this phenotyping method could both facilitate the detection of senescence mechanisms of cereal plants in large field trials as well as help to better identify the effects of the onset of senescence on grain yield and GPC.

Considering that early plant vigour and the onset of senescence are still scored visually in breeding programs, these novel methods can contribute to improvements in the plant breeding process due to its rapidity in screening large field trials.

## 6    Conclusions

Recent developments in plant breeding methods are mainly referable to research achievements on genome level. Several traits of important crops such as wheat, maize or rice could be improved using modern breeding strategies based on novel molecular techniques (e.g. next-generation sequencing or marker-assisted selection). In comparison to these considerable achievements, the plant breeding on phenotype level does not significantly differ between Mendel´s experiments on peas 1856 and commercial breeding today. Phenotypic traits of well promising breeding lines, cultivars or candidate plants are still assessed visually. An exception here are greenhouse experiments, where novel automated phenotyping methods were recently developed. However the major step during the breeding process is the validation of breeding candidates under field conditions, considering genotype-environment interactions. At this point plant breeders are faced with the challenge to score various plant traits visually in thousands of field plots. This procedure is laborious and less objective when doing it with several persons. Thus, high-throughput phenotyping methods are urgently needed to replace visual field scoring for managing large field trials and to accelerate the breeding process.

Therefore the present study was conducted to contribute to the high-throughput phenotyping of winter wheat cultivars under field conditions. After assessing the performance of active spectral reflectance sensors under varying conditions (temperature, light and measuring distance), as well as the penetration depth of those sensors into the canopy, spectral reflectance measurements were successfully applied for phenotyping two important breeding traits, early plant vigour and the onset of senescence, among a set of 50 winter wheat cultivars. Spectral reflectance sensors were therefore mounted on the mobile phenotyping platform Phenotrac 4 to provide the high-throughput character of the proposed method. Phenotypic differences for both traits could be clearly shown. The high-throughput phenotyping of plant vigour could improve the selection of cultivars in early development stages. Determining the onset of senescence with our proposed method will help plant breeders to identify fast and late-senescing (= stay-green) phenotypes. Information about the senescence behaviour of different wheat cultivars are of great importance for adapting crops to various environmental conditions.

The newly developed phenotyping methods presented in this study could help to establish spectral reflectance measurements as a rapid and accurate high-throughput phenotyping technique.

# References

Adamsen, F.G., Pinter, P.J., Barnes, E.M., LaMorte, R.L., Wall, G.W., Leavitt, S.W., Kimball, B.A., 1999. Measuring wheat senescence with a digital camera. Crop Sci. 39, 719–724.

Allen, W., Richardson, A., 1968. Interaction of light with a plant canopy. J. Opt. Soc. Am. 58, 1023–1028.

Araus, J., Labrana, X., 1991. Leaf photosynthesis and chloroplast senescence patterns in wheat flag leaves during grain filling. Photosynthetica 25, 33–37.

Babar, M.A., Reynolds, M.P., van Ginkel, M., Klatt, A.R., Raun, W.R., Stone, M.L., 2006. Spectral reflectance indices as a potential indirect selection criteria for wheat yield under irrigation. Crop Sci. 46, 578–588.

Barker, D.W., Sawyer, J.E., 2010. Using active canopy sensors to quantify corn nitrogen stress and nitrogen application rate. Agron. J. 102, 964–971.

Berger, B., Parent, B., Tester, M., 2010. High-throughput shoot imaging to study drought responses. J. Exp. Bot. 61, 3519–3528.

Bhullar, S.S., Jenner, C.F., 1985. Differential responses to high temperatures of starch and nitrogen accumulation in the grain of four cultivars of wheat. Funct. Plant Biol. 12, 363–375.

Blanco, A., Mangini, G., Giancaspro, A., Giove, S., Colasuonno, P., Simeone, R., Signorile, A., De Vita, P., Mastrangelo, A.M., Cattivelli, L., 2012. Relationships between grain protein content and grain yield components through quantitative trait locus analyses in a recombinant inbred line population derived from two elite durum wheat cultivars. Mol. Breed. 30, 79–92.

Bogard, M., Jourdan, M., Allard, V., Martre, P., Perretant, M.R., Ravel, C., Heumez, E., Orford, S., Snape, J., Griffiths, S., 2011. Anthesis date mainly explained correlations between post-anthesis leaf senescence, grain yield, and grain protein concentration in a winter wheat population segregating for flowering time QTLs. J. Exp. Bot. 62, 3621–3636.

Boligon, A.A., Lúcio, A.D.C., Lopes, S.J., Cargnelutti Filho, A., Garcia, D.C., 2011. Wheat seedling emergence estimated from seed analysis. Sci. Agric. 68, 336–341.

Booth, D.T., Cox, S.E., Meikle, T.W., Fitzgerald, C., 2006. The accuracy of ground-cover measurements. Rangeland Ecol. Manag. 59, 179–188.

Borrell, A.K., Hammer, G.L., Henzell, R.G., 2000. Does maintaining green leaf area in sorghum improve yield under drought? II. Dry matter production and yield. Crop Sci. 40, 1037–1048.

Borrell, A.K., Incoll, L.D., Simpson, R.J., Dalling, M.J., 1989. Partitioning of dry matter and the deposition and use of stem reserves in a semi-dwarf wheat Crop. Ann. Bot. 63, 527–539.

Busemeyer, L., Mentrup, D., Möller, K., Wunder, E., Alheit, K., Hahn, V., Maurer, H.P., Reif, J.C., Würschum, T., Müller, J., 2013. BreedVision - A multi-sensor platform for non-destructive field-based phenotyping in plant breeding. Sensors 13, 2830–2847.

Campbell, C.A., Davidson, H.R., Winkleman, G.E., 1981. Effect of nitrogen, temperature, growth stage and duration of moisture stress on yield components and protein content of Manitou spring wheat. Can. J. Plant Sci. 61, 549–563.

Campbell, C.A., Selles, F., Zentner, R.P., McConkey, B.G., McKenzie, R.C., Brandt, S.A., 1997. Factors influencing grain N concentration of hard red spring wheat in the semiarid prairie. Can. J. Plant Sci. 77, 53–62.

Campbell, J.B., 2002. Introduction to remote sensing. Guilford Press.

Chappelle, E.W., Kim, M.S., McMurtrey, J.E., 1992. Ratio analysis of reflectance spectra (RARS): an algorithm for the remote estimation of the concentrations of chlorophyll a, chlorophyll b, and carotenoids in soybean leaves. Remote Sens. Environ. 39, 239–247.

Christopher, J.T., Manschadi, A.M., Hammer, G.L., Borrell, A.K., 2008. Developmental and physiological traits associated with high yield and stay-green phenotype in wheat. Crop Pasture Sci. 59, 354–364.

Comar, A., Burger, P., de Solan, B., Baret, F., Daumard, F., Hanocq, J.-F., 2012. A semi-automatic system for high throughput phenotyping wheat cultivars in-field conditions: description and first results. Funct. Plant Biol. 39, 914-924.

De Vries, F.W.T.P., Brunsting, A.H.M., Van Laar, H.H., 1974. Products, requirements and efficiency of biosynthesis a quantitative approach. J. Theor. Biol. 45, 339–377.

Dellinger, A.E., Schmidt, J.P., Beegle, D.B., 2008. Developing nitrogen fertilizer recommendations for corn using an active sensor. Agron. J. 100, 1546–1552.

Derkx, A., Orford, S., Griffiths, S., Foulkes, J., Hawkesford, M.J., 2012. Identification of differentially senescing mutants of wheat and impacts on yield, biomass and nitrogen partitioning. J. Integr. Plant Biol. 54, 555–566.

Ellis, M.H., Rebetzke, G.J., Chandler, P., Bonnett, D., Spielmeyer, W., Richards, R.A., 2004. The effect of different height reducing genes on the early growth of wheat. Funct. Plant Biol. 31, 583–589.

Elsayed, S., Mistele, B., Schmidhalter, U., 2011. Can changes in leaf water potential be assessed spectrally? Funct. Plant Biol. 38, 523–533.

Erdle, K., Mistele, B., Schmidhalter, U., 2011. Comparison of active and passive spectral sensors in discriminating biomass parameters and nitrogen status in wheat cultivars. Field Crops Res. 124, 74–84.

Erdle, K., Mistele, B., Schmidhalter, U., 2013. Spectral high-throughput assessments of phenotypic differences in biomass and nitrogen partitioning during grain filling of wheat under high yielding western European conditions. Field Crops Res. 141, 16–26.

Feil, B., 1997. The inverse yield-protein relationship in cereals: possibilities and limitations for genetically improving the grain protein yield. Trends Agron. 1, 103–119.

Fiorani, F., Schurr, U., 2013. Future Scenarios for Plant Phenotyping. Annu. Rev. Plant Biol. 64, 267–291.

Fischer, A., Feller, U., 1994. Senescence and protein degradation in leaf segments of young winter wheat: Influence of leaf age. J. Exp. Bot. 45, 103–109.

Fitzgerald, G.J., 2010. Characterizing vegetation indices derived from active and passive sensors. Int. J. Remote Sens. 31, 4335–4348.

Fois, S., Motzo, R., Giunta, F., 2009. The effect of nitrogenous fertiliser application on leaf traits in durum wheat in relation to grain yield and development. Field Crops Res. 110, 69–75.

Foulkes, M.J., Sylvester-Bradley, R., Weightman, R., Snape, J.W., 2007. Identifying physiological traits associated with improved drought resistance in winter wheat. Field Crops Res. 103, 11–24.

Furbank, R.T., Tester, M., 2011. Phenomics–technologies to relieve the phenotyping bottleneck. Trends Plant Sci.

Gaju, O., Allard, V., Martre, P., Snape, J.W., Heumez, E., LeGouis, J., Moreau, D., Bogard, M., Griffiths, S., Orford, S., 2011. Identification of traits to improve the nitrogen-use efficiency of wheat genotypes. Field Crops Res. 123, 139–152.

Gallagher, J.N., Biscoe, P.V., Scott, R.K., 1975. Barley and its environment. V. Stability of grain weight. J. Appl. Ecol. 12, 319–336.

Gebbing, T., Schnyder, H., KÜhbauch, W., 1999. The utilization of pre-anthesis reserves in grain filling of wheat. Assessment by steady-state 13CO2/12CO2 labelling. Plant Cell Environ. 22, 851–858.

Ghassemi-Golezani, K., Dalil, B., 2011. Seed ageing and field performance of maize under water stress. Afr. J. Biotechnol. 10, 18377–18380.

Gong, Y.H., Zhang, J., Gao, J.F., Lu, J.Y., Wang, J.R., 2005. Slow export of photoassimilate from stay-green leaves during late grain-filling stage in hybrid winter wheat (Triticum aestivum L.). J. Agron. Crop Sci. 191, 292–299.

Govaerts, B., Verhulst, N., Sayre, K.D., De Corte, P., Goudeseune, B., Lichter, K., Crossa, J., Deckers, J., Dendooven, L., 2007. Evaluating spatial within plot crop variability for different management practices with an optical sensor? Plant Soil 299, 29–42.

Granier, C., Aguirrezabal, L., Chenu, K., Cookson, S.J., Dauzat, M., Hamard, P., Thioux, J.-J., Rolland, G., Bouchier-Combaud, S., Lebaudy, A., Muller, B., Simonneau, T., Tardieu, F., 2006. PHENOPSIS, an automated platform for reproducible phenotyping of plant responses to soil water deficit in Arabidopsis thaliana permitted the identification of an accession with low sensitivity to soil water deficit. New Phytol. 169, 623–635.

Gregersen, P.L., Culetic, A., Boschian, L., Krupinska, K., 2013. Plant senescence and crop productivity. Plant Mol. Biol. 82, 603–622.

Guyot, G., Baret, F., Major, D.J., 1988. High spectral resolution: Determination of spectral shifts between the red and the near infrared. International Archives of Photogrammetry and Remote Sensing 11, pp. 750-760.

Hatfield, J.L., Gitelson, A.A., Schepers, J.S., Walthall, C.L., 2008. Application of spectral remote sensing for agronomic decisions. Agron. J. 100, S–117.

Heege, H.J., Reusch, S., Thiessen, E., 2008. Prospects and results for optical systems for site-specific on-the-go control of nitrogen-top-dressing in Germany. Prec. Agric. 9, 115–131.

Hirel, B., Le Gouis, J., Ney, B., Gallais, A., 2007. The challenge of improving nitrogen use efficiency in crop plants: towards a more central role for genetic variability and quantitative genetics within integrated approaches. J. Exp. Bot. 58, 2369–2387.

Holland, K.H., Lamb, D.W., Schepers, J.S., 2012. Radiometry of proximal active optical sensors (AOS) for agricultural sensing. Selected topics in applied earth observations and remote sensing, IEEE Journal of 5, 1793–1802.

Holland-Scientific, 2008. CropCircle ACS-470 User´s Guide. Lincoln, NE.

Huete, A.R., 1988. A soil-adjusted vegetation index (SAVI). Remote Sens. Environ. 25, 295–309.

Jasper, J., Reusch, S., Link, A., 2009. Active sensing of the N status of wheat using optimized wavelength combination: Impact of seed rate, variety and growth stage, in: Precision Agriculture 09, Papers from the 7th European Conference on Precision Agriculture. Wageningen, pp. 23–30.

Jenner, C.F., Ugalde, T.D., Aspinall, D., 1991. The physiology of starch and protein deposition in the endosperm of wheat. Funct. Plant Biol. 18, 211–226.

Jiang, G.-H., He, Y.-Q., Xu, C.-G., Li, X.-H., Zhang, Q., 2004. The genetic basis of stay-green in rice analyzed in a population of doubled haploid lines derived from an indica by japonica cross. Theor. Appl. Genet. 108, 688–698.

Jordan, C.F., 1969. Derivation of leaf-area index from quality of light on the forest floor. Ecol. 50, 663–666.

Khah, E.M., Roberts, E.H., Ellis, R.H., 1989. Effects of seed ageing on growth and yield of spring wheat at different plant-population densities. Field Crops Res. 20, 175–190.

Kichey, T., Hirel, B., Heumez, E., Dubois, F., Le Gouis, J., 2007. In winter wheat (*Triticum aestivum* L.), post-anthesis nitrogen uptake and remobilisation to the grain correlates with agronomic traits and nitrogen physiological markers. Field Crops Res. 102, 22–32.

Kim, Y., Glenn, D.M., Park, J., Ngugi, H.K., Lehman, B.L., 2010. Active spectral sensor evaluation under varying condition. Transactions of the ASABE. 55:293-301.

Knipling, E.B., 1970. Physical and physiological basis for the reflectance of visible and near-infrared radiation from vegetation. Remote Sens. Environ. 1, 155–159.

Kyle, W.J., Davies, J.A., Nunez, M., 1977. Global radiation within corn. Bound. Layer. Meteorol. 12, 25–35.

Li, F., Miao, Y., Hennig, S.D., Gnyp, M.L., Chen, X., Jia, L., Bareth, G., 2010. Evaluating hyperspectral vegetation indices for estimating nitrogen concentration of winter wheat at different growth stages. Prec. Agric. 11, 335–357.

Li, L., Nielsen, D.C., Yu, Q., Ma, L., Ahuja, L.R., 2010. Evaluating the Crop Water Stress Index and its correlation with latent heat and CO2 fluxes over winter wheat and maize in the North China plain. Agric. Water Manag. 97, 1146–1155.

Link, A., Reusch, S., 2006. Implementation of site-specific nitrogen application-Status and development of the YARA N-Sensor. Presented at the NJF Report, Nordic Association of Agricultural Scientists, Stockholm, Lillehammer, pp. 37–41.

Lopes, M.S., Reynolds, M.P., 2012. Stay-green in spring wheat can be determined by spectral reflectance measurements (normalized difference vegetation index) independently from phenology. J. Exp. Bot. 63, 3789–3798.

Lukina, E.V., Stone, M.L., Raun, W.R., 1999. Estimating vegetation coverage in wheat using digital images. J. Plant Nutr. 22, 341–350.

Mayfield, A.H., Trengove, S.P., 2009. Grain yield and protein responses in wheat using the N-Sensor for variable rate N application. Crop Pasture Sci. 60, 818–823.

Mistele, B., Schmidhalter, U., 2008. Spectral measurements of the total aerial N and biomass dry weight in maize using a quadrilateral-view optic. Field Crops Res. 106, 94–103.

Mistele, B., Schmidhalter, U., 2010. Tractor-based quadrilateral spectral reflectance measurements to detect biomass and total aerial nitrogen in winter wheat. Agron. J. 102, 499–506.

Montes, J.M., Technow, F., Dhillon, B.S., Mauch, F., Melchinger, A.E., 2011. High-throughput non-destructive biomass determination during early plant development in maize under field conditions. Field Crops Res. 121, 268–273.

Murungu, F.S., 2011. Effects of seed priming and water potential on seed germination and emergence of wheat (Triticum aestivum L.) varieties in laboratory assays and in the field. Afr. J. Biotechnol 10, 4365–4371.

Novoa, R., Loomis, R.S., 1981. Nitrogen and plant production. Plant Soil 58, 177–204.

Pask, A., Pietragalla, J., 2011. Leaf area, green crop area and senescence. In: Pask A, Pietragalla J, Mullan D, Reynolds, M, eds. Physiological Breeding II: A Field Guide to Wheat Phenotyping. Mexico: CIMMYT.

Phillips, S.B., Keahey, D.A., Warren, J.G., Mullins, G.L., 2004. Estimating winter wheat tiller density using spectral reflectance sensors for early-spring, variable-rate nitrogen applications. Agron. J. 96, 591–600.

Pleijel, H., Mortensen, L., Fuhrer, J., Ojanperä, K., Danielsson, H., 1999. Grain protein accumulation in relation to grain yield of spring wheat (Triticum aestivum L.) grown in open-top chambers with different concentrations of ozone, carbon dioxide and water availability. Agric. Ecosyst. Environ. 72, 265–270.

Portz, G., Molin, J.P., Jasper, J., 2012. Active crop sensor to detect variability of nitrogen supply and biomass on sugarcane fields. Prec. Agric. 13, 33–44.

Przulj, N., Momcilovic, V., 2001a. Genetic variation for dry matter and nitrogen accumulation and translocation in two-rowed spring barley: I. Dry matter translocation. Eur. J Agron. 15, 241–254.

Przulj, N., Momcilovic, V., 2001b. Genetic variation for dry matter and nitrogen accumulation and translocation in two-rowed spring barley: II. Nitrogen translocation. Eur. J Agron. 15, 255–265.

Rajala, A., Niskanen, M., Isolahti, M., 2011. Seed quality effects on seedling emergence, plant stand establishment and grain yield in two-row barley. Agric. Food Sci. 20.

Raun, W.R., Solie, J.B., Johnson, G.V., Stone, M.L., Lukina, E.V., Thomason, W.E., Schepers, J.S., 2001. In-season prediction of potential grain yield in winter wheat using canopy reflectance. Agron. J. 93, 131–138.

Rebetzke, G.J., Richards, R.A., Fettell, N.A., Long, M., Condon, A.G., Forrester, R.I., Botwright, T.L., 2007. Genotypic increases in coleoptile length improves stand establishment, vigour and grain yield of deep-sown wheat. Field Crops Res. 100, 10–23.

Reusch, S., 2004. Optical Sensors for Site-Specific Nitrogen Fertilisation in Agricultural Crop Production. VDI Berichte 1829, 53–60.

Reynolds, M., Manes, Y., Izanloo, A., Langridge, P., 2009. Phenotyping approaches for physiological breeding and gene discovery in wheat. Ann. Appl. Biol. 155, 309–320.

Richards, R.A., Lukacs, Z., 2002. Seedling vigour in wheat-sources of variation for genetic and agronomic improvement. Crop Pasture Sci. 53, 41–50.

Roberts, D.F., Adamchuk, V.I., Shanahan, J.F., Ferguson, R.B., Schepers, J.S., 2009. Optimization of crop canopy sensor placement for measuring nitrogen status in corn. Agron. J. 101, 140–149.

Rondeaux, G., Steven, M., Baret, F., 1996. Optimization of soil-adjusted vegetation indices. Remote Sens. Environ. 55, 95–107.

Scharf, P., Stevens, G., Dunn, D., Oliveira, L., 2007. Crop sensors for variable-rate N application to cotton in the Midsouth. IPNI Annual Report.

Scharf, P.C., Shannon, D.K., Palm, H.L., Sudduth, K.A., Drummond, S.T., Kitchen, N.R., Mueller, L.J., Hubbard, V.C., Oliveira, L.F., 2011. Sensor-based nitrogen applications out-performed producer-chosen rates for corn in on-farm demonstrations. Agron. J. 103, 1683–1691.

Schmid, A., 2008. Erfassung des aktuellen Stickstoffstatus von Kulturpflanzen mit berührungsloser Sensorik zur Optimierung der teilflächenspezifischen Bestandesführung. Herbert Utz Verlag.

Schmidhalter, U., 2005. Sensing soil and plant properties by non-destructive measurements, In: Proceedings of the International Conference on Maize Adaption to Marginal

Environments, Nakhon. Ratchasima. Thailand, 6-9 March, Asksorn Siam Printing, Bangkok, Thailand, pp. 80-90.

Schmidhalter U, Glas J, Heigl R, Manhart R, Wiesent S, Gutser R, Neudecker E (2001) Application and testing of a crop scanning instrument–field experiments with reduced crop width, tall maize plants and monitoring of cereal yield. In: Proceedings of 3rd European Conference on Precision Agriculture, Montpellier, 953–958.

Schmidhalter, U., Jungert, S., Bredemeier, C., Gutser, R., Manhart, R., Mistele, B., Gerl, G., 2003. Field-scale validation of a tractor based multispectral crop scanner to determine biomass and nitrogen uptake of winter wheat, In: : Stafford, J., Werner, A. (Eds.), 4th European Conference on Precision Agriculture, Wageningen Academic Publishers, pp. 615–619.

Scotford, I.M., Miller, P.C.H., 2004. Estimating tiller density and leaf area index of winter wheat using spectral reflectance and ultrasonic sensing techniques. Biosyst. Eng. 89, 395–408.

Scotford, I.M., Miller, P.C.H., 2005. Vehicle mounted sensors for estimating tiller density and leaf area index (LAI) of winter wheat. Wageningen Academic Publishers, Wageningen, pp. 201–208.

Shibayama, M., Akiyama, T., 1989. Seasonal visible, near-infrared and mid-infrared spectra of rice canopies in relation to LAI and above-ground dry phytomass. Remote Sens. Environ. 27, 119–127.

Smith, R.C.G., Wallace, J.F., Hick, P.T., Gilmour, R.F., Belford, R.K., Portmann, P.A., Regan, K.L., Turner, N.C., 1993. Potential of using field spectroscopy during early growth for ranking biomass in cereal breeding trials. Crop Pasture Sci. 44, 1713–1730.

Solari, F., 2006. Developing a crop based strategy for on-the-go nitrogen management in irrigated cornfields. Ph.D. diss. Univ. of Nebraska, Lincoln, USA.
Solari, F., Hodgen, P.J., Shanahan, J., Schepers, J., 2004. Time of Day and Corn Leaf Wetness Effects on Active Sensor Readings, Agronomy Abstracts, No. 4253.

Spano, G., Di Fonzo, N., Perrotta, C., Platani, C., Ronga, G., Lawlor, D.W., Napier, J.A., Shewry, P.R., 2003. Physiological characterization of "stay green" mutants in durum wheat. J. Exp. Bot. 54, 1415–1420.

Steiner, J.J., Grabe, D.F., Tulo, M., 1989. Single and multiple vigor tests for predicting seedling emergence of wheat. Crop Sci. 29, 782–786.

Stevens, G., Wrather, A., Rhine, M., Vories, E., Dunn, D., 2008. Predicting rice yield response to midseason nitrogen with plant area measurements. Agron. J. 100, 387–392.

Subramanian, R., Spalding, E., Ferrier, N., 2013. A high throughput robot system for machine vision based plant phenotype studies. Machine Vision Applic. 24, 619–636.

Sylvester-Bradley R, Scott RK, Wright CE (1990) Physiology in the production and improvement of cereals. HGCA Research Review 18, 156 pp.

Tahir, I.S.A., Nakata, N., 2005. Remobilization of nitrogen and carbohydrate from stems of bread wheat in response to heat stress during grain filling. J. Agron. Crop Sci. 191, 106–115.

Taylor, J.C., Wood, G.A., Welsh, J.P., Knight, S., 2000. Exploring management strategies for precision farming of cereals assisted by remote sensing. Aspects Appl. Biol. 60, 53–60.

Teal, R.K., Tubana, B., Girma, K., Freeman, K.W., Arnall, D.B., Walsh, O., Raun, W.R., 2006. In-season prediction of corn grain yield potential using normalized difference vegetation index. Agron. J. 98, 1488–1494.

Thomas, H., Howarth, C.J., 2000. Five ways to stay green. J. Exp. Bot. 51, 329–337.

Thomas, H., Smart, C.M., 1993. Crops that stay green. Ann. Appl. Biol. 123, 193–219.

Thoren, D., Schmidhalter, U., 2009. Nitrogen status and biomass determination of oilseed rape by laser-induced chlorophyll fluorescence. Eur. J Agron. 30, 238–242.

Thoren, D., Thoren, P., Schmidhalter, U., 2010. Influence of ambient light and temperature on laser-induced chlorophyll fluorescence measurements. Eur. J Agron. 32, 169–176.

Tisné, S., Serrand, Y., Bach, L., Gilbault, E., Ben Ameur, R., Balasse, H., Voisin, R., Bouchez, D., Durand-Tardif, M., Guerche, P., Chareyron, G., Da Rugna, J., Camilleri, C., Loudet, O., 2013. Phenoscope: an automated large-scale phenotyping platform offering high spatial homogeneity. Plant J. 74, 534–544.

Tremblay, N., Wang, Z., Ma, B.L., Belec, C., Vigneault, P., 2009. A comparison of crop data measured by two commercial sensors for variable-rate nitrogen application. Prec. Agric. 10, 145–161.

Valério, I.P., Carvalho, F.I.F. de, Oliveira, A.C. de, Benin, G., Souza, V.Q. de, Machado, A. de A., Bertan, I., Busato, C.C., Silveira, G. da, Fonseca, D.A.R., 2009. Seeding density in wheat genotypes as a function of tillering potential. Scientia Agricola 66, 28–39.

Verhulst, N., Govaerts, B., Sayre, K.D., Deckers, J., Francois, I.M., Dendooven, L., 2009. Using NDVI and soil quality analysis to assess influence of agronomic management on within-plot spatial variability and factors limiting production. Plant Soil 317, 41–59.

Verma, V., Foulkes, M.J., Worland, A.J., Sylvester-Bradley, R., Caligari, P.D.S., Snape, J.W., 2004. Mapping quantitative trait loci for flag leaf senescence as a yield determinant in winter wheat under optimal and drought-stressed environments. Euphytica 135, 255–263.

Viscarra Rossel, R.A., 2008. ParLeS: Software for chemometric analysis of spectroscopic data. Chemom. Intell. Lab. Syst. 90, 72–83.

Walter, A., Studer, B., Kölliker, R., 2012. Advanced phenotyping offers opportunities for improved breeding of forage and turf species. Ann. Bot. 110, 1271–1279.

Wang, H., McCaig, T.N., DePauw, R.M., Clarke, J.M., 2008. Flag leaf physiological traits in two high-yielding Canada Western Red Spring wheat cultivars. Can. J. Plant Sci. 88, 35–42.

White, J.W., Andrade-Sanchez, P., Gore, M.A., Bronson, K.F., Coffelt, T.A., Conley, M.M., Feldmann, K.A., French, A.N., Heun, J.T., Hunsaker, D.J., 2012. Field-based phenomics for plant genetics research. Field Crops Res. 133, 101–112.

Winterhalter, L., Mistele, B., Jampatong, S., Schmidhalter, U., 2011. High throughput phenotyping of canopy water mass and canopy temperature in well-watered and drought stressed tropical maize hybrids in the vegetative stage. Eur. J Agron. 35, 22–32.

Winterhalter, L., Mistele, B., Schmidhalter, U., 2012. Assessing the vertical footprint of reflectance measurements to characterize nitrogen uptake and biomass distribution in maize canopies. Field Crops Res. 129, 14–20.

Wu, J., Yue, S., Hou, P., Meng, Q., Cui, Z., Li, F., Chen, X., 2011. Monitoring Winter Wheat Population Dynamics Using an Active Crop Sensor. Spectrosc. Spectral Anal. 31, 535–538.

Zadoks, J.C., Chang, T.T., Konzak, C.F., 1974. A decimal code for the growth stages of cereals. Weed Res. 14, 415–421.

Zillmann, E., Graeff, S., Link, J., Batchelor, W.D., Claupein, W., 2006. Assessment of cereal nitrogen requirements derived by optical on-the-go sensors on heterogeneous soils. Agron. J. 98, 682–690.

Nicht zuletzt danke ich meinen Eltern, die niemals Mühen gescheut haben meine Zukunftspläne zu unterstützen. Ihnen möchte ich diese Arbeit widmen, denn ich verdanke ihnen dort angekommen zu sein wo ich heute bin.

Die wichtigste Unterstützung während meiner Promotionszeit war und ist jedoch Sandra, die mich durch alle Höhen und Tiefen begleitet und mir jeden Tag den nötigen Rückhalt gibt. Ohne dich wäre diese Arbeit nicht entstanden. Ich danke dir, dass du immer für mich da bist.

# Curriculum Vitae

| | |
|---|---|
| Name | Sebastian Kipp |
| Geburtsdatum | 25.10.1984 |
| Geburtsort | Leverkusen |
| Staatsangehörigkeit | Deutsch |
| Schulabschluss | Abitur |

## Studium

| | |
|---|---|
| Seit 10/2010 | **Technische Universität München – Lehrstuhl für Pflanzenernährung**<br>Doktorand der Agrarwissenschaften |
| 10/2005 –<br>07/2010 | **Rheinische Friedrich-Wilhelms-Universität Bonn**<br>Diplom Ingenieur der Agrarwissenschaften (Dipl. Ing.-agr.) |

## Arbeitserfahrung

| | |
|---|---|
| Seit 10/2010 | **Wissenschaftlicher Mitarbeiter** an der Technischen Universität München |
| 01/2014 –<br>04/2013 | **Gastwissenschaftler** and der Australian Plant Phenomics Facility in Canberra/Australien und Adelaide/Australien |
| 03/2010 –<br>06/2010 | **Studentischer Mitarbeiter** beim Bundesverband Deutscher Pflanzenzüchter (BDP) in der Abteilung der Saatgut-Treuhandverwaltung (STV) in Bonn |
| 08/2009 –<br>02/2010 | **Gastwissenschaftler** am International Center for Agricultural Research in the Dry Areas (ICARDA) in Aleppo/Syrien |
| 08/2008 –<br>10/2008 | **Praktikum** bei der KWS Saat AG in der Abteilung Rapszüchtung in Einbeck |
| 01/2008 –<br>07/2009 | **Studentischer Mitarbeiter** beim Bundesverband Deutscher Pflanzenzüchter (BDP) in der Abteilung der Saatgut-Treuhandverwaltung (STV) in Bonn |
| 08/2007 –<br>10/2007 | **Praktikum** auf dem Milchviehbetrieb Baumhögger-Wieden KG in Leverkusen |
| 08/2007 –<br>10/2007 | **Praktikum** auf dem Obstbau- und Geflügelbetrieb Kuppel-Oderwald in Leverkusen |
| 07/2004 –<br>07/2005 | **Freiwilliges Soziales Jahr** beim Arbeiter-Samariter-Bund in Burscheid |

## Stipendien und Auszeichnungen

09/2013 | **Forschungsstipendium** der Bayer Science and Education Foundation

09/2013 | **Forschungsstipendium** der Prof. Werner Schulze-Stiftung

06/2013 | **Forschungsförderung** der Leonhard-Lorenz Stiftung

07/2012 | **Forschungspreis** der International Society of Precision Agriculture (ISPA)

08/2009 | **Forschungsstipendium** der Gesellschaft für Internationale Zusammenarbeit (GIZ)